D1 AND D2 DOPAMINE RECEPTOR BIASED AND HETEROMERIC SIGNALING: IMPLICATIONS FOR PROTEIN CONFORMATIONAL FLUIDITY

by
Lani S. Chun

A dissertation submitted to Johns Hopkins University in conformity with the requirements for the degree of Doctor of Philosophy.

Baltimore, Maryland

August 2015

Abstract

The D1R and D2R dopamine receptor (DAR) subtypes represent the two most abundant and highly targeted DARs, but the precise mechanisms of drug action at the molecular level are not well understood. A revolution in the understanding of G protein-coupled receptors depicts receptors as dynamic, conformationally fluid proteins. This led to the idea that receptor heteromerization or ligand binding can promote functionally selective/biased signaling. In this vein, two aspects of DAR signaling are studied: D1R-D2R heteromerization and biased D2R signaling.

In Chapter 2, the pharmacology and signaling mechanism for the D1R-D2R heteromer is investigated. Diverging from canonical D1R-$G_{s/olf}$ protein and D2R-$G_{i/o}$ protein coupling, the D1R-D2R heteromer was proposed to couple to G_q protein-mediated Ca^{2+} mobilization. In Chapter 2, it is shown that D1R-D2R-mediated Ca^{2+} signaling may not be completely G_q protein-dependent or heteromer-specific, and may largely depend on $G_{i/o}$ protein, $G_{s/olf}$ protein, and $G_{\beta\gamma}$ signaling. Furthermore, SKF83959 (previously reported as a D1R-D2R selective agonist) has significant cross-reactivity to other receptors, warranting careful interpretation of its use *in vivo*.

In Chapter 3, a high-throughput screen was conducted to interrogate a small-molecule library for novel D2R agonists using a Ca^{2+} mobilization assay. Following additional orthogonal screening of cAMP modulation and β-arrestin-2 recruitment, a G protein biased D2R agonist was identified (MLS1547). MLS1547 analogs were tested using the cAMP accumulation and β-arrestin-2 recruitment assays. These results provided the basis for pharmacophore modeling and molecular docking analyses to build structure-activity relationships (SAR) of the functionally selective properties of this series of compounds.

Chapter 4 extends the pharmacological profiling of MLS1547 by showing that MLS1547 stimulates a low but significant degree of D2R internalization. The pharmacophore model is also confirmed and extended by testing additional MLS1547 analogs and developing a refined SAR.

In Chapter 5, another high-throughput screen was conducted to detect β-arrestin-2 biased D2R selective ligands. Although one β-arrestin-2 biased agonist was identified, further testing was not possible, as a source for the compound was not available.

Taken together, these data expand the understanding of the spectrum of signaling capabilities available to the D1R and D2R by investigating two novel mechanisms of signaling.

Academic advisor, thesis mentor, and primary reader: Dr. David R. Sibley

Secondary readers: Drs. Sergi Ferré and Haiqing Zhao

Thesis committee members (alphabetical): Drs. Sergi Ferré, Samer Hattar, Rejji Kuruvilla, Amy Newman, David R. Sibley

Preface and Acknowledgements

I would first like to thank Dr. David R. Sibley (NINDS, NIH) for his continued support and mentorship. He has always been a patient and knowledgeable leader during my journey through graduate school. I could not have asked for a better mentor and guide. I would also like to acknowledge current and past members of the Sibley lab for their contributions. Dr. R. Benjamin Free has been ever generous with his time and advice, and has been a great advocate for my interests and ideas. Likewise, I could not have finished my dissertation projects without the support of Dr. Jennie Conroy, Dr. Amy Moritz, Trevor Doyle, Brittney Miller, Julie Meade, Adrian Padron, Nicole Miller, and Heather Pascual. All of my work in the Sibley Lab was supported by the NIH-NINDS Intramural Program.

I am grateful for the contributions of my collaborators, without whom, my project would not have been possible. For their high-throughput screening expertise and help with the medicinal chemistry, I would like to thank Dr. Jingbo Xiao, Dr. Xin Hu, Dr. Andrés E. Dulcey, Dr. Marc Ferrer, Dr. Noel Southall, and Dr. Juan J. Marugan (NCATS, NIH); and Dr. Jeff Aubé and Dr. Kevin Frankowski (University of Kansas).

For their molecular modeling expertise, I would like to thank Dr. Thijs Beuming (Schrödinger Inc. and Weill Medical College of Cornell University) and Dr. Le Shi (NIDA, NIH).

For their material and technical contributions to the confocal work, I would like to thank Dr. Da-Ting Lin and Dr. Yun Li (NIDA, NIH);

For their help investigating receptor internalization, my thanks go to Dr. Fang Liu (University of Toronto) and Dr. Yoon Namkung (McGill University). Also, thanks to Dr. Jonathan Javitch and Prashant Donthamsetti (Columbia University), as well as Dr.

Hideaki Yano (NIDA, NIH) for their advice and for providing many of the DNA constructs used in my assays.

My qualification, thesis, and defense committee members have also been an indispensable source of ideas and encouragement, and I would like to thank Dr. Sergi Ferré (NIDA, NIH), Dr. Samer Hattar (CMDB, Johns Hopkins University), Dr. Rejji Kuruvilla (CMDB, Johns Hopkins University) and Dr. Amy Newman (NIDA, NIH) for their continued involvement. Special thanks goes to Dr. Haiqing Zhao (CMDB, Johns Hopkins University) for being the JHU secondary reader of my dissertation.

Dr. Michael Lichten (NCI, NIH) and Dr. Orna Cohen-Fix (NIDDK, NIH) have been excellent JHU-GPP co-directors. Their Logic and Methods course helped me think like a scientist, and their warm counsel gave me strength when I felt overwhelmed. They are a big part of what makes the JHU-GPP a great program, and future students will be missing out when they pass the directorship baton on to the next set of co-directors.

I also have to give a HUGE thank you to Joan Miller, who is everything you want out of a department administrator. She is efficient and knowledgeable, is always easy to get in touch with, and has the memory of an elephant. I could not have gotten through graduate school without her calm influence and irreplaceable know-how.

Finally, I would like to thank my friends and family for their support and love. My parents have always looked out for my best interests and started me on this path by cultivating my curiosity and love of discovery.

Table of Contents

List of Tables

List of Figures

Chapter 1: Background and Significance

Dopamine Receptor Structure

Dopamine receptors (DAR) are class A (rhodopsin family), seven transmembrane, G protein-coupled receptors (GPCRs), of which five genes exist in mammals. Each gene encodes a DAR subtype (D1R - D5R), which are grouped by structure, pharmacology, and function into the D1-like (D1R[1–3] and D5R[4,5]) and D2-like (D2R[6–8], D3R[9], and D4R[10,11]) DAR sub-families.

When comparing the DARs, the highest degree of sequence homology exists within the transmembrane (TM) spanning domains, where the endogenous ligand dopamine (DA) binds. The D1R and D5R share 80% homology (Figure 1) in the TM domains while the D2R shares 75% and 53% TM sequence homology with the D3R and D4R (Figure 2), respectively[12]. The protein sequences diverge much more outside of the transmembrane domains, making them prime targets for the development of subtype selective allosteric ligands. Notably, the D2R also exists as two protein isoforms: D2R long (D2LR) and D2R short (D2SR). Post-transcriptional mRNA splicing results in the excision of 29 amino acids in the third intracellular loop of the receptor to form D2SR (Figure 2).

One of the best approaches for understanding receptor structure and function is to have a crystal structure or other atomic level view of the receptor (e.g. via protein NMR or cryo-electron microscopy). However, crystallization of GPCRs is generally very difficult due to their low abundance and hydrophobicity. Accordingly, of the five DAR subtypes, only the D3R has been successfully crystallized (PDB: 3PBL)[13]. Despite this limitation, the crystal structure of the D3R can provide insight to the structure of other DARs, and using the known structures of other class A GPCRs, pharmacological

structure-activity relationships, and mutational analyses, models with predictive value can be developed, suggesting how proteins and ligands interact with the receptor (see Chapter 3 and Figure 26).

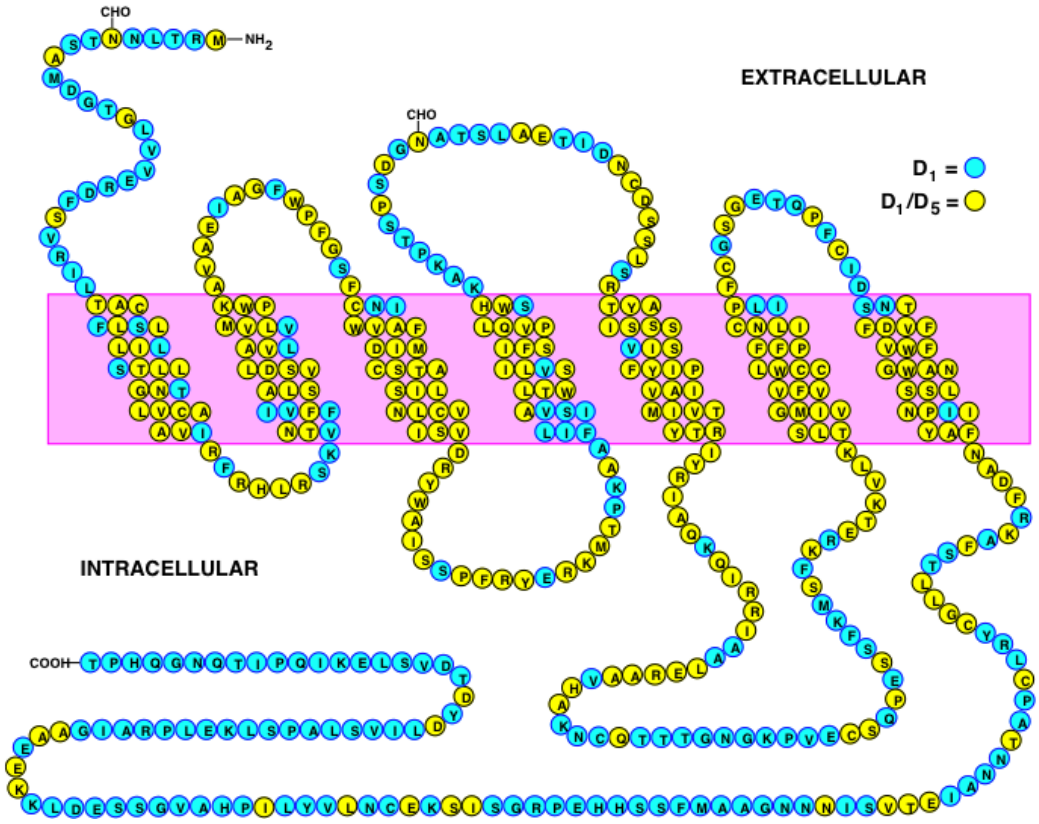

Figure 1: Amino acid sequence of the human D1R.
The membrane domain is depicted as a pink box. Residues unique to the D1R are shown in blue while those shared with the D5R are highlighted in yellow.

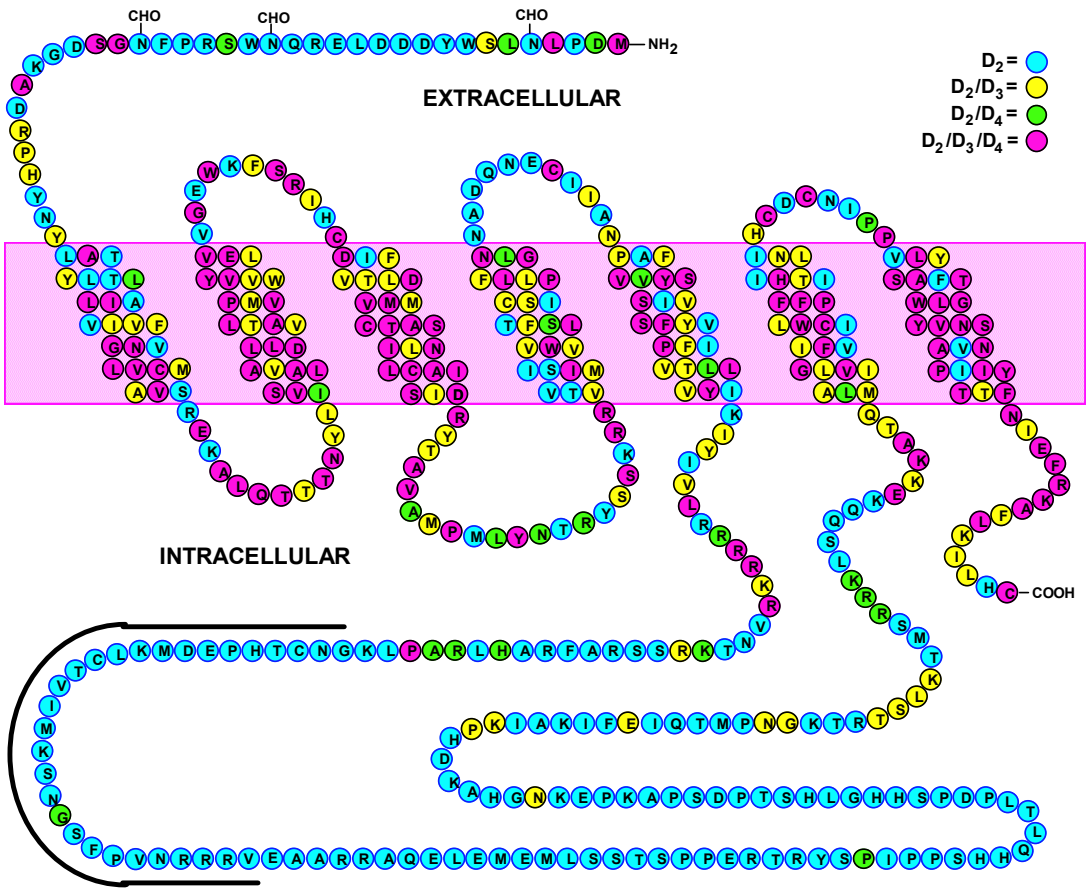

Figure 2: Amino acid sequence of the human D2LR.
The membrane domain is depicted as a pink box. Residues unique to the D2R are shown in blue. The black bar running parallel to the third intracellular loop indicates the 29 residues spliced out to form the D2SR. Residues shared between the D2R and D3R are highlighted in yellow. Residues shared between the D2R and D4R are highlighted in green. Residues common between the D2R, D3R, and D4R are highlighted in magenta.

Dopamine and Dopamine Receptor Expression and Function in Brain

Of the five DARs, the D1R is the most widely expressed subtype. It is expressed primarily in the striatum, nucleus accumbens (NAc), and olfactory tubercle, with lower levels in the cerebral cortex, hypothalamus, and thalamus[14,15]. The D2R is the second most highly expressed DAR in the brain, and like the D1R, the D2R is most highly expressed in the striatum, NAc, and olfactory tubercle, but it is also expressed in the substantia nigra (SN) and ventral tegmental area (VTA)[14–17]. The D2LR isoform is more abundant than the D2SR, and is highly expressed within the dorsal and ventral

striatum[18,19]. On the other hand, the D2SR is thought to function primarily as an autoreceptor, and has its strongest expression in the cell bodies and axons of dopaminergic neurons of the primary midbrain[20].

Expressed at a much lower level and the D1R and D2R are the D3R, D4R, and D5R. The D3R is particularly expressed in the ventral striatum, SN, VTA, hippocampus, septal area, and cortical areas[12]. The D4R is expressed at the lowest level compared to the other DARs, with expression in the frontal cortex, amygdala, hippocampus, hypothalamus, globus pallidus, SN, and thalamus[12]. The D5R is expressed mostly in the hippocampus and hypothalamus[21–23].

Within the brain, DA generally functions as a modulatory neurotransmitter that modulates the effects of glutamate and GABA signaling. Relatively few DA-producing (dopaminergic) neurons exist, with estimates ranging from 400,000 to 600,000 dopaminergic neurons in the human brain[24,25]. These neurons project from three major nuclei and release DA to large parts of the brain through four dopaminergic pathways (Figure 1):

1. Nigrostriatal pathway: dopaminergic neurons project from the SN pars compacta to the dorsal striatum, mainly targeting the GABAergic medium spiny neurons (MSN).
2. Mesolimbic pathway: dopaminergic neurons project from the VTA to the ventral striatum (NAc and olfactory tubercle). Again, the dopaminergic neurons mainly target GABAergic MSNs.
3. Mesocortical pathway: dopaminergic neurons project from the VTA to the cerebral cortex.

4. Tuberoinfundibular pathway: dopaminergic neurons project from the arcuate nucleus of the hypothalamus to the median eminence of the pituitary gland.

These pathways collectively regulate movement, reward, reinforcement, cognitive function, memory, and sleep[26–28], and dysfunction of dopaminergic systems may be involved in neuropsychiatric disorders such as schizophrenia, attention deficit hyperactivity disorder (ADHD), Parkinson's disease, and depression[29–31].

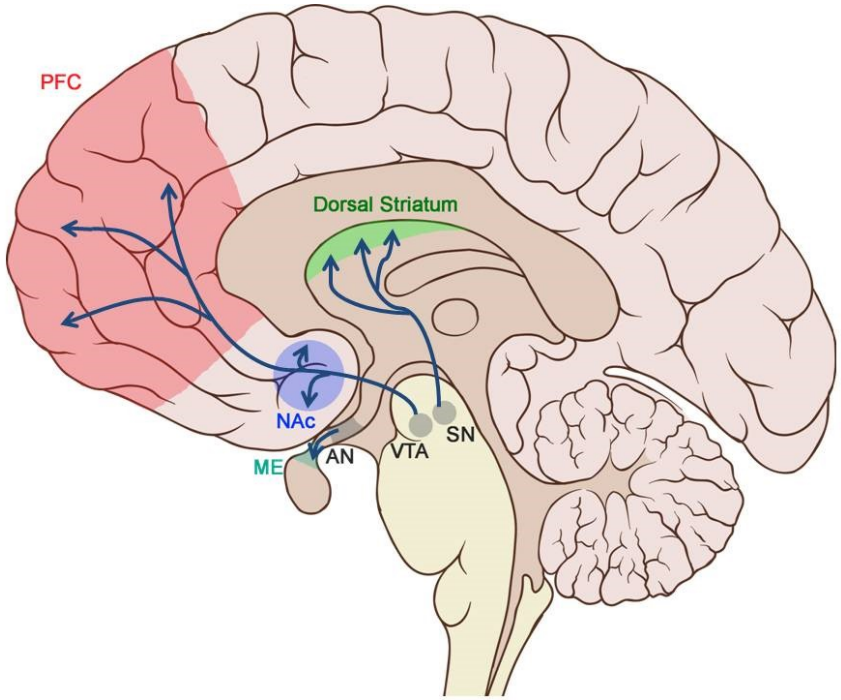

Figure 3: Diagram of the four main dopaminergic pathways.
Dopaminergic neurons project from three main nuclei (grey patches): the substantia nigra (SN), ventral tegmental area (VTA), and arcuate nucleus (AN) of the hypothalamus. Projections from these nuclei follow four distinct physiological pathways. The nigrostriatal pathway runs from the SN to the dorsal striatum (green). The mesolimbic pathway runs from the VTA to the nucleus accumbens (NAc, blue). The mesocortical pathway runs from the VTA to the prefrontal cortex (PFC, red). The tuberoinfundibular pathway runs from the AN to the median eminence of the pituitary gland (ME, teal). *Added text and arrows to figure from Creative Commons source: Patrick J. Lynch; illustrator; C. Carl Jaffe; MD; cardiologist Yale University Center for Advanced Instructional Media Medical Illustrations by Patrick Lynch, generated for multimedia teaching projects by the Yale University School of Medicine, Center for Advanced Instructional Media, 1987-2000. Patrick J. Lynch, http://patricklynch.net Creative Commons.*

Dopamine Receptor-mediated G Protein Signaling

The DARs primarily couple to, and signal through, heterotrimeric G proteins. These G proteins are GTPases which consist of a G_α subunit, a G_β subunit, and a G_γ

subunit. In its inactive state, the heterotrimeric G protein is bound to GDP. When activated by a receptor, the GDP is replaced with GTP, and the G_{α} subunit dissociates from the $G_{\beta\gamma}$ subunits to initiate signaling. Four main types of heterotrimeric G proteins are expressed in the brain[32–34]: adenylate cyclase inhibiting (G_i and G_o proteins), adenylate cyclase stimulating (G_s and G_{olf} proteins), phospholipase C β (PLCβ) stimulating (G_q and G_{11} proteins), and Rho family G proteins (G_{12} and G_{13} proteins).

Canonically, the D1-like receptors couple to the stimulatory $G_{s/olf}$ proteins to activate adenylate cyclase-mediated formation of cAMP while the D2-like receptors couple to the inhibitory $G_{i/o}$ proteins to inhibit adenylate cyclase[12,35] (Figure 4, Figure 5). Following activation, the D1-like receptor-mediated cAMP production causes the activation of protein kinase A (PKA), while D2-like receptor-mediated inhibition of cAMP production causes inactivation of PKA. PKA primarily works to modulate downstream protein activity and transcription, and one of its most well studied targets is the 32-kDa DA and cAMP-regulated phosphoprotein (DARPP-32), which is targeted by many other cellular proteins, and serves to combine multiple signaling inputs into one output[36]. Activation of DARPP-32 by the D1R and D5R causes enhancement of the NMDA receptor (NMDAR) signaling[37], which is important for synaptic plasticity, and has a role in learning and memory. This enhancement can by countered by the D2R, which inhibits the production of cAMP, hence decreasing PKA and subsequent DARPP-32 activation[38].

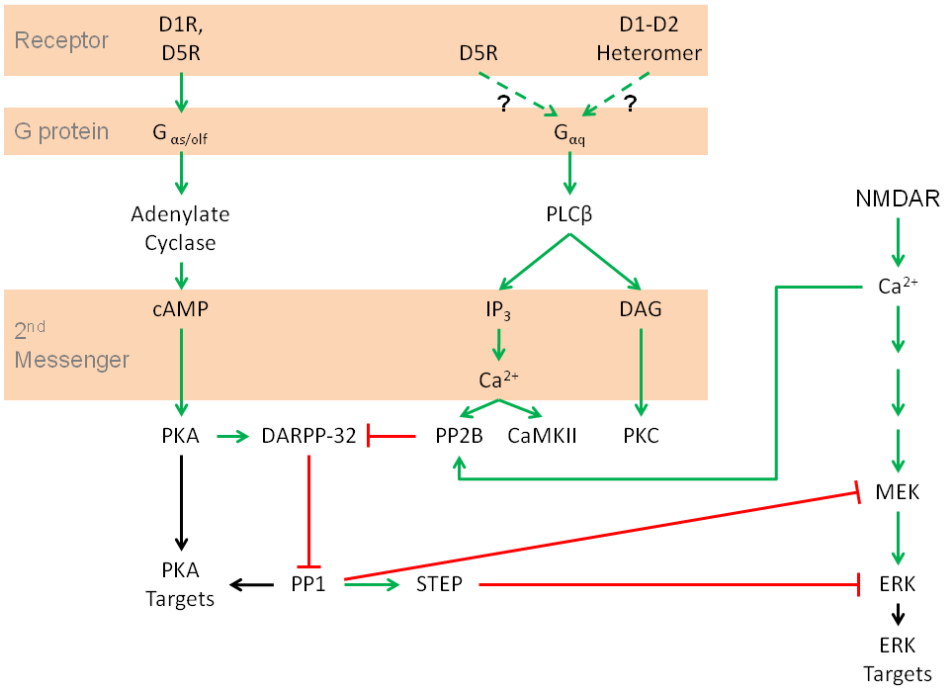

Figure 4: D1-like dopamine receptor signaling pathways.
Green arrows indicate activation, red lines indicate inhibition, and black arrows indicate an interaction that can be stimulatory or inhibitory depending on the cellular context. Abbreviations: DAG (diacylglycerol), DARPP-32 (32-kDa dopamine and cAMP-regulated phosphoprotein), ERK (extracellular signal-regulated kinase 1/2), MEK (MEK/ERK kinase), IP_3 (inositol triphosphate), NMDAR (NMDA receptor), PKC (protein kinase C), PKA (protein kinase A), PP1 (protein phosphatase), PP2B (protein phosphatase 2B/calcineurin), STEP (striatal-enriched tyrosine phosphatase).

There is some evidence that DARs can also couple to non-canonical signaling cascades. The D1-like and D2-like receptors can activate the G_q protein[39–42] (Figure 4) and stimulate $G_{\beta\gamma}$ release[42–44] (Figure 5) to activate PLCβ. The activation of PLCβ leads to the production of diacylglycerol and inositol triphosphate. Both second messengers lead ultimately to a change in long-term neural plasticity. D2-like receptor-mediated activation of the $G_{\beta\gamma}$ subunits is not limited to PLCβ activation and has been shown to lead to signaling through ion channels. More specifically, the D2R and D3R can activate the G protein-coupled inwardly-rectifying K^+ channel (GIRK)[45,46]. The D2R is also able to inhibit L/N-type Ca^{2+} channels[44,47]. Additionally, it has been suggested that a D1R-

D2R heteromer is able to form *in vitro* and couple to the G_q protein to activate PLCβ-mediated Ca^{2+} response (see Figure 4 and Chapter 2 for more details)[42,48].

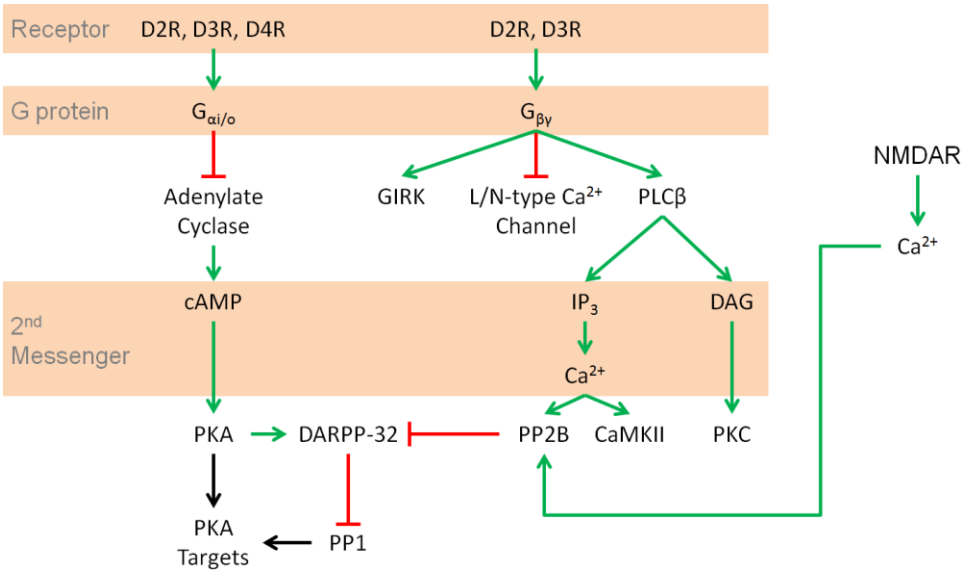

Figure 5: D2-like dopamine receptor signaling pathways.
Green arrows indicate activation, red lines indicate inhibition, and black arrows indicate an interaction that can be stimulatory or inhibitory depending on the cellular context. Abbreviations: DAG (diacylglycerol), DARPP-32 (32-kDa dopamine and cAMP-regulated phosphoprotein), IP_3 (inositol triphosphate), NMDAR (NMDA receptor), PKC (protein kinase C), PKA (protein kinase A), PP1 (protein phosphatase), PP2B (protein phosphatase 2B/calcineurin).

Regulation of DAR Signaling: G Protein-coupled Receptor Kinases and β-arrestins

Following activation, the DARs undergo rapid desensitization and internalization to regulate signaling activity. Desensitization involves the separation of the activated DAR from the G protein. This begins when a G protein-coupled receptor kinase (GRK) phosphorylates intracellular residues on the DAR[49,50]. Seven GRKs exist which are subdivided into the GRK1-like subfamily (GRK1 and GRK7), GRK2-like subfamily (GRK2 and GRK3), and GRK4-like subfamily (GRK4, GRK5, and GRK6)[49]. GRK1 and GRK7 are limited to regulating visual opsins and GRK4 has limited expression in the cerebellum, kidney, and testis[51], and has been shown to only regulate DAR function in

the kidney[52]. The GRK2, GRK3, GRK5, and GRK6 are more widely expressed and have all been associated with DAR regulation using *in vitro*, *in vivo*, and behavioral studies[27]. However, it is not known if a single GRK subtype regulates a single DAR subtype, and it is more likely that specific GRK-DAR interactions are tissue dependent.

Following GRK-mediated DAR phosphorylation, the scaffolding protein arrestin binds to the receptor, although it should be noted that, in some cases such as with the D2R, the phosphorylation event itself is not required for arrestin recruitment[53,54]. Arrestin binding promotes receptor desensitization by physically blocking the binding of G proteins to the receptor. Arrestin subsequently recruits the clathrin-binding AP2 protein[55–57] which promotes the formation of clathrin-coated pits, resulting in receptor endocytosis[53,58,59].

The arrestins are classified into two groups: the visual arrestins (arrestin 1 and arrestin 4) which are expressed in rod and cone cells of the eye, and the non-visual arrestins (arrestin 2 and arrestin 3, a.k.a. β-arrestin-1 and β-arrestin-2, respectively) which are ubiquitously expressed[60,61]. Although there is some evidence that β-arrestin-1 may interact with the DARs in the brain[62–64], this interaction has not been shown to regulate G protein-mediated DAR signaling. Instead, based on a variety of studies, β-arrestin-2 has been shown to be the primary regulator of DAR signaling in the brain[27]. Interestingly, it has been proposed that the sequence of residues that GRK phosphorylates on the receptor may regulate how arrestin functions following receptor binding[65,66] and may determine whether the receptor is recycled or degraded[67]. Furthermore, it has been reported that some GPCRs exhibit arrestin-independent mechanisms of receptor internalization[49] that

are largely dependent on the clathrin adaptor AP2[68] and various GRKs[68–75]. Thus far, no arrestin-independent internalization mechanisms have been reported for the DARs.

Chapter 2: D1R-D2R Synergy Promotes Ca^{2+} Signaling via Multiple Mechanisms

Background

Before the D1R-D2R heteromer was proposed, the subject of D1R and D2R cellular colocalization was, and still is, debatable. Most investigations of potential D1R and D2R cellular co-expression have been performed within the striatum, where over 90% of the neurons are MSNs. MSNs modulate cortical signals through two neuronal pathways that are defined by gene expression profiles and function (Figure 6). In the "direct" (striatonigral) pathway, MSN axons project towards and inhibit activity in the substantia nigra, allowing a net excitation of the motor cortex via the thalamus. In the "indirect" (striatopallidal) pathway, the striatum inhibits the activity of the globus pallidus. This allows the subthalamic nucleus to fire, resulting in net inhibition of the motor cortex. MSNs which form the direct pathway co-express D1R along with the neuropeptides dynorphin and substance P, while the MSNs of the indirect pathway co-express D2R and the neuropeptide enkephalin[76].

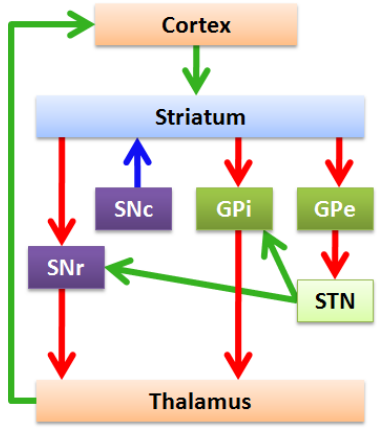

Figure 6: Connectivity diagram of the striatonigral and striatopalladial pathways. Excitatory glutamatergic pathways in green, inhibitory GABAergic pathways in red, and modulatory dopaminergic in blue. Abbreviations: SNr (substantia nigra pars reticulate), SNc (substantia nigra pars compacta), GPe (external globus pallidus), GPi (internal globus pallidus), STN (subthalamic nucleus).

Although there is evidence for concurrent expression of D1R and D2R in several brain regions, co-expression within the same neurons has been a matter of much debate. Immunolabeling of receptor proteins in striatal neural slices visualized by electron

microscopy suggested complete segregation of neurons expressing D1R and D2R[77,78], but other studies using fluorescence imaging provided evidence both for[48,79] and against[78] receptor co-localization in about 20% of striatal neurons. EGFP expression driven by either D1R or D2R gene promoters in BAC mice indicated complete cellular segregation of receptor expression[80]. *In situ* detection of D1R and D2R mRNA showed conflicting evidence[76,81–83], while reverse transcriptase PCR of single striatal neurons detected co-expression in about 17% of MSNs[84,85]. Additionally, the few MSNs that co-expressed enkephalin with dynorphin[29], or enkephalin with substance P[85], also co-expressed D1R and D2R. Interestingly, neurons co-expressing D1R and D2R may exhibit processes that exclusively express only D1R or only D2R receptors[48]. These findings, along with the methods of detection and visualization may be the reason for incongruent reports over D1R and D2R neuronal co-localization.

It was originally thought that the D1R and D2R were functionally opposed, based on their known regulation of adenylate cyclase (Figure 4, Figure 5)[86,87]. However, in the late 1980s, behavioral studies found that co-administration of D1R and D2R agonists elicited behaviors not seen when administered separately. These behaviors could be reduced with the addition of either a selective D1R or D2R antagonist, demonstrating the need for stimulation of both receptors at the same time. Electrophysiological studies presented similar results with simultaneous D1R and D2R stimulation in various regions of the brain such as the substantia nigra and nucleus accumbens[88]. Additional studies found evidence for D1R and D2R synergism in striatal neurons resulting in altered animal behavior[89–92]. While it was likely that behavioral changes induced by D1R and D2R ligands were due to integration of D1R and D2R signaling at the circuit level, the

question remained whether at least part of the behavioral changes could be attributed to D1R-D2R synergism at the cellular level.

In the 1990s, "D1-like" receptor stimulation was suggested to involve intracellular Ca^{2+} mobilization as a result of G_q-mediated activation of phospholipase C in striatal neurons[93–96]. This suggested that an alternate mechanism for D1R-related signaling existed. In 2004, Susan George and colleagues published data suggesting the existence of a D1R-D2R heteromer linked to stimulation of intracellular Ca^{2+} mobilization[48]. By heterologously co-expressing D1R and D2R in HEK293T and COS7 cells, they were able to observe an intracellular Ca^{2+} response after treatment with DA or co-treatment with selective D1R and D2R agonists. Ca^{2+} mobilization was not seen in cells transfected with only the D1R or D2R, with treatment with selective D1R or D2R agonists alone, or when the D1R-D2R co-transfected cells were stimulated with DA and incubated with either a D1R or D2R selective antagonist. This indicated that the Ca^{2+} response requires co-expression and co-activation of both D1R and D2R[48].

Additional publications from the George lab suggested the existence of D1R-D2R heteromers in the striatum, especially in the ventral striatum of human and rat brain. Importantly, studies using confocal FRET techniques argued for direct demonstration of the existence of D1R-D2R heteromers in 10-20% of the cell bodies and pre-synaptic terminals of MSNs within the nucleus accumbens[29,97–99], and the two DARs have been shown to co-internalize following selective activation of either receptor[100,101]. Moreover, they showed that the D1R-D2R heteromer stimulated G_q protein-mediated intracellular Ca^{2+} release[48,102], and they were able to see co-internalization of the two receptors following co-stimulation of the heteromer[100,101].

The George lab then identified and studied several structurally similar compounds from the benzazepine family that were able to selectively activate the D1R homomer (as defined by adenylate cyclase activation) or the D1R-D2R heteromer[103]. One such compound, SKF83822, only activates the D1R homomer, while another compound, SKF83959, was suggested to selectively activate the D1R-D2R heteromer[102] (Figure 7).

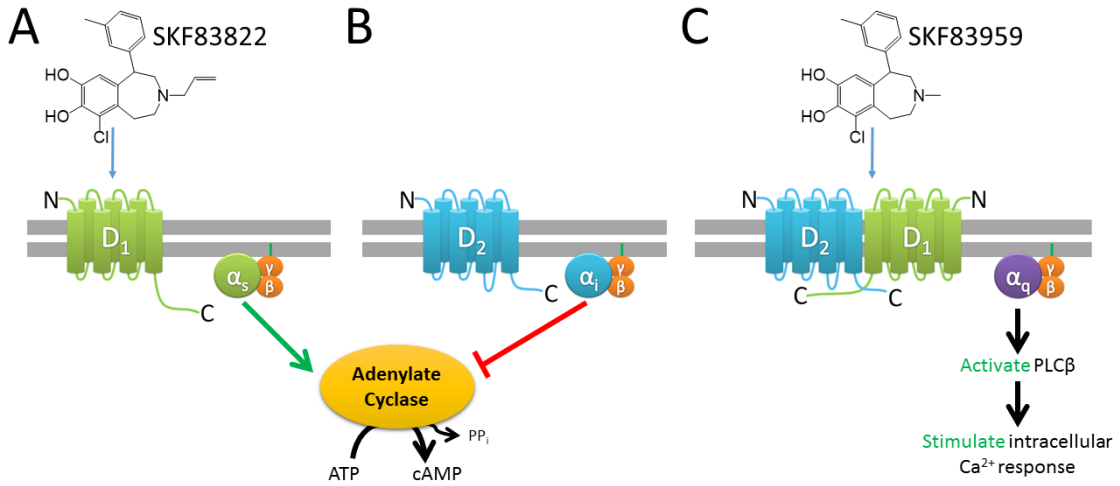

Figure 7: Differential effects of structurally similar benzazepines, SKF83959 and SKF83822, on DAR signal transduction.
A: SKF83822 acts as a D1R homomer agonist which activates stimulatory $G_{s/olf}$ proteins, causing cAMP formation. **B**: Benzazepines do not target homomeric D2Rs, which couple to inhibitory $G_{i/o}$ proteins, inhibiting cAMP formation. **C**: SKF83959 was suggested to activate the D1R-D2R heteromer to induce a phospholipase C β-induced Ca^{2+} response (Rashid et al., 2007). See Figure 4 and Figure 5 for more detailed signaling cascades.

Interestingly, other labs had already observed the unusual pharmacology of SKF83959. Undie et al. found that SKF83959 antagonized D1R-coupled cAMP formation and, instead, induced striatal intracellular Ca^{2+} mobilization in rats and monkeys[104]. SKF83959 did not cause epileptic seizures in rodents[105], unlike D1R agonists that stimulate cAMP production. Paradoxically, SKF83959 seemed to cause typical D1R agonist-like behaviors in rats[29], and is an effective anti-parkinsonian agent in MPTP-lesioned monkeys that are unresponsive to L-DOPA[106]. SKF83959's seemingly conflicting pharmacological actions have been proposed to be due to its unique D1R-D2R

heteromer-specific targeting, which might also account for its ability to treat L-DOPA-resistant parkinsonian monkeys with very little of the side effects that are typical of drugs used to treat Parkinson's disease[30]. These findings also presented tantalizing evidence that D1R-D2R heteromer specific drugs could be used to effectively treat neurological diseases without inducing the severe side effects seen with most drugs.

It is clear from these previous studies that the D1R and D2R can function synergistically to induce Ca^{2+} mobilization. However, these studies did not conclusively address whether the receptors function as a part of a dimer or a larger heteromeric complex. Also, all functional studies investigating D1R-D2R interactions in transfected cells used D2LR instead of D2SR, raising the issue that the observed phenomena might be isoform specific. Importantly, there is evidence that the 3rd intracellular loop (ICL), which is the only region of difference between D2LR and D2SR, can affect the G protein coupling and signaling capabilities for each D2R isoform[107]. Pei et al. found that a protein fragment unique to the 3rd ICL of the D2LR, which is absent in the D2SR, could associate with the D1R using a "pull down" assay[31]. The same fragment could also block co-immunoprecipitation of the D1R and D2R, consistent with the hypothesis that the 3rd ICL is an important region for D1R-D2R heteromer formation[31]. Pei et al. did not test the ability of other D2R regions to affect heteromer formation, nor did they do a co-immunoprecipitation of the D1R and D2SR, but their results do provide some evidence for isoform-dependent heteromerization of the D1R and D2R.

Many other GPCRs have been found to form homo- or hetero-oligomers with biochemical and functional characteristics that are unique to their oligomeric conformations[108–110]. These GPCR oligomers have been found to occur across different

classes, families, types, and subtypes[111]. Additionally, the internalization and degradation of GPCRs in homo- and hetero-oligomers has been found to differ from their homomeric counterparts[108,111–115]. The interaction between GPCR oligomers and their targets can be asymmetrical or symmetrical and, most intriguingly, a homo- or heteromer specific ligand can be functionally selective. Functional selectivity, also termed biased agonism, is a relatively new pharmacological concept. A ligand is functionally selective if it stimulates or inhibits one specific signaling pathway of a receptor that has many possible signaling pathways (see Chapter 3 Introduction).

GPCRs may exist in various constantly changing structural conformations, and a functionally selective ligand may bias the GPCR towards a specific conformation that limits its spectrum of signaling capabilities[116]. The evidence for a D1R-D2R heteromer selective ligand (SKF83959) along with the unknown structural and pharmacological properties of the heteromer is compelling. The discovery of novel small molecule ligands specifically targeting the D1R-D2R heteromer could aid, not only in drug discovery and development, but also in the characterization of the heteromer itself. This idea does not come without precedent, as other homo- and heteromeric GPCRs have been found to have oligomer-specific ligands with unique downstream coupling and signaling properties. For instance, a δ-opioid receptor antagonist, naltriben mesylate, exhibited biased antagonism when it was found to block *internalization* of heteromers composed of δ-opioid and μ-opioid receptors without inhibiting heteromer-mediated G protein *activation*[117]. Likewise, a κ-opioid receptor agonist, 6'-GNTI, was found to activate the κ-opioid receptor only when in a complex with the μ-opioid receptor[118].

While the precise mechanism for this type of signaling and its prevalence *in vivo* remains unclear, heteromer selective compounds could aid in furthering our understanding of heteromer structure, pharmacology and function *in vivo*. It has been reported that D1R-D2R co-activation results in increased Ca^{2+}/calmodulin-dependent protein kinase II α (CaMKIIα) levels in the striatum, resulting in enhanced brain-derived neurotrophic factor (BDNF) expression and increased neuronal maturation and differentiation[97,102,119]. BDNF is a growth factor that affects differentiation, growth, and survival of neurons and activation of the heteromer may have profound effects on neuronal plasticity. It was also shown that, when injected into rats, expression of glutamate decarboxylase-67 and the vesicular glutamate transporters 1 and 2 in striatal neurons was altered by SKF83959[120], which was interpreted to be due to selective D1R-D2R heteromer activation.

In the current study, we further investigate the biology and pharmacology of the proposed D1R-D2R heteromer and the mechanism of Ca^{2+} mobilization in heterologous expression systems. While we find that co-activation of both D1Rs and D2Rs are required for Ca^{2+} mobilization to occur, there appear to be multiple mechanisms through which this pathway is elicited. We also studied the pharmacological characteristics of SKF83959, to determine its putative activity as a heteromer selective ligand, and found that it was significantly less selective than previously proposed. In fact, we were not able to provide evidence for activation of the D1R-D2R heteromer by SKF83959. These results indicate that D1Rs and D2Rs can synergize to induce Ca^{2+} mobilization, although the mechanisms of activation are multiple and complex and there is not, as of yet, a selective pharmacology.

Materials and Methods

Materials – HEK293-tsa201 (HEK293T) cells were a gift from Dr. Vanitha Ramakrishnan. A D1R expressing stable cell line was purchased from Codex Biosolutions, Inc. (Gaithersburg, MD). [^{3}H]-SCH23390 (80.5 Ci/mmol) and [^{3}H]-methyl-spiperone (85.5 Ci/mmol) was obtained from PerkinElmer Life Sciences (Waltham, MA). Cell culture media and reagents were purchased from MediaTech/Cellgro (Manassas, VA). Cell culture flasks and materials and all assay plates were purchased from Greiner Bio-One (Monroe, NC). SKF83959 and SKF83822 were purchased from Tocris Bioscience/RD Systems (Minneapolis, MN). All other compounds and buffer components were purchased from Sigma-Aldrich (St Louis, MO), except where indicated.

Cell Culture and Transfection – HEK293T cells and D1R CODEX cells were maintained in Dulbecco's modified Eagle's medium (DMEM) supplemented with a final concentration of 10% fetal bovine serum, 100 units/ml penicillin, 100 μg/ml streptomycin, 1 mM sodium pyruvate, and 10 μg/ml gentamicin. Cells were incubated at 37°C, 5% CO_2, and 90% humidity. They were passaged and plated mechanically using Ca^{2+}-free Earle's balanced salt solution (EBSS) and pelleted by centrifugation at 1000 rpm for 10 min. For transfection studies, HEK293T cells were seeded in 150 mm plates at 10×10^6 cells per plate. After 24 h, cells were transfected according to the manufacturer's recommendations using Clontech's CalPhos^{TM} transfection kit (Clontech Laboratories, Inc., Mountain View, CA). The DAR plasmid constructs were FLAG-tagged rat D1R, D2SR, or D2LR in the pCD-SRα vector[121–123] and D4R in pcDNA3.1(+) vector[124]. Additional experiments were done using the G_q protein in the pcDNA3.1(+)

vector (Missouri S&T cDNA Resource Center, Rolla, MO) and various functionally dominant negative GRK2 mutants: GRK2 C-terminus 495-689 in pcDNA3(+), GRK2 K220R in pcDNA3(+), and empty pcDNA3.1(+)[125,126]. For all transfections, 5 μg of each DNA construct was used to transfect cells, with the exception of D1R, in which 10 μg was used.

Radioligand Binding Assays – 48 h after transfection, cells were dissociated from plates using Ca^{2+}-free Earle's balanced salt solution (EBSS), and intact cells were collected by centrifugation at 900 × g for 10 min. Cells were resuspended and lysed using 5 mM Tris-HCl and 5 mM $MgCl_2$ at pH 7.4 at 4°C. Cell lysate was pelleted by centrifugation at 20,000 × g for 30 min and resuspended in 5 mM Tris-HCl at pH 7.4. 100 μL cell lysate (containing 8 μg protein for D2R assays or 10 μg protein for D1R assays) was incubated for 90 min at room temperature with various concentrations of [^{3}H]-SCH23390 (D1R binding) or [^{3}H]-methyl-spiperone (D2R binding) in a final reaction volume of 250 μl. Non-specific binding was determined in the presence of 4 μM (+)-butaclamol. Bound ligand was separated from the unbound by filtration through a PerkinElmer Unifilter-96 GF/C 96 well micro-plate using the PerkinElmer Unifilter-96 Harvester, washing 3 times, 1 ml per well in ice-cold assay buffer. After drying, 50 μl of liquid scintillation cocktail (MicroScint PS, Perkin Elmer, Waltham, MA) was added to each well, plates were sealed, and analyzed on a PerkinElmer Topcount NXT^{TM}. For competition binding assays, a fixed concentration of 0.5 nM [^{3}H]-SCH23390 was incubated with various concentrations of SKF83959, and the remainder of the assay was performed as described above. K_i values were calculated from observed IC_{50} values using the Cheng-Prusoff

equation and a K_d value of 0.5 nM for SCH23390, as determined in independent saturation isotherms (data not shown). Expression of the D_4R was determined in an identical assay format as that for the D2R.

Competition Radioligand Binding Screen – A primary, single-point, radioligand competition binding assay was performed to assay for radioligand binding inhibition by SKF83959 (10 μM). Forty-three GPCRs and other drug targets were screened in the primary assay using radioligands with known binding properties. Percent inhibition was calculated by subtracting percent specific binding in the presence of the test compound from the percent specific binding in the absence of the test compound, (N=4). Receptors whose corresponding radioligands had greater than 50% inhibition at 10 μM SKF83959 underwent secondary radioligand competition binding assays to generate full competition curves. K_i determinations and receptor binding profiles were provided by the National Institute of Mental Health (NIMH) Psychoactive Drug Screening Program (PDSP), Contract # HHSN-271-2008-00025-C. The NIMH PDSP is directed by Dr. Bryan L. Roth (University of North Carolina, Chapel Hill, NC) and by Project Officer Jamie Driscol (NIMH, Bethesda, MD). For experimental details including radioligands used and associated K_d values for each individual receptor, please refer to the PDSP website http://pdsp.med.unc.edu/.

Ca^{2+} Mobilization Assays – Assays were performed as previously described. HEK293T cells were transiently transfected as described. 24 h after transfection, cells were plated in 384-well, optical, clear bottom, black walled plates (20 μL/well, 30,000 cells/well;

Greiner Bio-one, Monroe, NC). 48 h following transfection, cells were incubated for 60 min at room temperature in the dark with Fluo-8 NW Ca^{2+} dye and an extracellular signal quencher to block any signal from extracellular Ca^{2+} (Screen Quest™ Fluo-8 NW Calcium Assay Kit, AAT Bioquest, Inc., Sunnyvale, CA), as recommended by the manufacturer. The plates were then treated with various concentrations of antagonist or agonists (diluted in the presence of 0.2 mM sodium metabisulfite) as indicated in the results and figure legends. For agonist reads, plates were read in real time kinetically (every 0.6 sec) by recording a baseline read for 14 sec prior to addition of an agonist compound and then continually measured for 2 min after agonist addition. For antagonist reads, plates were read in real time kinetically (every 0.6 sec) by recording a baseline reading for 20 sec prior to addition of that antagonist. Then, three min later, agonist compound was added and the plates were read for an additional 3 min. All compound additions were done in unison using the 384-tip onboard robotics on an FDSS μCell (Hamamatsu, Bridgewater, NJ), and plates were continuously read using the FDSS μCell from the bottom throughout the assay with an excitation wavelength of 480 nm and an emission wavelength of 540 nm. Data were recorded and quantified as maximum minus minimum (max-min) RFU within the assay window using FDSS software. Data are expressed as a percentage of the control max-min RFU for given studies as indicated in the figure legends. In these experiments, D1R and D2R receptor expression levels typically varied between 1-3 pmol/mg protein. We found that co-expressing both receptors sometimes affected their expression compared to expressing them alone (data not shown). However, this did not affect the Ca^{2+} mobilization response, which, while not studied in detail, appeared to simply require a minimum level of dual receptor expression.

Statistical analysis – Data are expressed as a percentage of control values for individual experiments. Non-linear regression of all data was conducted on GraphPad Prizm 5.01 (GraphPad Software, Inc., La Jolla, CA). Results are expressed as mean ± S.E.M.

Cell Culture and Transfection—HEK293T cells were cultured in Dulbecco's modified essential medium (DMEM) supplemented with 10% fetal bovine serum, 1 mM sodium pyruvate, 50 units/ml penicillin, 50 μg/ml streptomycin, and 10 μg/ml gentamycin. Cells were grown at 37°C in 5% CO_2 and 90% humidity. Untagged rat D1R[122] in pcDNA3 and FLAG-tagged rat D2LR[127] were expressed singly or dually in HEK293T cells. Tag2B in pCMV (Stratagene, La Jolla, CA) was used as a negative control for FLAG-tagged D2LR. HEK293T cells were transfected using the calcium phosphate precipitation method for each experiment as follows: 5 million cells were seeded in 150 mm culture dishes, then transfected 24 h later with 15 μg of DNA of expression construct. After 24 h, the media was exchanged and experiments performed the following day.

Immunoprecipitation and Gel Electrophoresis – Cells were removed from culture dishes and collected by centrifugation (300 × *g*). They were then resuspended in 1 ml of solubilization buffer (50 mM HEPES, 1 mM EDTA, 10% glycerol, 1% Triton X-100, 150 mM NaCl, 50 mM NaF, 40 mM sodium pyrophosphate, and Complete-Mini; Roche Applied Science, Indianapolis, IN) protease inhibitor mixture and incubated on an orbital shaker at 4°C for 1 h. The lysates were transferred to 1.5 ml Axygen tubes and microfuged at 26,000 × g for 40 min. The lysates were pre-cleared using Protein G-agarose beads on an orbital shaker at 4°C for 3 h then microfuged for 5 min at 1000 × g.

Lysates transfected with FLAG-D2LR were transferred to 100 µl of anti-FLAG M2-agarose beads (Sigma-Aldrich, St. Louis, MO) equilibrated in solubilization buffer and rotated on an orbital shaker at 4°C overnight. Lysates of non-transfected cells or cells transfected with non-tagged D1R were removed from the Protein G-agarose pellets and stored at 4°C overnight. The anti-FLAG M2-agarose beads were collected via centrifugation and washed three times by resuspension and recentrifugation in solubilization buffer. The agarose was then subjected to a final wash in 1× TE buffer, pH 7.4 plus protease inhibitors. Proteins were eluted from the beads using 70 µl of NuPAGE-lithium dodecyl sulfate sample buffer (Invitrogen, Carlsbad, CA) at 37°C for 1 h, then microfuged at 2500 × g for 2 min to remove agarose beads and 30 µl of each supernatant was loaded on duplicate gels. 20 µl of lysate from non-transfected cells or cells transfected with untagged D1R was mixed with 40 µl of LDS buffer, mixed, then divided in half and loaded in duplicate gels. Proteins were resolved on duplicate 4–12% BisTris NuPAGE gels in MOPS buffer (Invitrogen, Carlsbad, CA) for 1 h at 195 V, constant voltage.

Western Blotting and Chemiluminescent Development – Proteins separated by PAGE were transferred onto polyvinylidene difluoride membranes for 1 h at 30 V constant voltage. Membranes were blocked in blocking solution (1% BSA, 0.01% Tween 20 in TBS) for 1 h at room temperature prior to incubation with the primary antibody. Primary antibodies used in this study include the following: rat monoclonal anti-D1R (clone 1-1-F11 S.E6, catalog number D-187, Sigma-Aldrich, St. Louis, MO) and rabbit polyclonal anti-D2L/SR (catalog number AB5084P, Chemicon, Temecula, CA). Primary antibody

solutions were diluted 1:10,000 for D1R primary and 1:1000 for D2L/SR primary in blocking solution. Each PVDF membrane was exposed to a single primary antibody solution (D1R or D2LR) overnight at 4°C on orbital shaker. Primary antibody solutions were removed and each membrane was washed three times, 5 min each in TBST. 1:10,000 dilutions in blocking solution were prepared for each HRP-conjugated secondary antibody (Jackson ImmunoResearch, West Grove, PA; anti-rat for the D1R and anti-rabbit for the D2LR). Membranes were incubated in appropriate secondary antibody solution for 1 h at room temperature on an orbital shaker. Membranes were washed three times, 5 min each in TBST. Proteins were visualized via the SuperSignal West Pico Chemiluminescent Substrate Kit or the SuperSignal West Dura Chemiluminescent Substrate (Pierce, Rockford, IL) according to the manufacturer's instructions, and images were recorded on film.

Results

Previous studies have suggested that the D1R-D2R receptor complex may signal as a heteromer and have implicated SKF83959 as a compound that may selectively activate this signaling complex[48,100,102,103]. However, these findings have not been corroborated and the mechanisms by which the D1R-D2R receptor complex signals remain unclear. To investigate the apparent ability of D1R-D2R receptor oligomerization to alter the G protein coupling of component receptors, we first transiently expressed the D1R either alone or concurrently with either the short (D2S) or long (D2L) isoforms of the D2R and measured intracellular Ca^{2+} mobilization via kinetic fluorescence imaging. Preliminary co-immunoprecipitation experiments revealed that D1R-D2R hetero-oligomers were indeed capable of forming under these expression conditions (Figure 8).

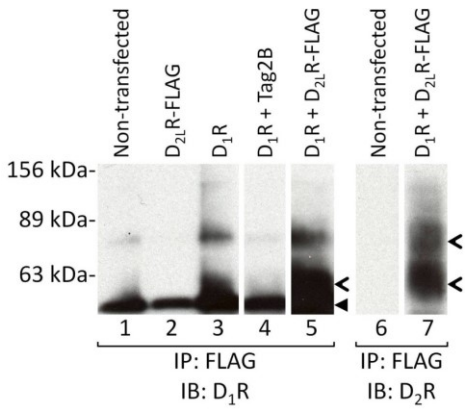

Figure 8: Co-immunoprecipitation of the D1R and D2LR.
Small arrows indicate the location of the D2LR in lane 7 and the D1R in lanes 3 and 5. The filled arrow indicates a non-specific background band as it is observed in non-transfected cells. HEK293T cells were transfected with either the FLAG-tagged D2LR, the non-tagged D1R, the D1R with a vector that expressed only the FLAG peptide (Tag2B), or the D1R with the FLAG-tagged D2LR, as indicated on the blots. Proteins were extracted and lysates were either electrophoresed or immunoprecipitated (IP) using anti-FLAG agarose beads, and immunoblotted (IB). IBs were probed using either a D2L/SR primary antibody or a D1R primary antibody. Lanes 1, 3, and 6 were loaded with whole cell lysate, while the remaining lanes underwent IP prior to being loaded on the gel. In this experiment, the D2R is IPed using an anti-FLAG antibody and appears in lane 7 as multiple glycosylated protein bands. The D1R appears as a single glycosylated protein band of ~60 kDa that is co-IPed with the D2R, as shown in lane 5. In contrast, the D1R does not co-IP with a peptide containing just the FLAG sequence (Tag2B), as shown in lane 4.

When cells were transfected with the D1R and D2LR or the D1R with D2SR, a clear dose-dependent activation of Ca^{2+} mobilization was observed in response to DA (Figure 9). Importantly, we observed no difference in coupling efficacy or agonist potency between the short and long isoforms of the D2R. However, when cells were transfected with any of the subtypes alone, the receptors failed to couple to Ca^{2+} mobilization (Figure 9). These data suggest that expression and activation of both the D1R and D2R are essential for coupling to Ca^{2+} mobilization and signaling.

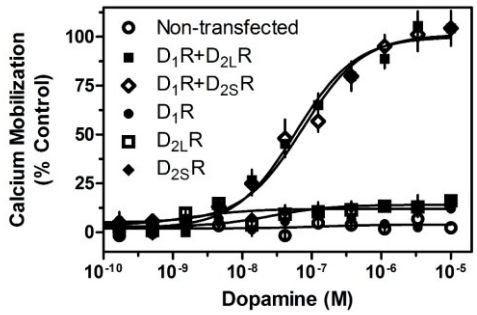

Figure 9: Agonist-induced Ca^{2+} mobilization in DA receptor transfected cells.
HEK293T cells were transiently transfected with D1R, D2LR, D2SR, D1R+D2LR, or D1R+D2SR as indicated and described in the methods. 24 h later, cells were plated in 384-well plates and assayed the following day for Ca^{2+} mobilization following stimulation by DA (D1R+D2LR EC_{50}=73.8 nM, D1R+D2SR EC_{50}=58.2 nM). Data are representative of three independent experiments done with the same assay conditions on different days. Data are expressed as percentage of control, normalized to the maximum signal seen via DA stimulation of D1R+D2LR transfected cells. Error bars indicate S.E.M. from multiple wells within the representative experiment.

To further investigate that the activation of both receptor subtypes is required to stimulate Ca^{2+} mobilization, we utilized receptor subtype selective antagonists. Concentration response inhibition curves for the D1R- selective (SCH23390) and the D2R selective (sulpiride) antagonists were generated for cells transfected with the D1R and D2R (Figure 10). Cells were simultaneously stimulated with 1 μM DA and examined for Ca^{2+} mobilization. We observed complete inhibition of the Ca^{2+} signal with *either* SCH23390 or sulpiride treatment. The potencies of the antagonists (SCH23390 IC_{50} ~8.0

nM, sulpiride IC_{50} ~0.7 nM) are consistent with their known affinities for their selective subtypes as determined in the Sibley laboratory (data not shown) as well as other groups[128,129]. More importantly, complete inhibition of the Ca^{2+} response is seen at antagonist concentrations that have no effect on the opposite receptor subtype. Thus, selectively blocking DA activation of either receptor subtype is sufficient to prevent Ca^{2+} mobilization further suggesting that both receptor protomers must be activated for this signaling to occur.

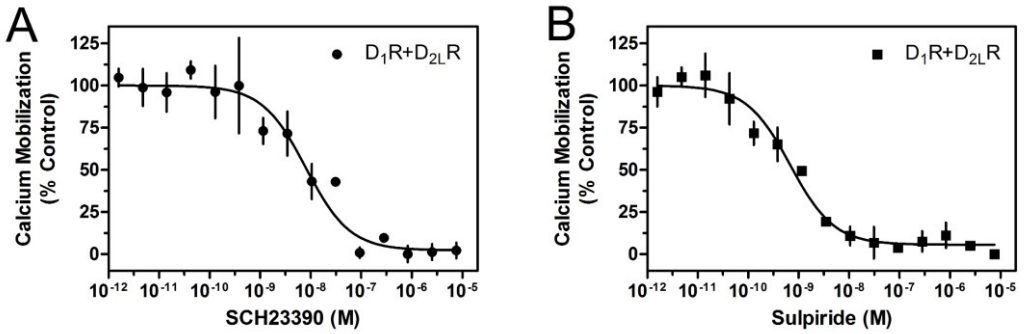

Figure 10: Inhibition of D1R+D2LR-mediated Ca^{2+} mobilization by either D1R- or D2R selective antagonists.
HEK293T cells were transfected with D1R+D2LR as described and 24 h later were plated in 384-well plates. Cells were incubated with the indicated concentrations of the D1R selective antagonist SCH23390 (**A**) or the D2R selective antagonist sulpiride (**B**), and then stimulated with an EC_{80} of DA (1 μM; SCH23390 IC_{50}=8.0 nM, sulpiride IC_{50}=0.7 nM). Data are expressed as a percentage of the control (10 μM) DA response and are representative of two independent experiments performed with the same assay conditions on different days. Error bars indicate S.E.M. from multiple wells within the representative experiment.

While the studies employing subtype selective antagonists suggested that both D1R and D2R are required for Ca^{2+} signaling, it might be possible that stabilizing one subtype into an inactive state within a heteromer might alter the conformation of the corresponding partner. Thus, to further elucidate the coupling mechanism, subtype selective agonists were used to determine if indeed activation of both protomers are required for Ca^{2+} mobilization. As seen in Figure 11, concurrent administration of a D1R selective (SKF83822) and a D2R selective (quinpirole) agonist to cells co-transfected

with D1R and D2R resulted in a Ca^{2+} mobilization response that nearly matched that of DA. In contrast, when D1R plus D2R co-transfected cells were stimulated with quinpirole alone, no Ca^{2+} mobilization was observed. Furthermore, when the co-transfected cells were stimulated with SKF83822, no Ca^{2+} mobilization was seen at concentrations selective for D1R. A small response was observed at 10 μM, but this was at a concentration where SKF83822 loses receptor subtype selectivity and can begin to stimulate the D2R as well. Previous studies showed that SKF83822 has an affinity for D1R in the ~2 nM range and D2R in the ~200 nM range[130]. Experiments done in our lab have demonstrated a D2R affinity that is greater than 10 μM (data not shown), supporting the idea that the SKF83822-mediated Ca^{2+} response seen at high concentrations is due to non-selective receptor activation. In addition, when cells were transfected with any of the subtypes individually, no signal was seen from any of the agonists (data not shown). Taken together, these data indicate that stimulation of both receptor subtypes is necessary for Ca^{2+} mobilization.

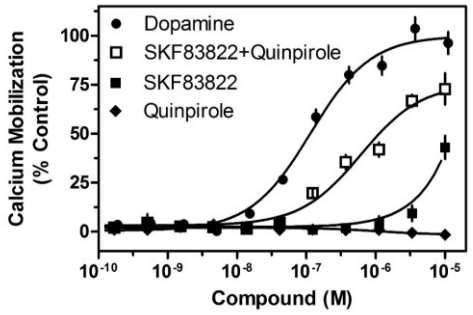

Figure 11: Stimulation of D1R+D2LR-mediated Ca^{2+} mobilization by either D1R- or D2R selective agonists.
HEK293T cells were transfected with D1R+D2LR as described, plated 24 h later in 384-well plates, and assayed for Ca^{2+} accumulation the following day. Cells were stimulated with one of the following agonists as indicated: DA, the D1R selective agonist SKF83822, the D2R selective agonist quinpirole, or both SKF83822 and quinpirole (D1R+D2LR EC_{50}=610.8 nM) combined. Control cells expressing the D1R, D2SR, or D2LR individually did not show a significant Ca^{2+} response to concurrent agonist administration. Data are expressed as a percentage of control maximum DA stimulated response and are representative of two independent experiments performed with the same assay conditions on different days. Error bars indicate S.E.M. from multiple wells within the representative experiment.

Previous studies suggested that SKF83959 may be a D1R-D2R heteromer selective compound and a significant Ca^{2+} response to this ligand has been reported in cells co-expressing the D1R and D2R[27,48,102,103]. This compound has also been reported to have seemingly paradoxical effects on the D1R, exhibiting both antagonist and agonist properties depending on the system[30,104,131]. In our current studies, we treated D1R and D2R co-transfected cells with SKF83959 and, surprisingly, were unable to elicit a Ca^{2+} response (Figure 12A). Furthermore, when SKF83959 was added in concert with the D2R selective agonist quinpirole, we were still unable to observe a significant Ca^{2+} response. It should be noted that SKF83959 consistently failed to stimulate Ca^{2+} mobilization even when this experiment was performed using different lots of compound from different vendors on separate days, as well as with different drug solvents (data not shown). We also had one lot of compound chemically analyzed to verify its purity (data not shown).

To demonstrate that the SKF83959 compound was pharmacologically active in our hands, we performed two separate experiments. In Figure 12B, we stimulated Ca^{2+} mobilization with DA and then dose-dependently added either the D1R selective antagonist SCH23390 as a control (see Figure 10A) or SKF83959 to see if it might function as an antagonist in this system. In fact it did, exhibiting even higher potency than SCH23390, although its efficacy of antagonism was less, exhibiting a maximum inhibition of ~50%.

Finally, we performed a radioligand binding competition assay with SKF83959 and cells transfected with the D1R (Figure 12C). SKF83959 was able to potently and

fully compete for radioligand binding to the D1R. These experiments (Figure 12B, C) demonstrate that SKF83959 is active in binding to the homomeric D1R as well as active as a partial antagonist of the Ca^{2+} response observed in D1R and D2R co-transfected cells. In contrast, it does not appear to function as an agonist with respect to stimulating Ca^{2+} mobilization in the D1R and D2R co-transfected cells.

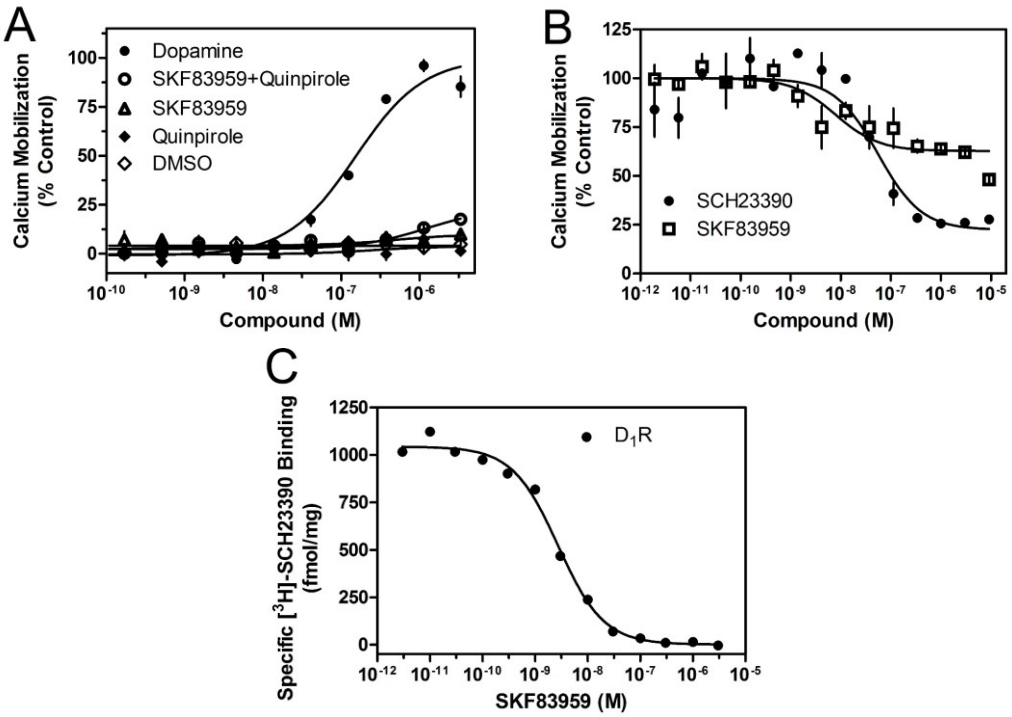

Figure 12: Pharmacological characterization of SKF83959 on D1R+D2LR-mediated Ca^{2+} mobilization.

HEK293T cells were transfected with D1R+D2LR as described, plated 24 h later in 384-well plates, and assayed for Ca^{2+} accumulation the following day. **A**: Cells were stimulated with one of the following conditions as indicated: DA, SKF83959, the D2R selective agonist quinpirole, or both SKF83959 and quinpirole combined. **B**: Cells were incubated with SKF83959 or the D1R selective antagonist SCH23390, then stimulated with an EC_{80} of DA (1 μM). Data are expressed as a percentage of control maximum DA-stimulated response and are representative of 2-3 independent experiments performed with the same assay conditions on different days. Error bars indicate S.E.M. from multiple wells within the representative experiment. **C**: HEK293 cells stably transfected with D1R (Codex Biosolutions, Inc., Gaithersburg, MD) were grown and membranes harvested according to the materials and methods. Membranes were incubated with various concentrations of SKF83959 and 0.5 nM [^{3}H]-SCH23390 as indicated. Graph is representative of two independent experiments done on different days. Data are expressed as specific binding in units of fmol/mg. K_i value was calculated using the Cheng-Prushoff equation and a radioligand K_d value of 0.5 nM as determined via saturation binding isotherms (data not shown). Average K_i for SKF83959 on D1R was 2.6 nM ± 0.7.

Given the apparent discrepancies of our findings with some previous studies[48,103,132], and the possibility that SKF83959 may not be as selective as previously thought, we sought to screen its selectivity against various GPCRs. This was accomplished through collaboration with the NIMH Psychoactive Drug-Screening Program (http://pdsp.med.unc.edu). For the primary screen, a single-point radioligand binding competition experiment was performed with 10 μM SKF83959 as a competitor against an appropriate receptor-specific radioligand of known properties. Forty-three GPCRs and signaling proteins were screened this way and twenty of them exhibited >50% inhibition at 10 μM SKF83959 (Table 1). In contrast, twenty-three GPCR targets were found to have <50% inhibition at 10 μM SKF83959 and were therefore considered relatively "inactive/low affinity" for SKF83959 (Table 2).

The twenty "active" receptors/proteins underwent secondary radioligand competition binding experiments to generate full competition curves for SKF83959 and K_i values for these receptors were determined and shown in Table 1. Of note is that the serotonin 5-HT2A, 5-HT2B, 5-HT2C, 5-HT5A and 5-HT6 receptors, the adrenergic α2A, α2B and α2C receptors, the D1, D2, and D5 receptors, and the serotonin transporter all have sub-micromolar K_i values. SKF83959 demonstrated very high (<100 nM) affinity for four of these GPCRs: the serotonergic receptor subtypes 5-HT2C, the adrenergic receptor subtype α2C, the D1, and D5 receptor subtypes, and the serotonin transporter. Notably, SKF83959 has also recently been shown to be a potent allosteric modulator of the sigma-1 receptor[133]. Taken together, these data indicate that SKF83959 has significantly high affinity for a wide number of receptors and thus caution should be taken when interpreting *in vivo* experimentation and the selectivity of this agent.

Table 1: SKF83959 competition binding experiments against various GPCRs.

Target	SKF83959 K_i (nM)	S.E.M.
5-HT1A	1648.0	352.3
5-HT2A	246.6	32.1
5-HT2B	405.0	145.1
5-HT2C	32.8	13.3
5-HT5A	277.8	141.8
5-HT6	546.0	56.0
α1A	1290.5	154.5
α1D	1115.5	232.4
α2A	323.7	120.6
α2B	163.1	17.8
α2C	31.1	7.6
D1R	1.7	0.8
D2R	567.0	150.0
D3R	1018.3	109.8
D4R	1975.7	756.4
D5R	4.0	0.1
H2	1699.3	640.3
M4	5238.5	1985.5
M5	3484.0	114.0
SERT	365.6	79.2

K_i values were derived from radioligand binding competition curves generated against each of the above targets (n=2) as described in the Materials and Methods section. Abbreviations: 5-HT1A (serotonergic receptor subtype 1A), 5-HT2A (serotonergic receptor subtype 2), 5-HT2B (serotonergic receptor subtype 2B), 5-HT2C (serotonergic receptor subtype 2C), 5-HT5A (serotonergic receptor subtype 5A), 5-HT6 (serotonergic receptor subtype 6), α1A (α-adrenergic receptor subtype 1A), α1D (α-adrenergic receptor subtype 1D), α2A (α-adrenergic receptor subtype 2A), α2B (α-adrenergic receptor subtype 2B), α2C (α-adrenergic receptor subtype 2C), M4 (muscarinic receptor subtype 4), M5 (muscarinic receptor subtype 5), SERT (serotonin transporter).

Table 2: List of various GPCR targets with low / no affinity for SKF93959.

5-HT1B	β2	H1	M3
5-HT1D	β3	H3	MOR
5-HT1E	BZP Rat brain	H4	NET
5-HT3	DAT	KOR	σ1
α1B	DOR	M1	σ2
β1	GABAA	M2	

Receptors showed less than 50% inhibition of binding by 10 μM SKF83959, and therefore were classified as having low to no affinity for the compound. The percent inhibition was calculated by subtracting % radioactivity bound to filter from 100% radioligand (n=4). The NIMH Psychoactive Drug Screening Program, as referenced in Table 1, generously provided the binding profiles. Abbreviations: 5-HT1B (serotonergic receptor subtype 1B), 5-HT1D (serotonergic receptor subtype 1D), 5-HT1E (serotonergic receptor subtype 1E), 5-HT3 (serotonergic receptor subtype 3), α1B (α-adrenergic receptor subtype 1B), β1 (β-adrenergic receptor subtype 1), β2 (β-adrenergic receptor subtype 2), β3 (β-adrenergic receptor subtype 3), BZP Rat Brain Site (allosteric benzodiazepine binding site on $GABA_A$ receptor), DAT (dopamine transporter), DOR (δ-opioid receptor), $GABA_A$ (ionotropic GABA receptor), H1 (histamine receptor subtype 1), H3 (histamine receptor subtype 3), H4 (histamine receptor subtype 4), KOR (κ-opioid receptor), M1 (muscarinic receptor subtype 1), M2 (muscarinic receptor subtype 2), M3 (muscarinic receptor subtype 3), MOR (μ-opioid receptor), NET (norepinephrine transporter), σ1 (sigma receptor subtype 1), σ2 (sigma receptor subtype 2).

While D1 and D2 receptors appear capable of signaling through Ca^{2+} mobilization when both receptors are stimulated, the mechanism of transduction remains unclear. To better understand the mechanisms involved, we tested the hypothesis that the receptors, perhaps within the context of a heteromer, may switch G protein-coupling selectivity and gain the ability to activate G_q. We first examined this possibility by over-expressing $G\alpha_q$ in cells expressing the D1R+D2R. Interestingly, the resulting DA-stimulated Ca^{2+} signal was increased by 200% when compared to cells transfected with the D1R+D2R alone (Figure 13A). Expression of only the $G\alpha_q$ protein in the absence of either receptor did not enable the ability of DA to stimulate Ca^{2+} mobilization (Figure 13A). In parallel studies, we examined how over-expression of $G\alpha_q$ with the D1R or D2R alone could couple to intracellular Ca^{2+} mobilization. While cells transfected with D1R or D2R alone did not give a Ca^{2+} response, consistent with Figure 9, when $G\alpha_q$ was over-expressed, the D1R was able to elicit a DA-stimulated Ca^{2+} signal in the absence of the D2R (Figure 13B), although the Ca^{2+} response was not as large as that seen with the D1R+D2R+$G\alpha_q$ transfection (cf. Figure 13A and B). No such phenomenon was observed with the D2R. Taken together, these data suggest that the G_q protein may be involved in Ca^{2+} mobilization mediated by a D1R-D2R heteromer, however, this interpretation is complicated by the fact that over-expression of $G\alpha_q$ can also lead to homomeric D1R coupling.

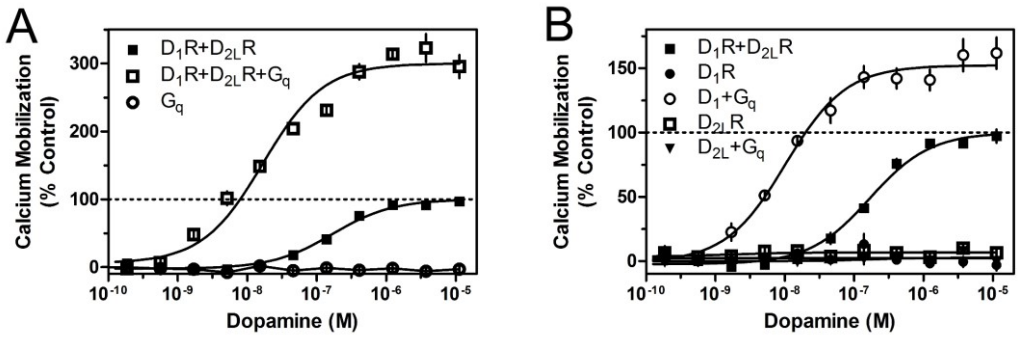

Figure 13: Influence of $G\alpha_q$ protein over-expression on D1R+D2LR-mediated Ca^{2+} mobilization. **A**: HEK293T cells were transfected with D1R+D2LR with and without $G\alpha_q$, or with $G\alpha_q$ alone (D1R+D2R EC_{50}=168.3 nM, EC_{max}=100%; D1R+D2R+G_q EC_{50}=16.8 nM, EC_{max}=300.1%). **B**: HEK293T cells were transfected with D1R+D2LR, D1R, or D2R with and without $G\alpha_q$ (D1R+G_q EC_{50}=10.3 nM, EC_{max}=152.2%). 24 h later cells were plated in 384-well plates and assayed the following day for Ca^{2+} mobilization following stimulation by the indicated concentrations of DA. Data are expressed as a percentage of control maximum DA stimulation for D1R+D2LR alone and are representative of 2-3 independent experiments performed with the same assay conditions on different days. Error bars indicate S.E.M. from multiple wells within the representative experiment.

Given our results with $G\alpha_q$ over-expression, we re-evaluated SKF83959-stimulation of Ca^{2+} mobilization under these conditions in the D1R and D2R co-expressed cells. We found that with $G\alpha_q$ over-expression, SKF83959 is able to stimulate Ca^{2+} mobilization in a manner similar to that of DA (Figure 14A), whereas it is unable to stimulate such a response in cells lacking $G\alpha_q$ over-expression (Figure 12 and Figure 14A). Interestingly, SKF83959 was also able to stimulate Ca^{2+} mobilization in cells expressing the D1R and over-expressing $G\alpha_q$, but not D1R alone (Figure 14A). These results led us to test the antagonist sensitivity of the SKF83959 responses as shown in Figure 14B. We found that the D1R selective antagonist, SCH23390, could completely ablate SKF83959 stimulation of Ca^{2+} mobilization in both D1R+$G_{q\alpha}$ transfected as and D1R+D2R+$G\alpha_q$ transfected cells. However, in contrast to what we observed for DA stimulation of D1R+D2R co-transfected cells, the D2R selective antagonist, sulpiride, was unable to block SKF83959 stimulation of Ca^{2+} mobilization. These results suggest that over-expression of $G\alpha_q$ enables SKF83959 to stimulate homomeric D1R present in

the D1R and D2R co-transfected cells, rather than enabling it to gain function as a D1R-D2R heteromeric selective agonist.

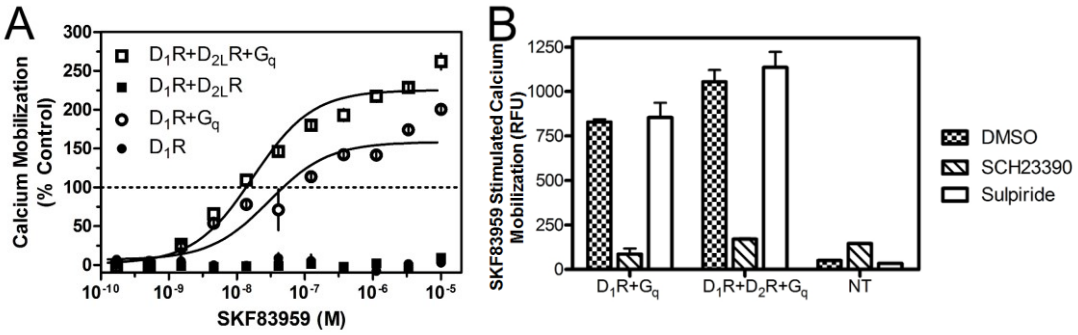

Figure 14: SKF83959 stimulates D1R-dependent Ca^{2+} mobilization in the presence of $G\alpha_q$. HEK293T cells were transfected with D1R or D1R+D2LR, with or without $G\alpha_q$, plated 24 h later in 384-well plates, and assayed for Ca^{2+} accumulation the following day. **A**: Cells were stimulated with SKF83959. The line at 100% denotes the maximal DA response of D1R+D2LR cells. **B**: Cells were incubated with the D1R selective antagonist SCH23390 (1 μM) or the D2R selective antagonist sulpiride (1 μM), and then stimulated with an EC_{80} of SKF83959 (100 nM). Error bars indicate S.E.M. from multiple wells within the representative experiment, which was replicated twice.

While the extant hypothesis, which our over-expression data support, is that G_q is central to the stimulation of Ca^{2+} mobilization, the central question is if direct coupling with a D1R-D2R heteromer may be involved. An alternative hypothesis is that the D1R and D2R signal through downstream pathways that converge on the G_q protein and/or other components of the Ca^{2+} mobilization process. In order to test whether D1R-D2R synergistic signaling is independent of G_i or G_s protein function, we interfered with the activity of G_i and G_s via treatment with toxins. D1R and D2R co-transfected cells were incubated overnight in media containing pertussis toxin (PTX) to inhibit G_i protein function[67] or cholera toxin (CTX) to interfere with G_s protein function[134]. Cells were then assayed for Ca^{2+} mobilization in response to DA stimulation. We found that treatment with either CTX or PTX drastically, but not entirely, reduced the Ca^{2+} response (Figure 15). These data support the involvement of D1R-G_s- and D2R-G_i-mediated mechanisms that majorly contribute to the Ca^{2+} response in the D1R and D2R co-transfected cells.

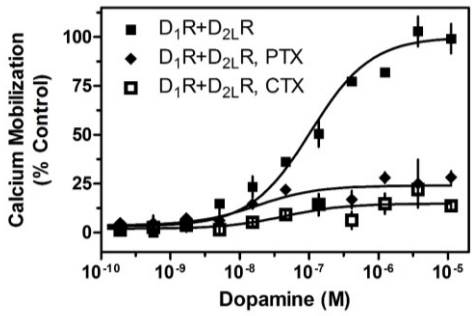

Figure 15: G protein dependency of D1R+D2LR-mediated Ca^{2+} mobilization.
HEK293T cells were transfected with D1R+D2LR. Cells were incubated overnight in 1 μg/ml pertussis toxin (PTX) or 1 μg/ml cholera toxin (CTX). 48 h post-transfection, cells were assayed for Ca^{2+} mobilization via stimulation with the indicated concentrations of DA (CTX EC_{max}=14%, inhibition=86% control, PTX EC_{max}=24%, inhibition=76% control). Data are expressed as a percentage of control maximum DA stimulation seen in untreated D1R+D2LR cells, and are representative of 2-3 independent experiments performed with the same assay conditions on different days. Error bars indicate S.E.M. from multiple wells within the representative experiment.

Another possibility, however, may be that general G_i-G_q "crosstalk" is occurring after receptor activation, which leads to PLC activation. Multiple cases of G_i-G_q cross-talk in other receptor systems and cell types have been documented[135–138], and G_i-G_q cross-talk in the D1R-D2R receptor system could account for the PTX sensitivity of the Ca^{2+} signal. In this model, any G_i-linked GPCR, not just the D2R would be able to support a G_q-mediated Ca^{2+} response. In order to test this possibility, we used the D4R, a G_i-linked DAR, which has not been found to form hetero-oligomers with the D1R[139]. We co-transfected the D1R and D4R and compared the DA response to that in the D1R+D2R transfected cells (Figure 16). In fact, the D4R was shown not to support a Ca^{2+} response in the presence of co-expressed D1R, indicating that non-specific G_i-G_q crosstalk, at least as previously described[135–138] does not explain the D1R-D2R heteromer-mediated Ca^{2+} response.

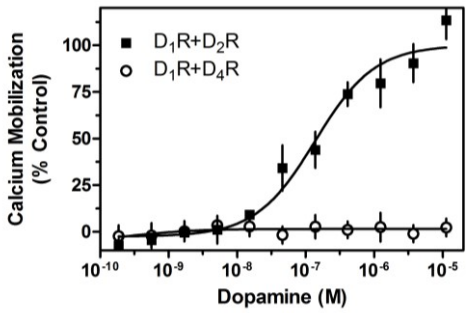

Figure 16: Dopamine does not elicit a Ca^{2+} response in cells co-expressing the D1R and D4R. HEK293T cells were transiently transfected with D1R+D2LR or D1R+D4R. 24 h later cells were plated in 384-well plates and assayed for Ca^{2+} mobilization through stimulation by the indicated concentrations of DA. Data are expressed as a percentage of control maximum DA stimulation seen in cells transfected with D1R+D2LR only (EC_{50} = 162.0 nM), and are representative of 2-3 independent experiments done with the same assay conditions on different days. Expression of the D4R was confirmed using radioligand binding assays as described in the Materials and Methods and was similar to that of the D2R. Error bars indicate S.E.M. from multiple wells within the representative experiment.

The potential involvement of multiple G_α-proteins led us to also investigate other mechanisms by which D1R and D2R activation could stimulate Ca^{2+} mobilization. Notably, $G_{\beta\gamma}$ subunits have been shown to increase cytoplasmic Ca^{2+} concentrations by stimulating PLCβ[27]. A recent publication found that the ghrelin receptor-D2R heteromer-linked Ca^{2+} response was PTX sensitive, required PLC activity, and could be ablated by sequestering the $G_{\beta\gamma}$ subunits[140]. To see if $G_{\beta\gamma}$ plays a role in the D1R-D2R heteromer-mediated Ca^{2+} release, we co-transfected the D1R and D2R with two different functionally dominant negative G protein-coupled receptor kinase 2 (GRK2) mutants. The mutants we used were GRK2 K220R and the GRK2 C-terminal 495-689 peptide fragment (GRK2 c-term), both of which are unable to phosphorylate GPCRs, but can bind to, and sequester $G_{\beta\gamma}$ subunits[125,126]. We found that over-expression of GRK2 K220R was able to completely ablate DA-stimulated Ca^{2+} mobilization in the D1R and D2R co-transfected cells (Figure 17A). Similarly, over-expression of GRK2 c-term drastically reduced, but did not completely ablate, the DA-stimulated Ca^{2+} response

(Figure 15B). These data suggest that the observed Ca^{2+} mobilization occurring in response to D1R and D2R activation is largely dependent on free $G_{\beta\gamma}$ subunits.

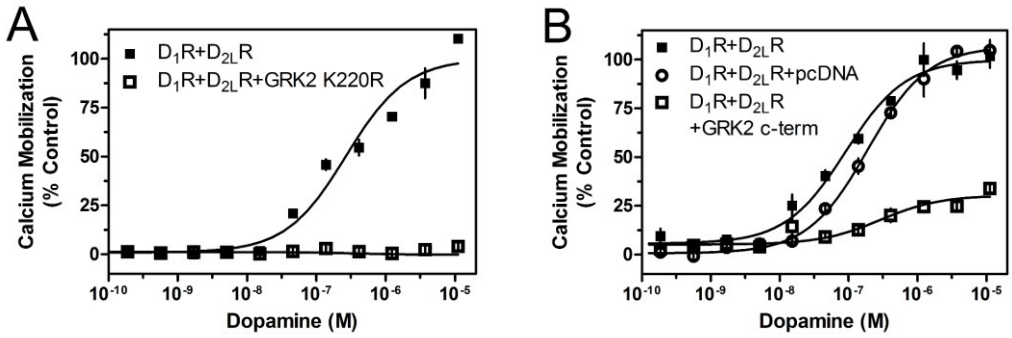

Figure 17: GRK2 influence on DA-mediated D1R+D2LR Ca^{2+} mobilization.
HEK293T cells were transiently transfected with D1R+D2LR, and either empty pcDNA vector the GRK2 catalytically inactive mutant (**A**) GRK2 K220R (D1R+D2R EC_{50}=269.1 nM), or the (**B**) GRK2 C-terminal 495-689 fragment (D1R+D2R EC_{50}=90.4 nM, E_{max}=100% control; D1R+D2R+pcDNA EC_{50}=188.5 nM, EC_{max}=106%; D1R+D2R+GRK2 c-term EC_{50}=288.1 nM, EC_{max}=30% control, 70% inhibition), as indicated and described in the methods. 24 h later cells were plated in 384-well plates and assayed following day for Ca^{2+} mobilization following stimulation by the indicated concentrations of DA. Data are expressed as a percentage of control maximum DA stimulation seen in cells transfected with D1R+D2LR only, and are representative of 2-3 independent experiments done with the same assay conditions on different days. Error bars indicate S.E.M. from multiple wells within the representative experiment.

Discussion

Receptor oligomers of many different GPCR types have been proposed to form homo- or hetero-oligomers with biochemical and functional characteristics that are unique to their oligomeric conformations[108]. These GPCR oligomers have been found not only to occur within a type of GPCR, but also across different classes, families, types, and subtypes[111]. In addition to signaling, internalization and degradation of GPCRs in homo- and hetero-oligomers has been found to differ from their homomeric activities[108,111,113–115]. Like previously described receptor oligomers, it has been shown that the D1R and D2R can co-IP with each other[31,48] (Figure 8), and fluorescence imaging has shown that the two receptors co-internalize when one or the other receptor is stimulated[100,101,141–143]. We have demonstrated that the Ca^{2+} response is unique to cells that co-express both D1 and D2 DARs and that the DARs must be co-stimulated, as an antagonist to either receptor blocks the transduction. However, the mechanism of action and whether heteromers versus homomers form the functional units for Ca^{2+}signaling remains unclear.

It has been suggested that the co-activation of the D1R-D2R complex causes a conformational change that results in the direct interaction between the C-terminus of the D1R and the third intracellular loop (ICL3) of the D2R[141]. The ICL3 is the only region of difference between D2LR and D2SR, and there is evidence that it results in differences in the G protein coupling and signaling capabilities of each D2R isoform[107]. Recently, it was proposed that the ICL3 of D2LR, but not the D2SR, could form a complex with the D1R[31], but the findings were based on the use of GST and TAT-fused D2R ICL3 fragments, which may not accurately mimic native receptor conformations and interactions. Later, it was shown that both D2R splice isoforms were able to co-

internalize with the D1R[141]. Our results show that both D2SR and D2LR can couple with the D1R to mobilize Ca^{2+} (Figure 9), and we have found that this is also true for both human (data not shown) and rat DARs. We have also confirmed that both receptors must be expressed in the same cell and co-activated to induce a Ca^{2+} response in HEK293T cells.

Our data also suggest that G_q protein signaling may play a role in the Ca^{2+} response elicited by the D1R-D2R complex. This was demonstrated by observing increased Ca^{2+} mobilization in response to DA in cells transfected with the D1R and D2R plus $G\alpha_q$. However, we also observed that the D1R alone may couple to $G\alpha_q$ when the alpha subunit is expressed in significantly high amounts. This is likely due to the D1R having a relatively low affinity for $G\alpha_q$, however, it may activate G_q-mediated Ca^{2+} mobilization under conditions where G_q expression is very high. This is also supported by the enhanced Ca^{2+} response we observe when the D1R and D2R are co-expressed in the presence of high levels of G_q protein, where the D1R is the protomer within the heteromer that likely activates $G\alpha_q$[103]. In this model, it is hypothesized that the D2R allosterically modulates the D1R[103,132]. We believe, however, that the enhanced Ca^{2+} mobilization seen in the D1R+D2R+$G\alpha_q$ transfected cells is not solely due to D1R homomer activation of G_q, as the degree of Ca^{2+} mobilization (300% of control, Figure 13A) is twice that seen in the D1R-$G\alpha_q$ transfected cells (Figure 13B). Interestingly, another study has also reported D1R-mediated Ca^{2+} release from internal stores in mouse Ltk- cells transfected with the human D1R[144], indicating that this is not an event particular to our experimental paradigm. Thus, while G_q may play a role in the apparent ability of the D1R-D2R heteromer to couple to Ca^{2+} signaling, this may be dependent on

the level of G_q protein expression, either on a total cellular basis, which would thus be cell-type dependent, or this signaling may be localized to specific membrane microdomains (see below).

It has also been suggested that SKF83959 may act as a D1R-D2R heteromer selective agonist, and it has been used as a putative heteromer selective probe *in vivo*. However, these studies are not without controversy as SKF83959 has a history of unusual pharmacology. Undie et al. found that SKF83959 inhibited D1R-stimulated cAMP formation and also induced striatal intracellular Ca^{2+} mobilization in rats and monkeys[104]. It lacked the side effects typical to D1R agonists that stimulate cAMP production but paradoxically seemed to cause typical D1R agonist-like behaviors in rats[29], and is an effective anti-parkinsonian agent in MPTP-lesioned monkeys unresponsive to L-DOPA[106]. In our hands SKF83959 did not stimulate a Ca^{2+} response in cells transfected with both the D1R and D2R, despite the fact that it was active in binding to the D1R. In fact, it appeared to act as an antagonist of the DA-stimulated Ca^{2+} response in D1R and D2R co-transfected cells. In contrast, when $G\alpha_q$ was over-expressed, SKF83959 stimulated a Ca^{2+} response in cells co-transfected with the D1R and $G\alpha_q$ as well as cells co-transfected with the D1R, D2R and $G\alpha_q$. However, we observed that while the D1R selective antagonist, SCH23390, completely blocked the SKF83959-stimulated Ca^{2+} response in both transfection conditions, the D2R selective antagonist, sulpiride, was ineffective in the D1R and D2R co-transfection condition. This contrasts with sulpiride's ability to completely block DA-stimulated Ca^{2+} mobilization in the D1R and D2R co-transfected cells (cf. Figure 10B and Figure 14B). This suggests that SKF83959 is not activating the D1R-D2R heteromer, but rather is activating only D1R homomers that

exist in the D1R and D2R co-transfected cells. This could be explained by the functionally selective, or biased agonism, properties of SKF83959 in that it can selectively activate D1R-G_q signaling, provided that there is sufficient $G\alpha_q$ present, but our current results do not support its ability to activate the D1R-D2R heteromer.

It has also been proposed that D1R-D2R heteromer activation via SKF83959 *in vivo* and *in vitro* results in increased Ca^{2+}/CaMKIIα levels in the striatum, further resulting in enhanced brain-derived neurotrophic factor expression and increased neuronal maturation and differentiation[97,102,119,120]. Given that our experiments indicated that SKF83959 could not induce D1R-D2R heteromer selective Ca^{2+} mobilization in a controlled cell environment, we conducted a single-point competition-binding screen against an array of forty-three GPCRs and additional signaling proteins (Table 1 and Table 2). We observed that SKF83959 demonstrated considerably high affinity for multiple receptors and other signaling proteins, and we conducted secondary competition binding experiments on the ones for which it showed the highest affinity. Surprisingly, SKF83959 showed nanomolar affinities for many different GPCRs including several serotonergic, adrenergic, dopaminergic, and muscarinic receptor subtypes (Table 1). Interestingly, it has been reported that the SKF83959-induced locomotor and grooming responses stimulated in wild-type mice were inhibited in D1R knock-out mice. The grooming and locomotor responses were not inhibited in D2R knock-out, $G\alpha_q$ knock-out, or catalytically inactive CaMKIIα knock-in mice[78]. This, as well as our functional data, questions whether or not SKF83959 may be useful as a selective probe to study D1R-D2R heteromer, or even D1-like receptor signaling *in vivo*.

Our data also suggested that Ca^{2+} signaling through the D1R-D2R receptor complex is largely sensitive to G_i and G_s inhibition by PTX and CTX, respectively. This led us to investigate additional hypotheses for the mechanism of D1R-D2R Ca^{2+} signaling. Recently, Kern et al. (2012) showed that the ghrelin receptor could hetero-oligomerize with the D2R. This heteromer induced Ca^{2+} release from internal cellular stores in a PLC dependent and PTX-sensitive manner, and seemed to require $G_{\beta\gamma}$ subunit activation. Previous studies have shown that GRK2 can bind to and sequester $G_{\beta\gamma}$ subunits[125] and catalytically inactive GRK2 mutants that retain $G_{\beta\gamma}$ binding have been used as tools to block $G_{\beta\gamma}$ signaling without the complication of added receptor desensitization[125,126]. Our data demonstrated that the catalytically inactive GRK2 K220R mutant completely ablated the DA-stimulated Ca^{2+} response in the D1R and D2R transfected cells while GRK2 c-term (a truncated GRK2 protein that only includes the $G_{\beta\gamma}$ binding domain) largely decreased the Ca^{2+} response. Since activated $G_{\beta\gamma}$ subunits can stimulate PLCβ activity[145], our results are consistent with the hypothesis that the DA-stimulated Ca^{2+} response significantly involves $G_{\beta\gamma}$ activation of PLCβ. Additionally, the N-terminal RGS domain of GRK2 has been shown to facilitate weak GTPase-activating protein-like activity on G_q, inhibiting PLC actvation[146,147]. This may explain the difference in degree of Ca^{2+} signal inhibition between the GRK2 K220R mutant and the truncated GRK2 c-term mutant[147]. Therefore, the activation of PLCβ may be $G_{q\alpha}$- as well as $G_{\beta\gamma}$-dependent and largely due to synergistic crosstalk between the D1R and D2R.

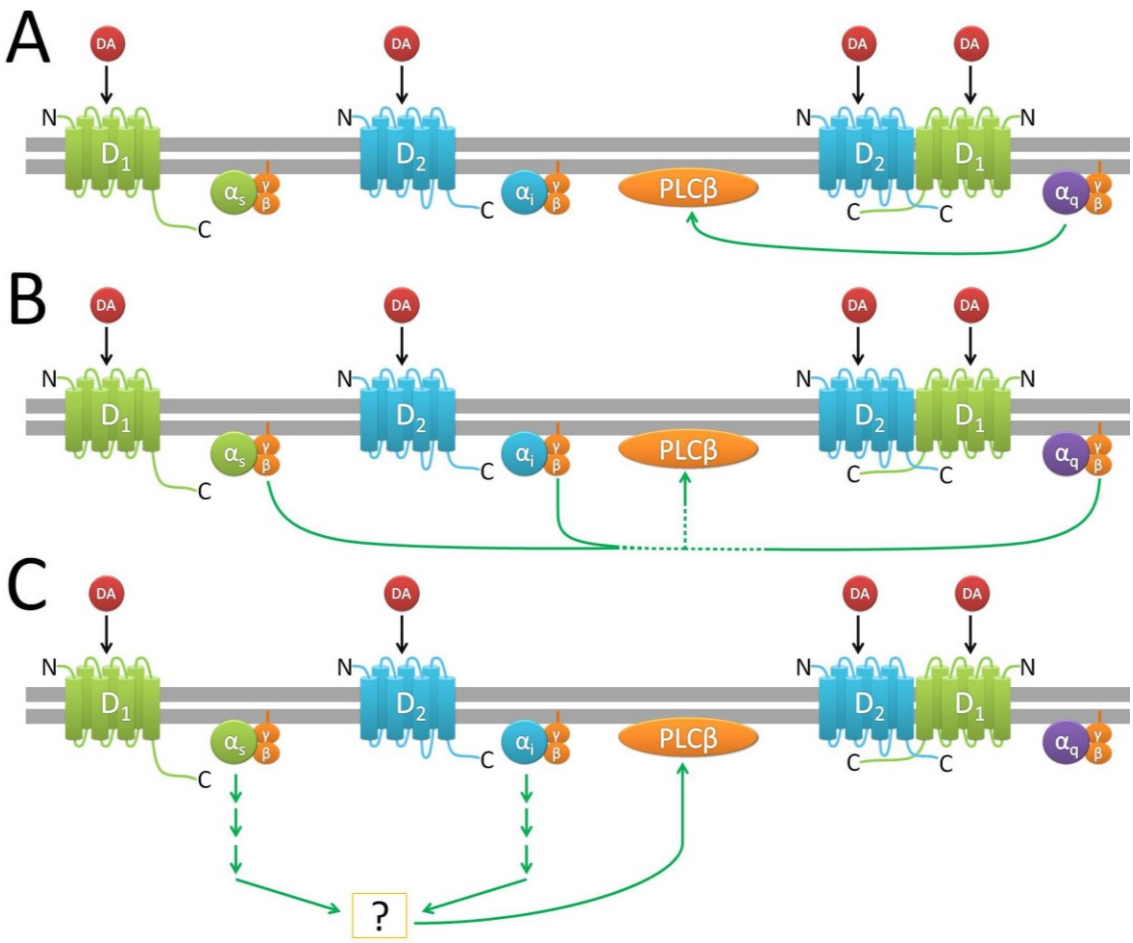

Figure 18: Various mechanisms of PLCβ activation that may occur when the D1R and D2R are co-expressed and co-activated.

Figure 18 represents several hypothetical signaling pathways for D1R-D2R receptor- Ca^{2+} signaling in HEK293 cells. Pathway A represents D1R-D2R heteromer activation of G_q leading to $G\alpha_q$ activation of PLCβ, as has been hypothesized in the literature[103]. Pathway B represents $G_{\beta\gamma}$ activation of PLCβ, where free beta/gamma subunits could arise through activation of either G_s, G_i or G_q. Pathway C represents co-activation of D1R and D2R homomers and cross-talk between G_s and G_i protein-mediated downstream signaling pathways ultimately leading to PLCβ activation. Given that PTX and CTX can nearly eliminate the DA-stimulated Ca^{2+} signaling, we believe that Pathway

A is largely inoperative in our system under basal conditions. Pathway C could readily account for the requirement for dual receptor activation, but the fact that $G_{\beta\gamma}$ sequestration largely eliminates the DA Ca^{2+} response would suggest that Pathway B is critically important. The PTX/CTX results further implicate G_s or G_i, however, the requirement for dual receptor activation in Pathway B is not completely clear. Certainly, additional work will be required to answer these questions, however, it is clear from these studies that D1R-D2R receptors can dually activate Ca^{2+} signaling through more than a single mechanism.

One additional consideration for D1R-D2R- Ca^{2+} signaling, which does not necessarily exclude the possibility of heteromer formation, may involve aggregation of the two DARs and their associated proteins in lipid rafts. Lipid rafts are a well-known but poorly understood platform for modulating certain protein-protein interactions in neurons as well as affecting GPCR ligand sensitivity, membrane trafficking, and signaling[148–153]. Lipid rafts would readily enable crosstalk between the D1R and D2R, and could assist in the multi-faceted signaling profile of the D1R-D2R receptor complex. In addition, differences in lipid raft composition, cell background, and assay detection may explain some of the differences observed between our data and the data generated by other groups. Despite the seeming complexity of the D1R-D2R receptor signaling mechanisms, it may yet be useful to study how synergistic concurrent activation of the D1R and D2R may induce effects not seen when either receptor is expressed alone. This can be examined by co-expressing mutants of the D1R and D2R which have been reported to be unable to form heteromers[141], and studying the effect of co-activation on the generation of a Ca^{2+} signal. Additionally, a compound that can selectively bias both receptors

towards a conformation that promotes PLC activation may be useful in providing a clearer understanding of the DAR system *in vivo*.

Chapter 3: Discovery and Characterization a G protein Biased Agonist MLS1547 that Inhibits β-arrestin-2 Recruitment to the D2R

Background

Among the DARs, the D2R is one of the most validated drug targets in neurology and psychiatry. However, most drugs targeting the D2R are problematic, either being less efficacious than desired or possessing adverse side effects due to the activation or blockade of multiple parallel signaling pathways. Despite recent advances, it remains unclear which signaling arms of the D2R are involved in the therapeutic effects of various agents used to treat neuropsychiatric disease states associated with the D2R.

One of the best characterized signaling pathways of the D2R is G_i/G_o-mediated inhibition of adenylate cyclase, which reduces intracellular cAMP levels and thereby attenuates phosphorylation of the DARPP-32 by PKA[154]. DARPP-32 is a protein phosphatase that acts as an integrator of cell signaling of many neurotransmitters, including DA (Figure 4, Figure 5)[155]. Reduction of DARPP-32 phosphorylation inhibits its activity and associated downstream signaling pathways[154,155]. Notably, administration of antipsychotic drugs, such as haloperidol or clozapine, has been shown to increase the level of DARPP-32 phosphorylation[156].

A more recently characterized D2R G protein-independent signaling pathway occurs through agonist recruitment of β-arrestin-2 to the receptor, which inhibits protein kinase B (Akt). Typically, regulation of Akt is associated with the insulin and neurotrophin pathways. The first link between the D2R and Akt was seen when D2R activation caused reduced Akt activity and increased activation of the Akt target glycogen synthase kinase 3β (GSK3β), while D2R inhibition caused precisely the opposite reaction[157,158]. Additionally, mice that lacked β-arrestin-2 did not show reduced Akt when

the D2R was stimulated, pointing to β-arrestin-2 as the intermediary signaling protein between the D2R and Akt[159]. Through further study, it was found that following recruitment to the D2R, β-arrestin-2 forms a complex with Akt and protein phosphatase 2A, which results in dephosphorylation of Akt and subsequent activation of GSK3β[160,161].

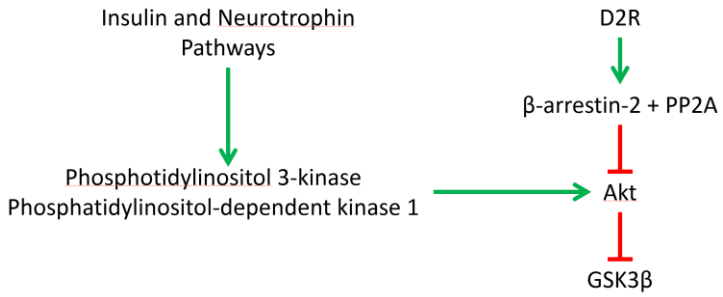

Figure 19: D2R β-arrestin-2 G protein-independent signaling.
Protein kinase B (Akt) has classically been associated with the insulin and neurotrophin pathways. However, a new pathway has been described wherein the D2R-β-arrestin-2-protein phosphatase 2A (PP2A) complex is able to inhibit Akt-mediated inhibition of glycogen synthase kinase 3β (GSK3β). Green arrows indicate activation and red lines indicate inhibition.

The D2R-β-arrestin-2-Akt signaling occurs at a much slower timescale compared to the D2R-G protein signaling[162], which could be explained by the hypothesis that G proteins may be pre-coupled to GPCRs, while arrestins require receptor activation to be recruited to the receptor[110]. Interestingly, Caron and colleagues have argued that *inhibition* of this pathway in D2R-expressing neurons is correlated with antipsychotic properties[163,164], whereas Roth and colleagues have suggested that *stimulation* of the D2R-β-arrestin-2 pathway may actually enhance antipsychotic efficacy[165,166].

A promising approach to dissecting the importance of these signaling pathways, and resolving associated controversies, is to study them using ligands that exhibit functionally selective or biased signaling properties[167,168]. Many GPCRs are able to transduce signals through more than one intracellular pathway. Although in most cases the endogenous transmitter will activate all signaling pathways, synthetic agonists may

preferentially activate one signaling pathway over another, or even activate one while inhibiting another[169–171]. While the mechanisms underlying functional-selectivity are not known, a leading hypothesis is that GPCRs can adopt multiple functionally "active" conformational states that are either stabilized or induced by these selective ligands[172,173]. Functionally selective compounds have been reported for many GPCRs and the mechanisms for biased signaling vary widely[174]. Biased signaling units may consist of GPCR homomers or require receptor homo- or heteromerization[48,117,175]. Coming from the other direction, biased ligands can bind allosterically[175,176], orthosterically[165,177], or bitopically[178,179] and can be small molecules[177], large compounds[180], or even short peptide sequences called pepducins[176,181].

Although relatively few biased ligands have been described for the D2R[182–186] existing examples strongly support the concept of the D2R being able to adopt multiple signaling-biased confirmations. Recently, a structural basis for functional-selectivity of several GPCRs has been proposed[180,187–189] suggesting that rational design of functionally selective compounds may be possible.

Recently, Jin and colleagues developed and characterized a series of analogs of the atypical antipsychotic aripiprazole that are partial agonists of D2R-mediated β-arrestin recruitment yet fail to stimulate G_i-linked cAMP inhibition[165,166]. Likewise, we currently describe the identification of an arrestin biased compound for the D2R (see Results). In contrast, no biased ligands had previously been described with the opposing pharmacology for the D2R, that is, stimulation of G protein signaling pathways without activation of β-arrestin recruitment. In this project, we now report the discovery of a novel, highly efficacious G protein biased agonist for the D2R with no detectable β-

arrestin-2 recruitment to the receptor. Identification of such functionally selective ligands may provide the requisite pharmacological probes with which to dissect these two signaling pathways and elucidate their function *in vivo*. Functionally selective agonists may also result in improved therapies for certain neuropsychiatric disorders, such as Parkinson's disease (in which D2R stimulation is desired) and schizophrenia (where inhibition of D2R signaling is the goal).

Materials and Methods

Ca^{2+} mobilization Assay – Flp-In T-Rex 293 cells were stably transfected with human D2SR and Gqi5 protein using the Flp-In T-Rex expression system (Life Technologies, Grand Island, NY). The cell line was constructed by co-transfecting SFD2s/FRT/TO and pOG44, followed by hygromycin B selection. Gqi5/pIRESpuro3 (Clontech) was then transfected into the D2R stable cell line, followed by selection with puromycin. D2R expression is controlled by tetracycline induction, while Gqi5 is continuously expressed.

D2R-stimulated Ca^{2+} mobilization was measured using methods similar to those previously published by our laboratory[42] and in Chapter 2. Cells were induced with 1 μM tetracycline added directly to the culture media and plated in as described in Chapter 2 in 384- or 1536-well, optical, clear bottom, black-walled plates (Greiner Bio-one, Monroe, NC). 20 μL/well (20,000 cells/well) were added to 384-well plates, and 3 μL/well (4,000 cells/well) to a 1536-well plate. See Chapter 2 Materials and Methods for the procedure following plating.

cAMP Inhibition Assay – D2R-mediated inhibition of forskolin-stimulated cAMP production was assayed using the DiscoveRx HitHunter assay kit (DiscoveRx Inc., Fremont, CA). CHO-K1 cells stably expressing the human D2R long isoform (DiscoveRx) were seeded in CP2 media at a density of 5,000 cells/well in 384-well black, clear-bottom plates. After 16-24 h of incubation at 37°C, 5% CO_2, and 90% humidity, the media was removed and replaced with 5 μl / well PBS. Cells were treated with 2.5 μl of various concentrations of compound diluted in PBS in the presence of an ~EC_{80} concentration of forskolin (100 μM) and 0.2 mM sodium metabisulfite and incubated for

60 min at 37°C, 5% CO_2, and 90% humidity. DiscoveRx HitHunter reagents were then added, and cells incubated in the dark at room temperature, according to manufacturer recommendations. Luminescence was measured on a Hamamatsu FDSS μCELL (Hamamatsu Photonics K. K., Bridgewater, NJ) for 8.5 sec. Data were collected as RLUs and values were normalized to a percentage of the maximum forskolin-stimulated cAMP signal. Data fit to a single site model and the Hill coefficients of the concentration response curves did not significantly differ from unity.

β-Arrestin Recruitment Assay – The ability of the agonist-activated receptor to recruit β-arrestin-2 was determined using the DiscoveRx PathHunter (DiscoveRx Inc., Fremont, CA) technology that involves enzyme complementation of fusion-tagged receptor along with an arrestin recruitment modulating sequence and β-arrestin-2 proteins. Control experiments determined that this PathHunter receptor construct will couple to G protein-mediated signaling with similar efficacy as an unmodified construct (data not shown). Assays were conducted, with minor modifications, as previously published by our laboratory[190,191]. Briefly, CHO-K1 cells expressing D2R long isoform (DiscoveRx) were seeded in CP media (DiscoveRx) at a density of 2,625 cells/well in 384-well black, clear-bottom plates. Following 24 h of incubation, the cells were treated with multiple concentrations of compound in PBS containing 1% DMSO and incubated at 37˚C for 90 min. DiscoveRx reagent was then added to cells according to the manufacturer's recommendations followed by a 30-60 min incubation at room temperature. Luminescence was measured on a Hamamatsu FDSS μCELL reader (Hamamatsu, Bridgewater, NJ). Data were collected as relative luminescence units (RLU) and

subsequently normalized to a percentage of the control luminescence seen with a maximum concentration of DA, with zero percent being RLU seen in the absence of any compound. The Hill coefficients of the concentration response curves did not significantly differ from unity.

β-Arrestin-2 BRET Assay – To directly assess induction of D2R-β-arrestin-2 interaction we employed a bioluminescence resonance energy transfer (BRET) assay that utilizes a cell line stably transfected with an Rluc-8 fusion-tagged D2R (short isoform) under a tetracycline-inducible promoter, as well as mVenus fusion-tagged β-arrestin-2[192,193]. The cell line was constructed using Flp-In T-REX 293 cells (Invitrogen, Life Technologies) transfected with pIRESpuro3/mVenus/β-arrestin-2, where the mVenus tag is on the N-terminus of the human β-arrestin-2. Clones were then analyzed for expression of the construct following selection with 2 μg/ml puromycin. The cell line with the highest level of expression was then transfected with pcDNA5/FRT/TO-SFD2LRluc8 and POG44 followed by hygromycin selection and subsequent functional screening to select the final stable line. Addition of the Rluc-8 substrate coelenterazine *h* results in an emission at 485 nm. However, when in close proximity with mVenus, resonance energy transfer leads to a shift in the emission spectrum from 485 nm to 510-540 nm, thereby quantifying the interaction between the receptor and the β-arrestin-2 protein. Cells were induced for 24 h by addition of 1 μM tetracycline directly to the culture media resulting in membrane receptor expression of approximately 5.8 pmol/mg protein. Cells were then removed from the plates using Earle's balanced salt solution without Ca^{2+} (EBSS-), pelleted by centrifugation, re-suspended (200,000 cells/ml) in Dulbecco's Phosphate Buffered Saline

(DPBS) (Mediatech, Manassas, VA) plus 0.05 g/500 ml sucrose and seeded into 96-well solid bottom white assay plates (20,000 cells/well) (Greiner Bio-one, Monroe, NC). Cells were allowed to sit for 45 min at room temperature and were then treated with 5 μM coelenterazine *h* (Nanolight Technology, Pinetop, AZ), incubated for 5 min and then stimulated with agonist using an onboard robotics 8 channel pipet head in a Flexstation III (Molecular Devices, Sunnyvale, CA). Original data are collected 5 min after agonist addition as a ratio of 525nm/485nm emission. Data are expressed as normalized to the percentage of the maximum DA-induced ratio.

Radioligand Binding Assays – Radioligand competition binding assays were conducted with slight modifications as previously described by our laboratory[42]. HEK293 cells stably transfected with human D1R, D2R, D3R, D4R, or D5R (Codex Biosolutions, Inc., Gaithersburg, MD) were dissociated from plates using EBSS-, and intact cells were collected by centrifugation at 900 × g for 10 min. Cells were re-suspended and lysed using 5 mM Tris-HCl and 5 mM $MgCl_2$ at pH 7.4 at 4°C. Cell lysate was pelleted by centrifugation at 30,000 × g for 30 min and re-suspended in EBSS with Ca^{2+} at pH 7.4. Cell lysates (100 μl, containing ~8 μg protein for D2-like receptor assays or ~10 μg protein for D1-like receptor assays) were incubated for 90 min at room temperature with the indicated concentrations of MLS1547 and either 0.5 nM [^{3}H]-SCH23390 (D1R and D5R), or 0.5 nM [^{3}H]-methylspiperone (D2R, D3R, and D4R) in a final reaction volume of 250 μl. Non-specific binding was determined in the presence of 4 μM (+)-butaclamol. Bound ligand was separated from free by filtration through a PerkinElmer Unifilter-96 GF/C 96 well micro-plate using the PerkinElmer Unifilter-96 Harvester, washing 3 times,

1 ml per well in ice-cold assay buffer. After drying, 50 µl of liquid scintillation cocktail (MicroScint PS, Perkin Elmer, Waltham, MA) was added to each well, plates were sealed, and analyzed on a PerkinElmer Topcount NXT^{TM}.

Pharmacophore Modeling – All modeling was performed using tools in the Schrödinger suite (Schrödinger Inc., New York, NY). While the main goal of pharmacophore modeling is to explain the molecular features that are associated with active compounds, such capability can benefit from the inclusion of "inactive" compounds in the model building procedure. In our case, to differentiate G protein biased from non-biased agonists in such a model we defined a so called "biased activity" measure that is similar to the "bias factor"[194], but without taking the exponential form:

$$biased\ activity = \log_{10}\left(\frac{E_{max}}{EC_{50}}\right)_{G\ protein} - \log_{10}\left(\frac{E_{max}}{EC_{50}}\right)_{arrestin}$$

For G protein biased agonists that did not exhibit measurable β-arrestin-2 stimulation, we assigned an E_{max} of 5% and an EC_{50} of 1 mM in order to generate bias factors, via the above equation, that can be compared to those for less biased agonists. Our rationale for selecting these values is that the β-arrestin-2 assay cannot reliably detect a signal of 5%, or less, over basal and 1 mM is 10-fold higher than the maximum concentration tested for any compound. Notably, the $\log_{10}(E_{max}/EC_{50})$ values from the G protein assay drive the ranking of these fully biased ligands.

Based on this "biased activity" measure, ten compounds, displaying either the strongest or weakest G protein-bias were selected: NCGC9125, NCGC9126, NCGC6387, NCGC9141 and MLS1547 for the biased set, and NCGC9134, NCGC9132, NCGC5872,

NCGC9131 and NCGC6388 for the non-biased set (see Results). For each compound, the 3D structure was built using the program Maestro (v9.5), and a single protonation state was chosen, with the 4-position of the piperazine bearing the positive charge in all cases. Multiple conformers were generated using the ConfGen program (v2.5). At least 10 conformers per ligand were generated, which required sampling with the "intermediate" search strategy of the program.

The goal of a pharmacophore search is to identify the largest set of pharmacophore features with specific 3-dimensional relationships, i.e., inter-feature distances that are common amongst all active compounds. The pharmacophore model was built using the program Phase (v3.6). The default pharmacophore features include positive (P), negative (N), hydrogen-bond acceptor (A), hydrogen-bond donor (D), aromatic (R) and hydrophobic (H) types. For the compounds studied here, the following functional groups were assigned to the hydrophobic (H) feature using a procedure that has been described by Green et al.[195]: isopropyl, aromatic halogens, aromatic CH_3, and methoxy-CH_3. The location of a given hydrophobic site is a weighted average of the positions of the non-hydrogen atoms in the associated fragment.

In addition, to allow ambiguous alignment of non-polar features, aromatic groups in the ligands were assigned to both the R and H feature types. When we assigned these features to the selected ligands, the largest number of features in a pharmacophore hypothesis that produced matches for all 5 biased compounds was found to be 4. These 4-point pharmacophores were of the HHPR, AHHP, HPRR and AHPR variants (the order of the features is arbitrary). For each of these variants, a number of 3D hypotheses were enumerated and clustered based on all occurring inter-feature distances. From this initial

set of hypotheses, the one that best matched the active compounds was then determined by a more rigorous custom scoring function ("survival score"), which consisted of 1) the *alignment score* based on the RMSD of feature positions, 2) the *vector score* of aligned features with a directional character (aromatic, donor and acceptor), and 3) the pairwise *volume overlap* of all the ligands aligned to the pharmacophore. This default scoring of all possible variants revealed that the HHPR and HRPR hypotheses were best able to explain the data. To eliminate the hypotheses that also matched the non-biased compounds, the 5 most non-biased compounds were used to rescore the hypotheses ("inactive score"). The finally selected pharmacophore was the HRPR variant (see Results) with the best "survival"-"inactive" score.

Construction of a novel active D2R model – Our active D2R model was based on an active model of the D3R, for which an inactive crystal structure is available[13]. The active D3R model was created by applying a set of spatial constraints obtained by comparing the inactive and active states of the β_2 adrenergic receptor (β2AR). In brief, the inactive and active structures of the β2AR (PDB: 2RH1[196] and PDB: 3SN6[197] respectively) were aligned and, by subtracting the coordinates of the Cα atoms of the inactive from the active form, a set of delta-coordinates were created. These deltas were added to the coordinates of the aligned D3R structure to generate a set of spatial constraints. Using these constraints, the inactive model of the D3R was transformed into an active form by using a hybrid minimization-Monte Carlo scheme, implemented in the program Prime (v3.3). The active D3R model was then used as a template in building the D2R homology model using Prime. Docking of compounds into the active-state model of the D2R was

achieved using the program Glide (v6.0), using the SP scoring function. To determine the binding mode of the congeneric series, a single reference compound (MLS1547) was first docked in the orthosteric binding site (OBS) revealed by the bound eticlopride in the D3R structure, which is formed by residues from TMs 3, 5, 6, and 7. We found the pyridine moiety of MLS1547 preferred to point towards TM2. Interestingly, for two well-studied D2R antagonists, spiperone and azaperone that share a common 4-fluophenyl-4-butanone moiety, as proposed/validated previously[198], if we assume that such a moiety is bound in the OBS, then the pyridine moiety of azaperone similarly points towards TM2 as MLS1547 (data not shown). We also docked MLS1547 in another D2R model in an active conformation based on a D3R active model[199] and equilibrated using MD simulations. Encouragingly results from both D2R models were consistent. All other compounds were then docked using core-constraints on the core substructure shared by all compounds to ensure the core in the OBS adopted a similar binding mode.

Results

In an effort to discover G protein biased agonists of the D2R, we screened a ~380,000 compound small molecule library in the Molecular Libraries Probe Production Center Network (MLPCN) at the National Center for Advancing Translational Sciences (NCATS) (Figure 20). The primary screen used a stably transfected cell line expressing the human D2R and a chimeric G_{qi5} protein enabling robust Ca^{2+} mobilization upon activation of the D2R. This screen identified 2,288 compounds with significant D2-G_{qi5} agonist activity, defined as compounds that, when screened at 40 μM, elicited a response larger than 3-fold over the standard deviation of mean signal from control wells with no compound. Agonists were also screened for Ca^{2+} mobilization in parental, non-transfected cell line and any compound showing activity was eliminated. The active compounds were then subjected to verification by generating full concentration-response curves for each compound. Subsequently, the hit compounds that exhibited full dose-response-activity relationships were evaluated in two orthogonal assays - one was to evaluate their ability to inhibit cAMP accumulation, a primary G protein signaling mechanism for the D2R[154], and the other was to test their ability to recruit β-arrestin-2, an important signaling response independent of G protein activation[161,162].

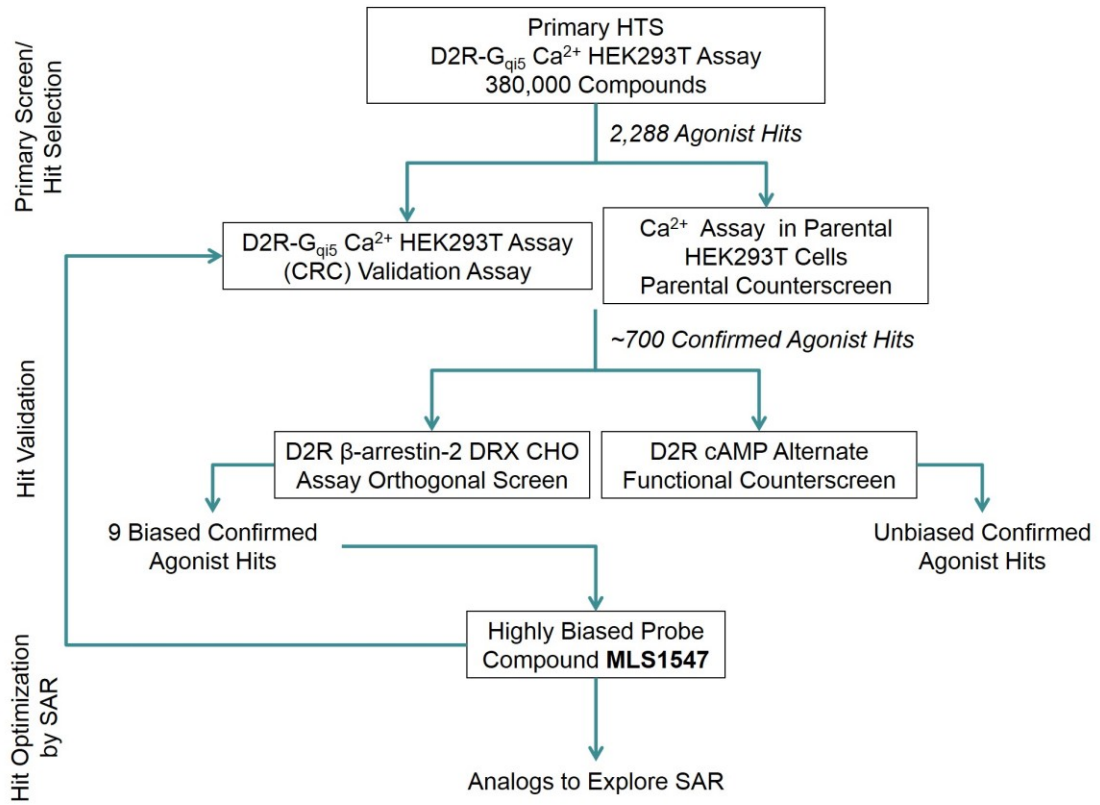

Figure 20: Flowchart of D2R G protein biased ligand screen.
Abbreviations: CRC (concentration response curve), HTS (high-throughput screen), MLS1547 (MLS000051547), SAR (structure-activity relationships).

As would be expected, our results revealed that the vast majority of the hit compounds were equally active in both the G protein- and β-arrestin-2-mediated signaling assays (see Figure 21). However, a small subset of hits (about two dozen) showed either greatly diminished efficacy and/or potency in the β-arrestin-2 recruitment assay. One of these compounds, MLS000051547 (MLS1547, Figure 22A), was selected for further characterization as it appeared to have high efficacy in the G protein-mediated signaling assays, but no measurable activity in the β-arrestin-2 recruitment assay.

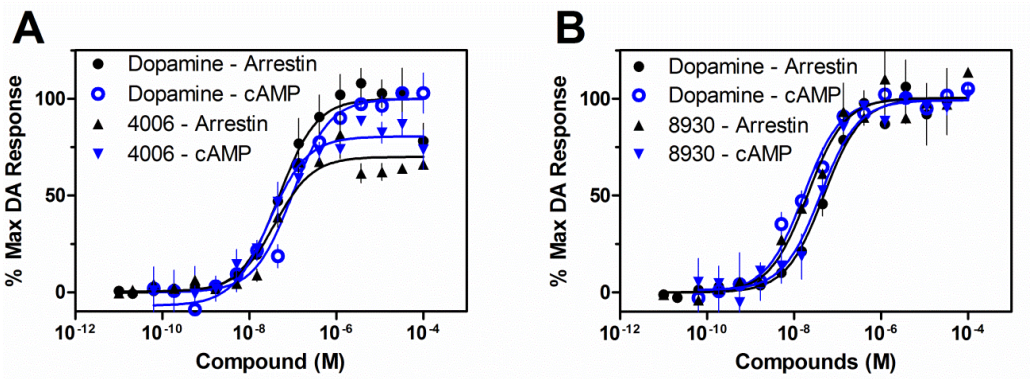

Figure 21: Examples of compounds with little to no bias between G protein- and β-arrestin-2-mediated signaling.

Compounds were assayed for agonist activity in both D2R-mediated inhibition of cAMP and D2R-mediated arrestin recruitment assays. Results were normalized to 100% maximum dopamine response for each group. **A**: NCGC00124006 was screened as an agonist in both assays giving E_{max} values of 80.5% in the cAMP inhibition assay and 69.9% in the arrestin recruitment assay. Corresponding EC_{50} values were 0.29 and 0.39 μM in the cAMP inhibition and arrestin recruitment assays, respectively. **B**: NCGC00138930 was screened as an agonist in both assays giving E_{max} values of 99.3% in the cAMP inhibition assay and 100.4% in the arrestin recruitment assay. Corresponding EC_{50} values were 0.04 μM and 0.02 μM in the cAMP inhibition and arrestin recruitment assays, respectively. Data are representative graphs from screening assays. Dopamine was run as a non-biased control and mean values for dopamine are reported in Tables 1 and 2.

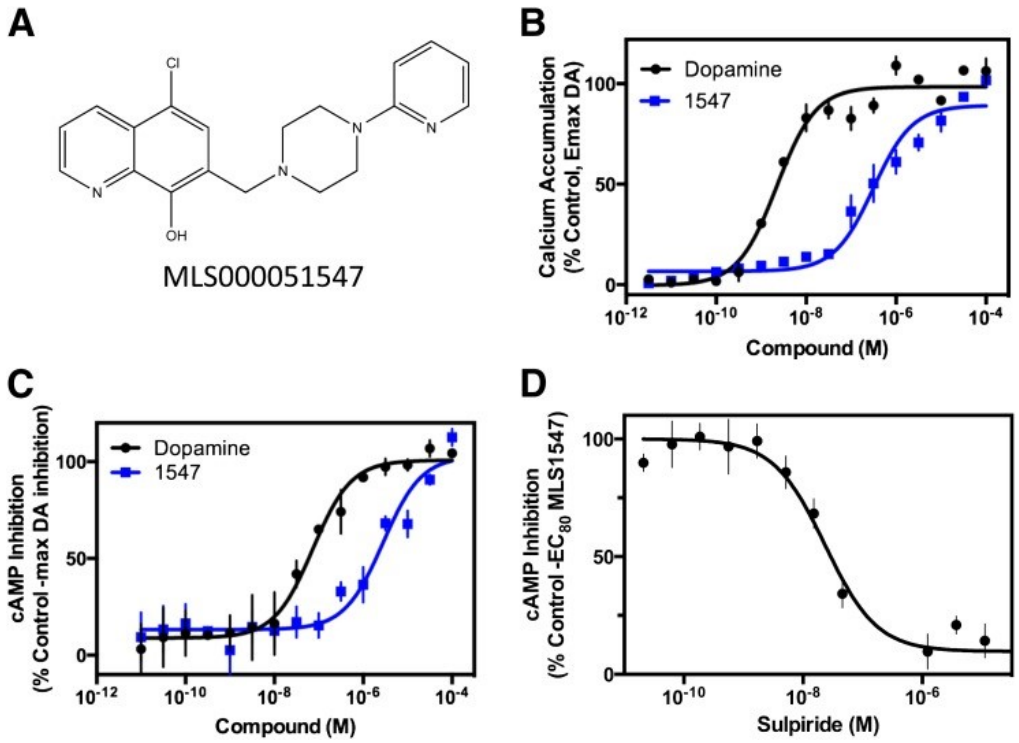

Figure 22: MLS1547 stimulates D2R G protein-mediated signaling.
A: Structure of MLS000051547 (MLS1547). **B**: HEK293 cells stably expressing D2R and G_{qi5} were assayed for MLS1547 stimulation of Ca^{2+} accumulation. Cells were stimulated with the indicated concentrations of dopamine or (EC_{50}=2.5 nM ± 0.3, E_{max}=101.7% ± 0.1) or MLS1547 (1547) (EC_{50}=0.37 μM ± 0.2, E_{max}=89.3% ± 4.3) **C**: CHO cells stably expressing the D2R were assayed for MLS1547 inhibition of forskolin-stimulated cAMP. Cells were stimulated with the indicated concentration of dopamine (EC_{50}=0.06 μM ± 0.02, E_{max}=100.4% ± 1.6) or MLS1547 (EC_{50}=0.26 μM ± 0.07, E_{max}=97.1% ± 3.7). **D**: CHO cells stably expressing D2R were assayed for sulpiride reversal of MLS1547 inhibition of forskolin-stimulated cAMP accumulation. Cells were stimulated with an EC_{80} concentration of MLS1547 in the presence of increasing concentrations of the D2R antagonist sulpiride (IC_{50}=22.0 nM ± 2.8). Data are representative of 3-5 independent experiments run in triplicate and plotted as a percentage of the maximum response observed with dopamine (**B** and **C**), or as a percentage of the response seen with an EC_{80} concentration of MLS1547 (**D**), as indicated.

Indeed, Figure 22B shows that MLS1547 behaved as a highly efficacious agonist in the D2-G_{qi5} Ca^{2+} mobilization assay with an EC_{50} value of 0.37 μM and an E_{max} of ~90%. In order to insure that this activity is physiological, and not restricted to the chimeric G protein nature of the G_{qi5} assay, we examined the ability of MLS1547 to inhibit forskolin-stimulated cAMP accumulation in cells stably expressing the D2R. Figure 22C shows that, similar to DA, MLS1547, completely inhibited the stimulation of cAMP by forskolin with an EC_{50} of 0.26 μM suggestive of it having high efficacy at

D2R-mediated G protein-linked signaling. We further found that the inhibition of cAMP accumulation by MLS1547 was completely blocked by co-treatment with the D2R antagonist sulpiride, as shown in Figure 22D. The IC_{50} of 22 nM for sulpiride's inhibition of MLS1547's action is similar to sulpiride's potency for blocking DA's response in this cAMP assay (data not shown). Taken together, these data indicate that MLS1547 is a highly efficacious agonist at the D2R for stimulating G protein-mediated signaling.

The ability of MLS1547 to stimulate recruitment of β-arrestin-2 to the D2R was evaluated using the DiscoveRx β-arrestin-2 PathHunter assay, which relies on the complementation and activation of β-galactosidase when β-arrestin-2 is recruited to the receptor. Notably, β-arrestin-2 is the arrestin protein functionally coupled to the D2R *in vivo*[200]. While incubation with DA resulted in robust recruitment of β-arrestin-2 in a dose-dependent manner, MLS1547 failed to exhibit activity in this assay (Figure 23A) despite it being a highly efficacious agonist of G protein-mediated signaling. However, other possible explanations for these discrepant results could include interference of the compound with the enzyme-linked signaling resulting in a suppression of signal. To address these alternative explanations, we employed a bioluminescence resonance energy transfer (BRET) assay that directly measures the physical interactions between the β-arrestin-2 protein and the D2R. Furthermore this also serves as a control for a different cell background, as these assays were conducted in HEK293 cells. As seen in Figure 23B, however, MLS1547 failed to stimulate any observable recruitment of β-arrestin-2 to the D2R in this assay, despite robust recruitment by DA. Taken together, these findings indicate that, while MLS1547 is a highly efficacious agonist at G protein-mediated

signaling, it is unable to stimulate measurable β-arrestin-2 recruitment, thus establishing it as a highly G protein biased agonist at the D2R.

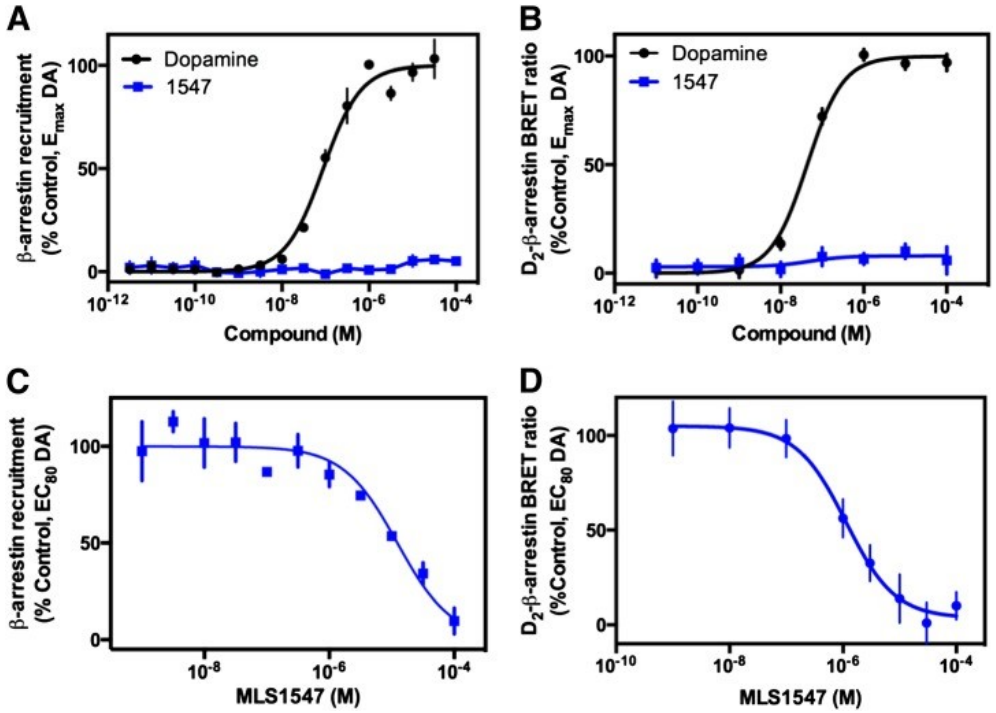

Figure 23: MLS1547 acts as an antagonist for dopamine-stimulated β-arrestin-2 recruitment to the D2R.

A: DiscoveRx PathHunter cells were assayed for agonist-induced recruitment of β-arrestin-2 to the D2R. Cells were stimulated with the indicated concentrations of dopamine or MLS1547 (1547), and EC_{50} and E_{max} values were obtained for dopamine, 0.09 μM ± 0.03 and 99.0% ± 0.6, respectively (mean ± SEM, n=3). MLS1547 failed to stimulate measurable β-arrestin-2 recruitment. **B**: HEK293 cells were stably transfected with Rluc-8-fused D2R and mVenus-fused β-arrestin-2, stimulated with various concentrations of dopamine (EC_{50}=0.05 μM ± 0.01, E_{max}=99.8% ± 1.9) or MLS1547 (1547) as indicated, and examined for BRET as described in the Materials and Methods. MLS1547 failed to stimulate any measurable D2R-β-arrestin-2 interactions. Data for panels **A** and **B** are representative of 3-5 independent experiments run in triplicate and plotted as a percentage of maximum response observed with dopamine as indicated. **C**: DiscoveRx PathHunter cells were stimulated with an EC_{80} concentration of dopamine (1 μM), then assayed for the ability of MLS1547 to antagonize this response (IC_{50}=9.9 μM ± 0.9). Data are expressed as the percentage of the maximum response observed with 1 μM dopamine and represent the mean ± SEM values of three individual experiments performed in triplicate. **D**: The same cells described for the BRET assay in B above were stimulated with an EC_{80} of dopamine (1 μM) and assayed for the ability of MLS1547 (IC_{50}=3.8 μM ± 1.8) to antagonize this response. Data are expressed as mean ± SEM of six independent experiments run in quadruplicate.

Since MLS1547 activates G protein-linked pathways, yet does not appear to stimulate β-arrestin-2 recruitment, MLS1547 would be expected to antagonize the DA-induced β-arrestin-2 response by blocking DA binding to the receptor. In fact, as seen in

Figure 23C, MLS1547 fully antagonized DA-mediated β-arrestin-2 recruitment to the D2R in the DiscoveRx assay, with an IC_{50} of 9.9 μM. Similar results were obtained when MLS1547 was examined for antagonist activity in the D2R β-arrestin-2 BRET assay, demonstrating an IC_{50} of 3.8 μM (Figure 23D). In summary, while MLS1547 is an agonist of D2R-stimulated G protein-mediated signaling, it does not stimulate β-arrestin-2 recruitment to the receptor, instead acting as an apparent antagonist of DA-mediated β-arrestin-2 recruitment.

In order to determine the affinity of MLS1547 for the D2R, we used standard radioligand binding competition analyses. MLS1547 was found to completely displace [^{3}H]-methyl-spiperone binding to the D2R with a calculated K_i value of 1.2 μM ± 0.2 (Figure 24). Displacement studies were also conducted on the other DA receptor subtypes (Figure 25) resulting in K_i values of 2.3 μM ± 0.2 (D3R) and 0.32 μM ± 0.04 (D4R), mean ± SEM (n=3), suggesting a less than 10-fold difference in affinity between the members of the D2-like family. When the D1-like receptors were examined by measuring the ability of MLS1547 to displace [^{3}H]-SCH23390 binding to D1 and D5 receptors, the extrapolated K_i values for both receptors were >50 μM (Figure 25).

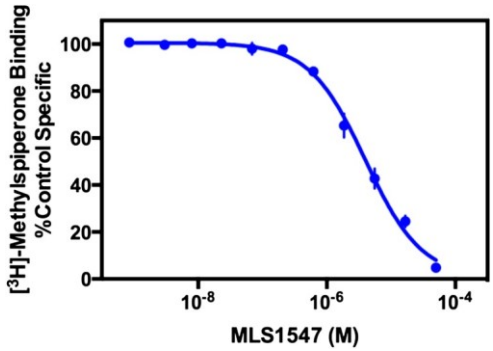

Figure 24: Competition binding assay using MLS1547 and the D2R.
Membranes from HEK293 cells stably transfected with the human D2R were harvested for radioligand competition binding assays as described in the Materials and Methods. Membranes were incubated with the indicated concentrations of MLS1547 and 0.5 nM [^{3}H]-methylspiperone. The data are representative of four independent experiments and expressed as a percentage of the binding seen in the absence of any competing ligand. The K_i for MLS1547 was calculated to be 1.2 μM ± 0.2 (mean ± SEM, n=4).

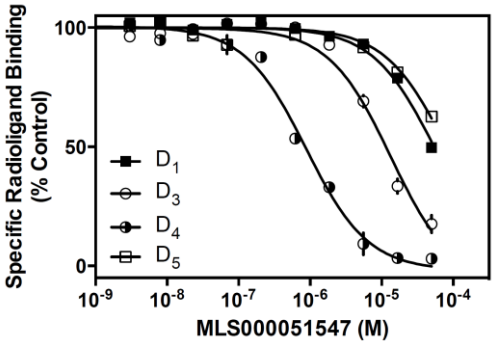

Figure 25: Competition binding of MLS1547 for dopamine receptor subtypes.
Membranes from HEK293 cells stably transfected with human D1R, D3R, D4R, or D5R (Codex Biosolutions, Inc., Gaithersburg, MD) were harvested for radioligand competition binding. Briefly, membranes were incubated with the indicated concentrations of MLS1547 and either 0.5 nM [^{3}H]-SCH23390 (D1R and D5R), or 0.5 nM [^{3}H]-methylspiperone (D3R and D4R). The curves shown are representative of four independent experiments done on different days. Data are expressed as a percentage of the binding seen for each individual receptor subtype in the absence of any competing ligand. K_i values were calculated using the Cheng-Prusoff equation and radioligand K_d values determined via saturation binding isotherms on each individual receptor. Average K_i values are reported in the Results section.

A series of MLS1547 analogs were either obtained from commercial sources, or, in a few cases, synthesized to investigate the structure-activity relationship (SAR) of pathway selectivity for this set of compounds. These analogs were assayed in the D2R DiscoveRx cAMP assay as well as in the D2R DiscoveRx β-arrestin-2 recruitment assay (Table 3 and Table 4) Although none of the analogs were more potent than MLS1547, a

subset of the analogs were also G protein biased in that they inhibited cAMP accumulation yet lacked β-arrestin-2 recruitment activity (Table 3). However, another subset of compounds exhibited agonist activity in both the cAMP and β-arrestin-2 assays with little to no bias (Table 4). These findings were used to formulate a preliminary SAR of G protein bias in this series of compounds.

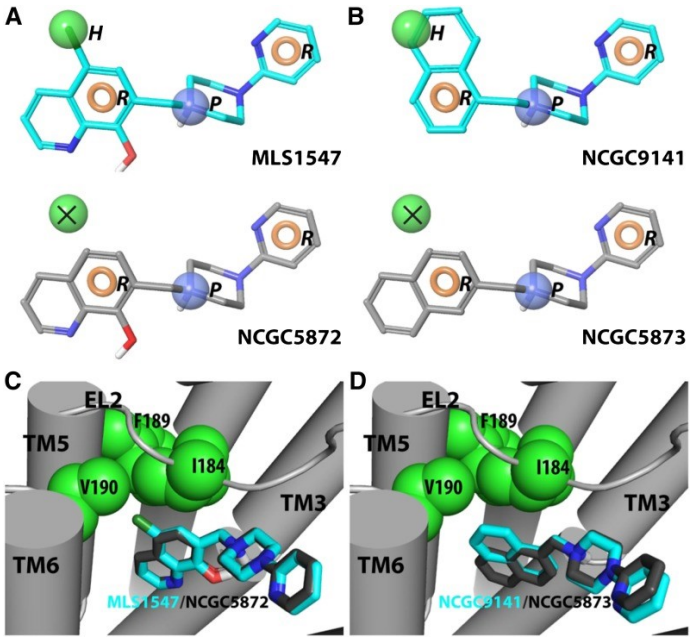

Figure 26: Pharmacophore model for G protein biased and non-biased agonist interactions with the D2R.
A and **B**: HRPR pharmacophore with aligned biased compounds MLS1547 and NCGC9141. Biased compounds align well to all four features: two aromatic (beige), one hydrophobic (green) and a positive (blue) feature. **Middle**: Compared to the biased compound MLS1547, the non-biased compound NCGC5872 (left) lacks the -Cl group and cannot align both the hydrophobic and aromatic features, while the different attachment points of the naphthalene ring in compounds NCGC9141 and NCGC5873 cause the former, but not the latter to align well to the 4-point pharmacophore. In this case, one of the aromatic rings in NCGC9141 aligns the hydrophobic feature. **C** and **D**: docked poses of biased (cyan) and unbiased (grey) compounds in an active model of the D2R. Note the more extensive interaction of non-polar features in the biased compounds with a hydrophobic pocket formed by residues in EL2 and TM5.

To do this, a pharmacophore model was constructed to distinguish between the highly G protein biased (Table 3) and less/non-biased D2R agonists (Table 4). Specifically, we selected ten compounds, displaying either the strongest or weakest G

protein-bias, and then assigned default pharmacophore features (positive (P), acceptor (A), donor (D), aromatic (R) and hydrophobic (H)) to these ligands (see Methods). We found that a 4-point HRPR hypothesis was best able to explain the experimental data (Figure 26A and B). Specifically, the alignment of the "H" feature in these compounds is the key difference between the completely biased (Table 3) and less/non-biased (Table 4) agonists of this scaffold. As shown by two representative biased/non-biased pairs in Figure 26, the completely biased compounds align optimally to the "H" feature, whereas the less/non-biased compounds do not (Figure 26A and B).

In parallel, we docked these compounds into a novel active-state model of the D2R using MLS1547 as a reference compound. For the MLS1547 compound, we observed two plausible orientations with the pyridine moiety pointing towards either TM5 in the orthosteric binding site (OBS) or toward TMs 2 and 7, away from the OBS (data not shown). Based on the SAR derived from Table 3, it appears that the N in the pyridine ring likely makes an H-bond with a receptor residue, as there is a ~10 fold increase in the potency of MLS1547 compared to that of NCGC319125. When the pyridine points towards TM5, however, a corresponding H-bond donor cannot be identified in the OBS. Thus, it is more likely that MLS1547 adopts the alternate orientation with the pyridine pointing toward TMs 2 and 7, in which the N on the pyridine ring may interact with T412 in TM7 to form an H-bond. These docking results were confirmed using a model with the D2R in an active conformation based on another D3R active model[199] and equilibrated using molecular dynamics simulations (data not shown). Encouragingly, results from both models were similar.

Using the MLS1547 pose with the pyridine pointing toward TMs 2 and 7, we used a core-restrained protocol to dock the other compounds into the active D2R model in order to compare the binding modes of the fully G protein biased vs. less/non-biased agonists. The resulting poses show that the completely biased compounds from Table 3 have a significantly higher tendency to interact with the extracellular portion of TM5. Specifically, the chloro (-Cl) group of MLS1547 interacts with a hydrophobic pocket formed by Ile184^{EL2}, Phe189$^{5.38}$, and Val190$^{5.41}$ (Figure 26).

Interestingly, this is consistent with our finding from the pharmacophore modeling that the fully G protein biased, but not the less/non-biased compounds, can be well-aligned to the "H" feature of the aforementioned HRPR pharmacophore. While recent publications suggest a possible role for aromatic -Cl groups in an H-bond formation, it is not atypical to consider -Cl as a hydrophobic group as well. Indeed, there are multiple examples in the literature where a methyl/-Cl swap resulted in roughly the same potency, and was better tolerated than the unsubstituted hydrogen[201].

Table 3: Analogs of MLS1547 exhibiting complete G protein bias.
The compounds were assayed in agonist mode using the DiscoveRx cAMP and arrestin assays.

		D2R cAMP Response		D2R β-arrestin Recruitment	
Structure	Compound ID	Emax (% Control ± SEM)	EC_{50} (μM ± SEM)	Emax (% Control ± SEM)	EC_{50} (μM ± SEM)
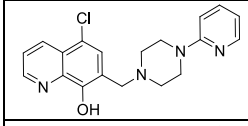	MLS1547	97.1 ± 3.7	0.26 ± 0.07	Inactive	Inactive
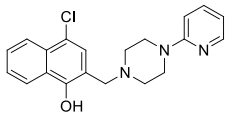	NCGC00319124	87.3 ± 14.7	5.5 ± 0.9	Inactive	Inactive
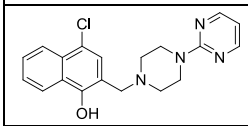	NCGC00319127	93.9 ± 4.6	4.7 ± 1.7	Inactive	Inactive
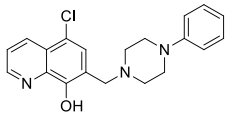	NCGC00319125 (a.k.a. NCGC1-D01)	66.8 ± 3.9	2.8 ± 1.2	Inactive	Inactive
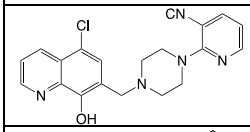	NCGC00346387	94.8 ± 2.1	1.4 ± 0.8	Inactive	Inactive
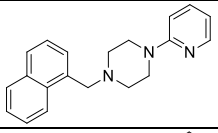	NCGC00319141 (a.k.a. NCGC1-D03)	89.5 ± 5.2	0.7 ± 0.7	Inactive	Inactive
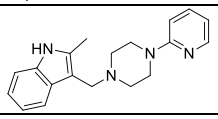	MLS000860449	84.9 ± 2.7	4.5 ± 3.0	Inactive	Inactive
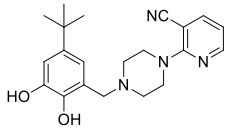	NCGC0319129	74.8 ± 23.8	9.5 ± 5.6	Inactive	Inactive
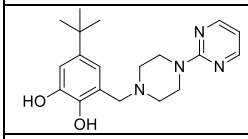	NCGC00319126	62.8 ± 7.7	1.1 ± 0.6	Inactive	Inactive
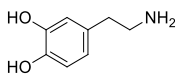	Dopamine	100	0.06 ± 0.02	100	0.09 ± 0.03

Table 4: Partially or non-biased analogs of MLS1547.
The compounds were assayed in agonist mode using the DiscoveRx cAMP and arrestin assays.

		D2R cAMP Response		D2R β-arrestin Recruitment	
Structure	Compound ID	Emax (% Control ± SEM)	EC_{50} (μM ± SEM)	Emax (% Control ± SEM)	EC_{50} (μM ± SEM)
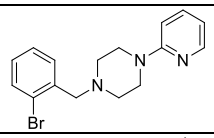	NCGC00319139	95.5 ± 2.0	0.03 ± 0.01	89.3 ± 9.4	2.0 ± 0.5
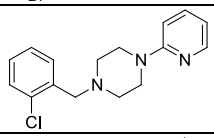	NCGC00319137	84.1 ± 4.5	0.02 ± 0.001	84.7 ± 2.5	1.6 ± 0.3
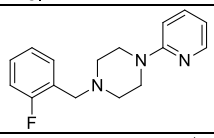	NCGC00319136	93.8 ± 1.4	0.1 ± 0.04	76.4 ± 2.9	0.7 ± 0.07
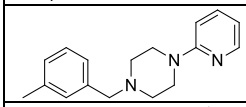	NCGC00092785	77.0 ± 10.9	0.04 ± 0.01	73.8 ± 1.2	0.4 ± 0.02
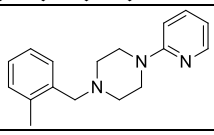	NCGC00319134	86.1 ± 14.4	0.1 ± 0.04	74.7 ± 1.8	0.3 ± 0.03
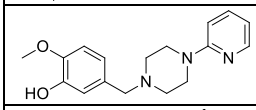	NCGC00319131	89.6 ± 0.5	0.2 ± 0.1	66 ± 0.2	0.8 ± 0.01
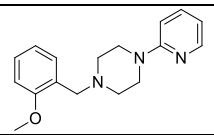	NCGC00319132	78.9 ± 10	0.1 ± 0.01	59.2 ± 4.2	0.3 ± 0.04
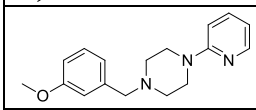	NCGC00319133	86.5 ± 14.7	0.01 ± 0.001	87.6 ± 2.0	0.2 ± 0.03
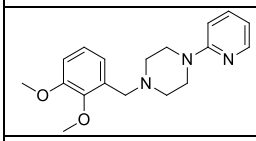	NCGC00319130	71.0 ± 17.1	0.1 ± 0.02	66.0 ± 0.2	2.1 ± 0.4
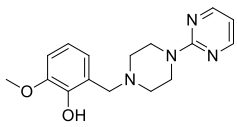	NCGC00319135	83.3 ± 14.4	1.4 ± 0.1	68.9 ± 4.9	13.2 ± 6.6
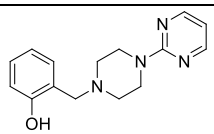	NCGC00319140	92.5 ± 5.5	2.0 ± 0.2	66.2 ± 18.6	20.5 ± 9.6

Table 4, continued: Partially or non-biased analogs of MLS1547. The compounds were assayed in agonist mode using the DiscoveRx cAMP and arrestin assays.

		D2R cAMP Response		D2R β-arrestin Recruitment	
Structure	Compound ID	Emax (% Control ± SEM)	EC_{50} (μM ± SEM)	Emax (% Control ± SEM)	EC_{50} (μM ± SEM)
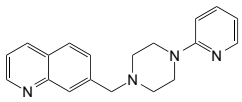	NCGC00346388	90.9 ± 1.9	0.2 ± 0.1	56.8 ± 7.1	1.0 ± 0.6
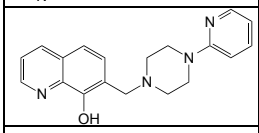	NCGC00345872 (a.k.a. NCGC2-5)	97.1 ± 0.9	0.3 ± 0.1	58.0 ± 8.4	0.9 ± 0.3
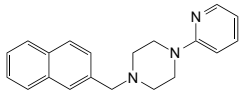	NCGC00345873 (a.k.a. NCGC2-6)	93.1 ± 1.6	0.1 ± 0.07	63.3 ± 8.9	0.9 ± 0.6
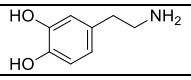	Dopamine	100	0.06 ± 0.02	100	0.09 ± 0.03

Discussion

Preceding this study, no G protein biased D2R ligands had been reported. Here we report the discovery of a highly G protein biased D2R agonist (MLS1547) that inhibits arrestin recruitment to the receptor (Figure 22, Figure 23). In lieu of attempting to rationally design a biased compound based on known D2R ligands, a high throughput screen was implemented which led to the detection of MLS1547. We then used chemical analogs of MLS1547 to identify SAR that led to the development of a model for biased D2R signaling (Figure 26).

One of the key difficulties involving functionally selective ligands is how exactly to characterize and quantify the degree of signaling bias[174,194,202,203]. In the simplest terms, one must take both signaling potency and efficacy of all associated signaling cascades into account to determine bias. Additionally, in some cases, different signaling cascades may have completely different spatio-temporal characteristics[162], further complicating the determination of ligand bias. One group has developed a mathematical formula to determine a ligand's "bias factor"[194]. We used the bias factor formula without the exponential form to calculate "bias activity", as described in the Materials and Methods. Using this bias activity measure, five of the most biased compounds (NCGC9125, NCGC9126, NCGC6387, NCGC9141 and MLS1547) were compared to five of the least biased compounds (NCGC9134, NCGC9132, NCGC5872, NCGC9131 and NCGC6388) to develop the pharmacophore model.

It is tempting to speculate that the structural basis for the different efficacies of these two groups of agonists critically depends on whether a compound can interact with the hydrophobic pocket near the extracellular portion of TM5 mentioned above. Interestingly, interactions with the extracellular portion of TM5 have previously been

proposed as the structural basis for the arrestin signaling bias of the serotonergic agonist ergotamine at the 5-HT2B receptor, whereas ergotamine is notably non-biased at the related 5-HT1B receptor[180]. Thus, comparing crystal structures of ergotamine bound to both receptors, it was found that the extracellular portion of TM5 is tilted significantly more towards the OBS in the 5-HT2B receptor, compared to the 5-HT1B receptor[180]. This suggests a mechanism whereby agonists that prevent such a tilting would bias towards G protein activation, compared to the arrestin pathway. Future experiments to test this SAR prediction for the D2R and other GPCRs will be required. It is interesting to note, however, that in the D2R, mutations of four residues at the cytoplasmic end of TM5 disrupt arrestin recruitment much more than they impact cAMP signaling[204], suggesting that differential propagation of signals through TM5 may play an important role in determining signaling bias. Interestingly, several D2R mutants with mutations in the third transmembrane domain were described which were either G protein biased or arrestin biased when stimulated with DA[205].

In summary, MLS1547 is the first example of a G protein biased agonist of the D2R. While it robustly activates G protein-mediated signaling, the compound does not appear to significantly promote arrestin recruitment to the receptor. Rather, through occupancy of the receptor, MLS1547 functions as an apparent antagonist of DA-induced arrestin recruitment to the D2R. Administration of compounds with this pharmacological profile to animals would be expected to stimulate G protein biased signaling of the D2R while simultaneously inhibiting the effects of endogenous DA signaling through the β-arrestin-2/Akt/GSK3β pathway. Such compounds may also engender less arrestin-mediated receptor desensitization or internalization, thereby further amplifying the G

protein signaling arm. Recently, β-arrestin biased agonists have been developed for the D2R that exhibit varying degrees of agonist efficacy[165,166]. Functionally selective probes for both of the major signaling arms of the D2R should now help to dissect their roles in normal physiology and behavior as well as elucidate their involvement in the therapeutic effects of various pharmaceutical agents.

Chapter 4: SAR Investigation MLS1547 and its Analogs Reveals Molecular Signatures Essential for Compound Bias

Background

Most agonists, in particular the endogenous neurotransmitter will typically activate all associated signaling pathways in parallel with equal or similar efficacy. However, it is now recognized that some agonists may be functionally selective, resulting in a variety of possible downstream signaling configurations[206]. In Chapter 3, the discovery of a G protein biased D2R agonist (MLS1547) was described and data that was obtained from structurally similar analogs was used to generate a pharmacophore model to explain how this molecular scaffold engenders signaling bias.

Here, MLS1547 signaling is studied further by determining its ability to induce receptor internalization. As a G protein biased D2R agonist, it is expected that little to no D2R internalization would be stimulated by MLS1547. Indeed, G protein biased ligands for other GPCRs have shown a lack of receptor internalization despite the activation of other parallel signaling cascades[207,208]. Here, we show that D2R stimulation by MLS1547 shows a marked lack of receptor internalization compared to non-biased agonist, yet this may be dependent on the cellular context.

To refine and build on the pharmacophore model (Figure 26), additional SAR data was obtained through an iterative chemical synthesis approach. 46 distinct analogs were synthesized and tested for G protein and β-arrestin-2 signaling activity. Data from these new MLS1547 analogs were combined with data for analogs in Chapter 3 to deduce the influence of different areas of the scaffold on dictating receptor signaling bias. These findings enhance our understanding of biased signaling interactions, refine the existing

model of MLS1547 signaling, and may have implications for the development of functionally selective compounds for the D2R.

Materials and Methods

Materials – Original screening quantities of MLS1547 was obtained from the Molecular Libraries Screening Center Network Library and subsequently purchased from MolPort (Riga, Latvia), for follow-up triage studies. Subsequent batches of the compound were synthesized along with all analogs in house at the Kansas Specialized Chemistry Center, as described below. Compounds were tested in-house via NMR to confirm purity (>99%) and structural accuracy. Identical results were obtained with all batches from all suppliers. All other chemicals were obtained from Sigma-Aldrich (St. Louis, MO) unless otherwise indicated within the methods. All tissue culture media, selection agents, and components were obtained from Mediatech, Inc. (Manassas, VA).

cAMP inhibition assay – Assays were performed essentially as previously described (see Chapter 3 Materials and Methods). For antagonist mode assays, compounds were diluted in PBS in the presence of 100 μM forskolin and 0.2 μM sodium metabisulfite, and an EC_{80} of DA. Data for antagonist mode assays were collected as relative luminescence units (RLUs), and values were normalized to a percentage of max sulpiride inhibition.

β-Arrestin-2 recruitment assay – Assays were conducted, with minor modifications, as previously published by our laboratory (see Chapter 3 Materials and Methods). Compounds were diluted in PBS in the presence of 0.2 μM sodium metabisulfite and an EC_{80} of DA for antagonist mode assays. Data were collected as RLUs and subsequently normalized to a percentage of EC_{80} DA activation for antagonist mode assays.

Primary glia and striatal neuron culture – Isolation and culturing of cells was conducted as described previously[209,210]. ***Glia Cultures***: Briefly, dissection buffer consisting of ACSF (119 mM NaCl, 5 mM KCl, 1 mM $MgCl_2$, 30 mM dextrose, 25 mM HEPES, pH 7.4, without Ca^{2+}) and glia media (DMEM supplemented with 10% FBS, 10 units/ml penicillin, 10 μg/ml streptomycin, and Glutamax) were prepared and stored at 4°C until use. Embryonic or neonatal mice were euthanized by rapid decapitation. Cerebral cortexes were dissected, and digested in papain solution (100 ml papain and 20 μl 1% DNase I in 2 ml dissection buffer) at 37°C for 20 min. Following digestion, tissue was rinsed with 10 ml pre-warmed glia media, triturated with a fire-polished glass Pasteur pipette, diluted in glia media and filtered through a 70 μm cell-strainer. Cells were then seeded into collagen coated T75 flasks (2-3 embryos/flask) and placed into a 37°C cell culture incubator overnight, fed the next day and dissociated with 0.05% trypsin when nearing confluence in 10-12 days. Glia were cultured directly onto collagen coated inserts (Millipore PICM03050) placed in 6 well plates (one confluent T75 flask per 6-well plate/ 2 ml/insert) and used for conditioning neuronal cultures. ***Neuronal Cultures***: Pregnant mice (E15-18) were euthanized with CO_2, and embryonic mice were euthanized by decapitation. The striatum was dissected from the brain tissue and placed into a 15 ml conical tube with ice-cold dissection buffer, for culture of MSNs. Tissues are dissociated with papain as described above and counted. Neurons were then seeded on poly-L-Lysine coated glass coverslips previously incubated in a 37°C incubator overnight in plating media (Neurobasal supplemented with 5% heat-inactivated horse serum, 10 units/ml penicillin, 10 μg/ml streptomycin, Glutamax; 2% B27 supplement) at a density of 0.4×10^6 cells per well of a 6-well plate, and cultured in a 37°C incubator overnight (neurons

are DIV 0). The next day (DIV 1), coverslips containing neurons were placed underneath the glia culture inserts, one coverslip/well. For transfection of primary striatal neurons, each neuronal culture/coverslip was transfected with 1 μg of D2R-pHluorin DNA construct[211] using 2 μl of Lipofectamine 2000 (Invitrogen, Calrlsbad, CA) according to the manufacturers recommendation. Briefly, Lipofectamine 2000 reagent and DNA construct were diluted in supplement free Neurobasal medium, incubated for 20 min at room temperature. Glia culture inserts were removed momentarily from the 6-well plates and 200 μl Lipofectamine/DNA mixture was added to each coverslip, followed by return of the glia culture inserts to each well. Neurons were incubated with the Lipofectamine/DNA mixture at 37°C for 2-4 h. After the 2-4 h incubation period, glia inserts were removed again and the media containing the Lipofectamine/DNA mixture was removed, glia culture inserts were returned to each well, and the glia media from each insert was changed. Neurons were cultured for an additional 24-72 h prior to imaging.

D2R immunocytochemistry – MSNs were transfected with pH-DRD2 for 48 h as described above[211], washed with ACSF, and incubated with rabbit polyclonal anti-GFP antibody (1:200 dilution; a gift from Dr. Richard L. Huganir, Department of Neuroscience, Johns Hopkins University School of Medicine/HHMI) for 1 h at 4°C to stain surface receptors. Neurons were subsequently fixed with Parafix (4% sucrose, 4% paraformaldehyde in PBS, pH 7.4), permeabilized with 0.25% Triton X-100 in PBS, blocked with 10% normal donkey serum in PBS at 37°C for 1 h, and subsequently stained with a mouse monoclonal GFP antibody at a dilution of 1:100 (a gift from Dr.

Richard L. Huganir) to stain for total pH-DRD2 to amplify green fluorescent signal from superecliptic pHluorin at neutral pH. Neurons were then washed four times and subsequently stained with Alexa Fluor 647 Red-X donkey anti-Rabbit IgG (H+L; 1:100 dilution; CAT 647 711-605-152, Jackson Immunoresearch Laboratories, Inc.) and Alexa Fluor 488 donkey anti-mouse IgG (H+L; 1:200 dilution; CAT 705-545-147, Jackson Immunoresearch Laboratories, Inc.) secondary antibodies. Images were acquired on an inverted Zeiss fluorescent microscope using a 40× objective (NA, 1.30) and a 2.5× relay lens between the microscope and the camera. Fluorescent intensities were quantified using ImageJ (NIH, http://rsb.info.nih.gov.ezproxy.welch.jhmi.edu/ij/). The ratio between surface to total of pH-DRD2 signal was normalized to the control group (pH-DRD2 without DA stimulation).

Total Internal Reflection Fluorescence Microscopy – Total internal reflection fluorescence (TIRF) imaging was conducted on a custom made in house system with a 100-mW Cyan laser for excitation, and an Electron Multiplying Charge Coupled Device (EMCCD) camera for a detector. Prior to imaging experiments, a coverslip containing transfected neurons as described above was assembled into a live-imaging chamber and incubated with ACSF. Transfected neurons were identified visually under epifluorescent imaging, and subject to a 1 min photo-bleach to eliminate pre-existing pHluorin fluorescence on the plasma membrane. Following photobleaching, recording is performed for 1 min at 10 Hz with each recording containing 600 images and the gain setting of the electron multiplier set to maximum. Individual insertion events are identified in the recording ImageJ, and analyzed manually.

Biotinylated D2R internalization assay – HEK293 cells were transfected with HA-D2R. 72 h after transfection, cell surface proteins were labeled with Sulfo-NHS-SS-Biotin (30 min on ice). After washes, cells returned to incubator with different treatments for 30 min. Cells were then incubated with MESNA to cleave biotin from surface proteins. Cell lysate was incubated with avidin beads to precipitate biotin labeled (internalized) proteins. Western blotting was then used to detect internalized D2R and TfR with specific HA antibody and TfR antibody. The concentrations of quinpirole, 1547, 3-PPP, and Aripiprazole are all 10 μM. Western Blot of Anti-HA-D2R, to detect internalized D2R, and anti-TfR was used as loading control. Densitometric analysis of internalized D2R/TfR. One-way ANOVA test, * $P<0.05$; ** $P<0.01$.

BRET biosensor-based D2R internalization assay – The receptor internalization biosensor was constructed using a modified GFP10. They were synthesized at GeneScript® (Piscataway, NJ) and subcloned into pcDNA 3.1/zeo(-) using infusion technology (Clontech, CA). For assays HEK293SL cells were cultured in DMEM supplemented with 5% fetal bovine serum and 20 μg/ml gentamycin and maintained at 37°C in 5% CO_2 and 90% humidity. Cells were seeded at 7.5×10^5 cells per 100 mm dish a day before transfection and transfected using calcium phosphate as previously described. After 18 h of transfection, the medium was replaced, and the cells were re-plated onto poly-ornithine coated white 96-well plates (~25,000 cells per well). The next day, cells were washed once with pre-warmed Tyrode's buffer (140 mM NaCl, 2.7 mM KCl, 1 mM $CaCl_2$, 12 mM $NaHCO_3$, 5.6 mM D-glucose, 0.5 mM $MgCl_2$, 0.37 mM

NaH_2PO_4, 25 mM HEPES, pH 7.4), and then stimulated with various concentrations of ligands in Tyrode's buffer for 30 min at 37 °C. The cell-permeable substrate, coelenterazine 400a was added at a final concentration of 5 μM in Tyrode's buffer 3~4 min before BRET measurements. Measurements were performed by using Synergy2 (BioTek®) microplate reader with a filter set of 410 ± 80 nm and 515 ± 30 nm for detecting the Rluc8 *renilla* luciferase (donor) and GFP10 (acceptor) light emissions, respectively. The BRET signal was determined by calculating the ratio of the light intensity emitted by the GFP10 over the light intensity emitted by the Rluc8 and performed in triplicate. Data are expressed as a mean ± SEM of the BRET ratio.

Results

D2R internalization is weakly stimulated by MLS1547

MLS1547 has been shown to act as a biased D2R agonist, displaying high efficacy at stimulating G protein linked signaling, but failing to recruit β-arrestin-2 as observed using several *in vitro* assays[212]. As previously discussed, one advantage of a compound biased in this manner is that in theory it would have the ability to activate G protein signal in neurons without causing rapid desensitization/tolerance usually associated with arrestin recruitment by non-biased agonists. This led us to delve further into MLS1547 signaling bias by examining agonist-mediated D2R internalization. As it is thought that most agonist-induced D2R internalization is mediated by β-arrestin-2[200] we predicted that MLS1547 would have a diminished ability to stimulate receptor internalization when compared to a non-biased agonist.

In a first approach, we used a BRET-based biosensor in transiently transfected HEK293 cells that employs a modified GFP protein that is cell surface-localized[213]. Co-transfection of D2R-Rluc8 and the cell surface-localized GFP protein results in constitutive BRET when they are expressed at the cell surface and in close proximity. Upon agonist stimulation the receptor is internalized but the GFP protein remains in the plasma membrane resulting in a decrease in the BRET ratio due to separation of the BRET donor (D2SR-Rluc8) and acceptor (GFP). As shown in Figure 27A, stimulation with DA resulted in a dose dependent decrease in the BRET ratio with an EC_{50}=0.14 μM ± 0.04. When cells are stimulated with MLS1547 they failed to elicit a significant change in BRET ratio at concentrations up to 30 μM, a concentration that results in full activation of G protein signaling (cf. Figure 22 and Figure 23). Figure 27B demonstrates single concentration data using 10 μM of DA or 30 μM of MLS1547, where DA

treatment resulted in significant receptor internalization when compared to the untreated control, whereas MLS1547 treatment did not result in any significant change in BRET. These initial findings suggest that MLS1547 does not promote D2R internalization.

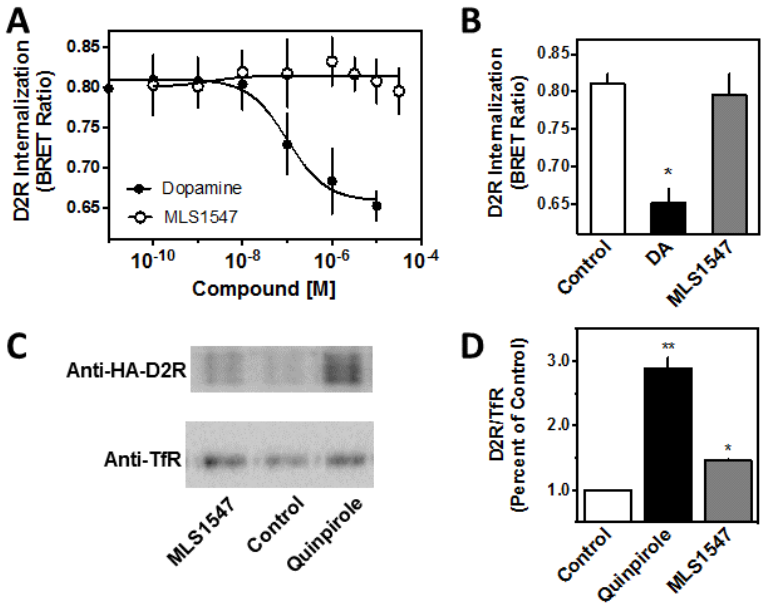

Figure 27: Investigation of D2R internalization in non-neuronal cell systems.
A: HEK293 cells were transiently transfected with D2R-Rluc8 and a modified GFP10, which together produce constitutive BRET. On the day of assay, the cells were stimulated with either dopamine (DA) or MLS1547 for 30 min at 37ºC before BRET measurement. The data are graphed as mean dose-response curves from three experiments. DA exhibited an EC_{50} of 0.14 ± 0.04 mM for BRET reduction/D2R internalization, while MLS1547 treatment failed to alter the BRET signal. **B:** Maximum BRET signal obtained after treatment with vehicle (control, 0.81 ± 0.02), 10 µM DA (0.65 ± 0.02), or 30 µM MLS1547 (0.79 ± 0.03). All data are expressed as mean ± SEM of the BRET ratio from three independent experiments. *P<0.05, unpaired Student's t-test compared to untreated controls. **C:** HA-tagged D2R was transiently transfected into HEK293 cells and surface D2R was biotinylated as described in Methods. After washing, cells were treated with either vehicle (control), 10 µM quinpirole, or 30 µM MLS1547 or for 30 min at 37ºC. Biotin was cleaved from D2R that remained on the cell surface, followed by cell lysis and isolation of biotinylated (internalized) D2R using avidin beads. Western blotting was used to detect D2R and also transferrin receptor (TfR) (as a gel loading control). A single experiment, representative of three, is shown. **D:** Densitometric analyses were performed and the data expressed as D2R/TfR ratios, relative to the untreated controls (1.0). Treatment values are provided as mean ± S.E.M: quinpirole = 2.8 ± 0.2 and MLS1547 = 1.5 ± 0.03. One-way ANOVA followed by Bonferroni's post-test was performed: *p<0.05, and **p<0.01.

We next took a different approach to assess agonist-induced internalization using a cell surface biotinylation assay and transient expression of HA-tagged D2R in HEK293 cells. In this type of experiment, the D2R is labeled with biotin at the cell surface followed by agonist treatment of the cells. Biotin is then cleaved from cell surface

proteins and internalized receptors (that are protected from cleavage) are isolated via binding to avidin beads[214]. Figure 27C shows a Western blot of internalized D2R protein after treatment with 10 μM of MLS1547 or 10 μM of the D2R agonist quinpirole. The D2R is visualized using an antibody directed to an HA tag on the receptor (top blot). Visualization of the transferrin receptor (TfR) was also performed as a gel loading control (bottom blot). The blots were quantified using densitometric analysis and graphed as a percentage of D2R protein divided by the loading control (TfR), with untreated control levels being set to 1 (Figure 27D). Notably, treatment with the D2R agonist quinpirole resulted in a robust loss of cell surface D2R protein following treatment (Figure 27D), but MLS1547 treatment also resulted in statistically significant receptor internalization. However, this response was only a fraction of that produced by quinpirole (Figure 27D). Thus these results differed somewhat from those obtained using the BRET assay in that MLS1547 promoted a small degree of receptor internalization.

As the above experiments used non-neuronal cells (HEK293) to examine D2R internalization, we wished to examine this response within a neuronal context. Thus, we performed studies to examine D2R internalization and recycling in striatal neurons from E15-E18 mouse embryos using both immunocytochemistry (ICC) and TIRF microscopy[209–211]. Figure 28A shows quantification of ICC assays following a 45 min incubation with 10 μM DA, 30 μM MLS1547, 30 μM sulpiride, or no compound (control). Data are expressed as the ratio of surface to total receptors normalized to the control. Sulpiride was used as a negative control, and as expected, no significant D2R internalization was detected after sulpiride treatment (surface:total=1.05 ± 0.08). DA treatment resulted in a significant decrease in relative D2R surface expression when

compared to the control (DA surface:total = 0.72 ± 0.02, control surface:total=1.00 ± 0.02, p <0.0001). Notably, MLS1547 caused a statistically significant degree of receptor internalization when compared to the control (MLS1547 surface:total = 0.90 ± 0.03, p<0.0262). However this response was much less than that observed with DA (p<0.0001).

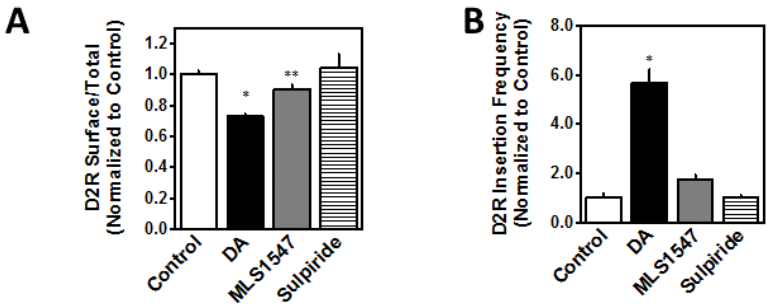

Figure 28: Investigation of D2R internalization in neuronal cell systems.
A: Medium spiny neurons were prepared and transfected with the D2R-pHluorin construct (pH-DRD2) as described in Methods. 48 hr later, the neurons were treated with vehicle (control) or 10 µM dopamine (DA), 30 µM MLS1547, or 30 µM sulpiride for 45 min. Neurons were washed and then stained with a polyclonal GFP antibody to detect surface D2R followed by fixation, permeabiization and re-staining with a monoclonal GFP antibody to detect total cellular D2R. The ratios between surface to total pH-DRD2 signal were normalized to the control group in each experiment and are expressed as mean ± S.E.M of the indicated number of cells (n): control = 1.00 ± 0.02, n = 746; DA = 0.72 ± 0.02, n = 627; MLS1547 = 0.90 ± 0.03, n = 812, sulpiride = 1.05 ± 0.08, n = 171. One-way ANOVA followed by Bonferroni's post-test was performed: *p<0.0001 and **p<0.0262. **B:** Medium spiny neurons expressing the D2R-pHluorin construct were exposed to vehicle (control) or 10 µM DA, 30 µM MLS1547, or 30 µM sulpiride for 20 min and the number of reinsertion events/(min×µm^2) were visualized in real time as described in Methods. The average reinsertion frequencies for the drug treatments were normalized to the control group in each experiment and are expressed as mean ± S.E.M of the indicated number of cells (n): control = 1.00 ± 0.20, n = 51; DA = 5.70 ± 0.54, n = 49; MLS1547 = 1.73 ± 0.22, n = 50, sulpiride = 1.56 ± 0.34, n = 15. One-way ANOVA followed by Bonferroni's post-test was performed, *p<0.0001.

For TIRF microscopy studies, the same neurons used in the ICC studies were used to look at vesicle reinsertion. As described in the Materials and Methods[209,211], cells were transfected with a D2R construct tagged with a pH dependent GFP (pHluorin) that loses fluorescence in the acidic environment of vesicles. This enables the visualization of vesicle exocytosis or "reinsertion", as pHluorin fluorescence is regained the moment the vesicle fuses with the cell membrane. It has been shown that an increase in measured

receptor internalization correlates to an increase in reinsertion frequency, which is theorized to be due to recycling of D2Rs back to the cell membrane following agonist-stimulated endocytosis[210,211]. The frequency of D2R-containing vesicle reinsertion is measured via real-time TIRF microscopy by photobleaching a neuron and then treating cells for 20 min with 10 μM DA, 30 μM MLS1547, 30 μM sulpiride, or no treatment (control). Vesicle re-insertions to the membrane were counted for 5 min, and displayed as the number of reinsertions per minute per μm^2 cell surface membrane (Figure 28B). DA treatment caused a significant increase in re-insertion frequency when compared to the control (DA frequency=5.70 ± 0.54, control frequency=1.00 ± 0.20, $p < 0.0001$), correlating to an increase in receptor internalization. MLS1547 treatment in resulted in a small but statistically non-significant increase in reinsertion frequency (frequency=1.73 ± 0.22) when compared to the control.

Taken together, our data show that MLS1547 promotes little (biotinylation and ICC assays) to no (BRET and TIRF assays) D2R internalization, confirming the notion that it is a highly G protein biased agonist. The small degree of internalization seen in the biotinylation and ICC assays may suggest that MLS1547 is incompletely biased, that is, it has a low efficacy for recruiting β-arrestin-2 that was not observed directly in the arrestin recruitment assays. Alternatively, D2R internalization may not be solely dependent on arrestin, and MLS1547 may be promoting receptor internalization via a non-arrestin-mediated mechanism. Future experiments will be required to distinguish between these possibilities.

MLS1547 analog structure-activity relationships

As our goal is to develop an *in vivo* probe for G protein-mediated D2R signaling, we engaged in further chemical optimization. Previously, we obtained 22 MLS1547 analogs and tested them in functional assays for cAMP accumulation and β-arrestin-2 recruitment. In order to better understand the importance of various functional groups, as well as to strive for a more potent and more selective compound, a structured iterative chemical synthesis of 46 additional analogs of MLS1547 was conducted. Figure 29A illustrates the parental compound and the previously developed pharmacophore model highlighting four regions of the molecule that are believed to be important for G protein bias. These include a hydrophobic binding moiety (green ball), two aromatic groups (orange balls), and a positively charged feature (pink ball). Keeping this in mind, Figure 29B shows the four main areas of the molecule that we selected for derivation to develop a more detailed SAR in this series of compounds.

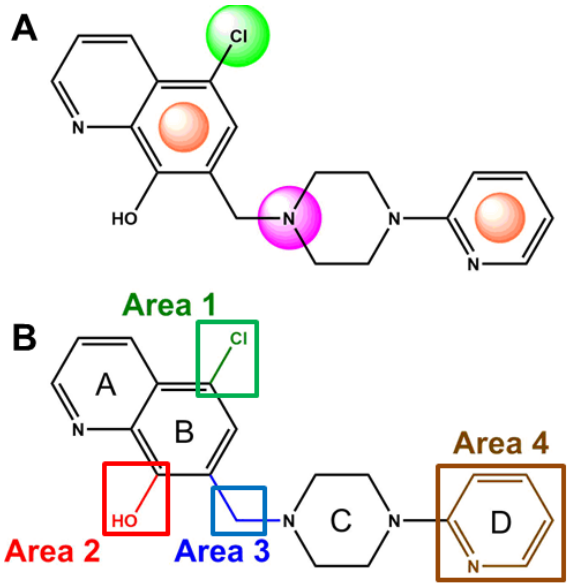

Figure 29: Structure of parent compound, MLS1547.
A: Pharmacophore model depicting four required features for agonist activity and G protein bias. Green represents a hydrophobic component, orange represents the two aromatic components, and purple represents a positively charged component. **B:** The four main areas of the scaffold that were modified are indicated.

SAR: a hydrophobic binding moiety is necessary for G protein bias

We have previously postulated that a hydrophobic binding pocket comprised of D2R residues I184, F189, and V190 was involved in G protein biased signaling (Figure 26)[212]. The chloro group (Figure 29B, area 1) on MLS1547 was postulated to interact with this pocket and prevent the tilting of TM5 during receptor activation. With this in mind, our first approach was to further investigate the influence of this hydrophobic binding moiety on compound bias by constructing multiple analogs of MLS1547 that vary in this part of the molecule. Table 5 and Table 6 show analogs that were designed to address the importance of the hydrophobic binding moiety (Figure 29B, area 1) in maintaining compound bias.

In Table 5, it can be seen that removing the chloro group in area 1 (NCGC2-5) caused a gain in arrestin agonist activity (loss of signaling bias), whereas replacing the chloro group with a bromo group such as with KU2-1, caused a decrease in G protein agonist potency (EC_{50} from 260 nM to 8 μM) and efficacy. Similar Cl→H substitutions within the context of related MLS1547 derivatives (KU2-4, KU2-6, KU2-7, KU2-8) support the need for the hydrophobic moiety in order for the compound to exhibit strong G protein signaling bias.

We previously found that a naphthalene group can provide the necessary hydrophobic feature for G protein bias, but only if oriented correctly such that it can engage the hydrophobic pocket in the D2R (Figure 26D)[212]. For instance, NCGC1-D03 is highly G protein biased whereas NCGC2-6 is not (Table 6). Other analog pairs following this change in naphthalene orientation exhibited similar phenomena. Interestingly, compounds with indole groups substituted for the naphthalene group (KU7-1 and KU7-6), yet in a similar orientation as the non-biased NCGC2-6 compound, also exhibited

non-biased signaling activity (Table 6). In aggregate, these data confirm and strengthen our previously proposed pharmacophore model for G protein signaling bias of the MLS1547 scaffold. Thus a hydrophobic moiety is integral to G protein biased signaling activity at the D2R, and this moiety can be provided either through a halogen group or a hydrophobic ring in the correct orientation.

Table 5: Removing a hydrophobic moiety by changing chloro group on ring B causes a loss in G protein bias.

Scaffold	R	Sibley ID	D2 cAMP HitHunter Assay				D2 Arrestin PathHunter Assay			
			E_{max} (% Control ± SEM)	EC_{50} (μM ± SEM)	I_{max} (% Control ± SEM)	IC_{50} (μM ± SEM)	E_{max} (% Control ± SEM)	EC_{50} (μM ± SEM)	I_{max} (% Control ± SEM)	IC_{50} (μM ± SEM)
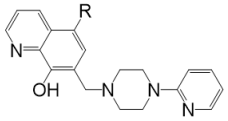	Cl	MLS1547	95.4 ± 8.9	2.2 ± 0.6	NA	NA	NA	NA	100 ± 0	20.4 ± 5.3
	Br	KU2-1	75.0 ± 3.9	7.9 ± 2.1	22.9 ± 4	2.8 ± 1.5	NA	NA	123.5 ± 6.4	6.7 ± 1.9
	H	NCGC2-5	97.1 ± 0.9	0.3 ± 0.09	NA	NA	58 ± 8.4	0.9 ± 0.3	NA	NA
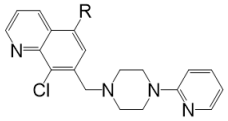	H	KU2-4	56.8 ± 8.3	6.6 ± 5.5	108.6 ± 89	34.6 ± 21.6	30.1 ± 1.1	7.3 ± 1.8	79.9 ± 12.1	17.9 ± 9.4
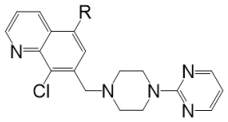	H	KU2-6	59.3 ± 4.9	1.2 ± 0.4	NA	NA	53.4 ± 7.8	15.6 ± 8.8	NA	NA
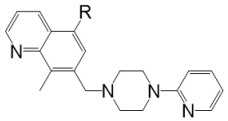	H	KU2-7	48.9 ± 5.4	1.4 ± 0.7	45.8 ± 12.6	11.5 ± 4	22 ± 1.6	9.3 ± 2.9	69.3 ± 9.8	4.6 ± 1.7
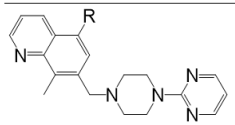	H	KU2-8	58.7 ± 2.8	0.8 ± 0.4	NA	NA	46.5 ± 1.5	7.6 ± 1	73.2 ± 10.6	8.3 ± 2.9

Yellow compounds are previously reported in Chapter 3. Red compounds appear in multiple tables.

Table 6: Removing a hydrophobic moiety by moving linker location on ring B causes a loss in G protein bias.

Scaffold	R	Sibley ID	D2 cAMP HitHunter Assay				D2 Arrestin PathHunter Assay			
			E_{max} (% Control ± SEM)	EC_{50} (μM ± SEM)	I_{max} (% Control ± SEM)	IC_{50} (μM ± SEM)	E_{max} (% Control ± SEM)	EC_{50} (μM ± SEM)	I_{max} (% Control ± SEM)	IC_{50} (μM ± SEM)
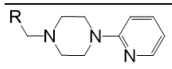		NCGC1-D03	89.5 ± 5.2	0.7 ± 0.7			NA	NA		
	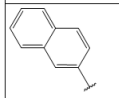	NCGC2-6	93.1 ± 1.6	0.1 ± 0.07			63.3 ± 8.9	0.9 ± 0.6		
	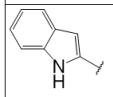	KU7-1	75.4 ± 7.6	0.2 ± 0.1	45.6 ± 12	11.8 ± 6	60.9 ± 6.4	0.7 ± 0.1	30 ± 1.0	3.3 ± 0.9
	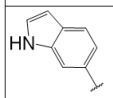	KU7-6	51.9 ± 13.8	1.6 ± 1.3	43.2 ± 11.6	11.3 ± 1.8	60.8 ± 6.0	9.3 ± 6.1	38.8 ± 4.1	1.6 ± 1.0
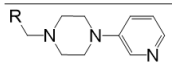	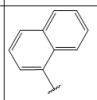	KU6-15	70.0 ± 10.0	13.3 ± 8.6	24.6 ± 5.4	9.1 ± 6.3	34.9 ± 4.1	7.7 ± 0.3	72.1 ± 6.3	8.0 ± 4.7
		KU6-9	NA	NA	68 ± 11.6	5.3 ± 2.4	NA	NA	94.2 ± 2.5	4.2 ± 1.0
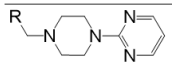	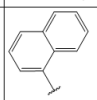	KU6-13	90.1 ± 12.7	8.5 ± 4.0		>100	85.6 ± 4.5	14.5 ± 1.5	NA	NA
		KU6-7	51.6 ± 3.5	0.8 ± 0.1	54.9 ± 12.9	10.3 ± 6.1	70.6 ± 8.9	2.6 ± 1.1	66.2 ± 11.3	40.6 ± 27.1
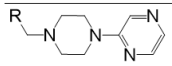		KU6-14	66.5 ± 20.6	27.3 ± 18.2		>100	NA	NA	NA	NA
	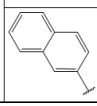	KU6-8	NA	NA		>100	54.7 ± 5.1	24.8 ± 15.5	NA	NA

Yellow compounds are previously reported in Chapter 3. Red compounds appear in multiple tables.

SAR: the hydroxyl group enhances G protein and arrestin agonist activity

We next examined the importance of the hydroxyl group (Figure 29B, area 2) attached to ring B by constructing analogs seen in Table 7. Other analog sets in Table 7 show that replacing the hydroxyl group with either a chloro (KU3-2, KU3-3, or KU3-4, KU2-4), methyl (KU4-3, KU4-4, KU4-5 or KU2-7), or methoxy (KU2-3, KU2-2) group generally results in a complete loss, or diminishment, of agonist activity. Notably, we observed that the two methoxy derivatives (KU2-2 and KU2-3) functioned as antagonists of both D2R signaling assays suggesting that, while they lost agonist efficacy, they retained affinity for the receptor. In contrast, the chloro and methyl derivatives were ineffective as antagonists and lost all functional activity at the D2R. These data suggest that the hydroxyl group on ring B is a strong driver of both affinity and efficacy in this series of compounds and plays a vital role in driving G protein bias and activity.

Table 7: Changing the hydroxyl group on ring B to a less polar functional group causes loss in G protein and arrestin agonist activity.

			D2 cAMP HitHunter Assay				D2 Arrestin PathHunter Assay			
Scaffold	R	Sibley ID	E_{max} (% Control ± SEM)	EC_{50} (μM ± SEM)	I_{max} (% Control ± SEM)	IC_{50} (μM ± SEM)	E_{max} (% Control ± SEM)	EC_{50} (μM ± SEM)	I_{max} (% Control ± SEM)	IC_{50} (μM ± SEM)
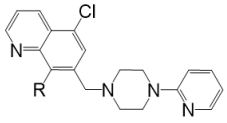	OH	MLS1547	95.4 ± 8.9	2.2 ± 0.6	NA	NA	NA	NA	100 ± 0	20.4 ± 5.3
	Cl	KU3-2	NA	NA	NA	NA	NA	NA	NA	NA
	CH3	KU4-3	NA	NA	NA	NA	NA	NA	NA	NA
	OCH3	KU2-3	NA	NA	79.9 ± 0.8	2.5 ± 0.8	NA	NA	114.9 ± 0.7	4.5 ± 0.8
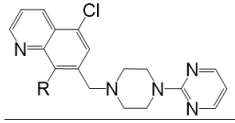	OH	KU1-1	92.8 ± 2.1	0.7 ± 0.2	NA	NA	21.6 ± 5.7	0.5 ± 0.3	92.8 ± 2.2	4.6 ± 2.4
	Cl	KU3-3	NA	NA	NA	NA	NA	NA	NA	NA
	CH3	KU4-4	NA	NA	NA	NA	NA	NA	NA	NA
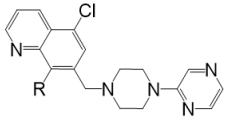	OH	KU1-6	83.8 ± 8.5	3.5 ± 3.4	15 ± 10.4	9.9 ± 5.4	NA	NA	127.2 ± 11.4	7.8 ± 1.6
	Cl	KU3-4	NA	NA	NA	NA	NA	NA	NA	NA
	CH3	KU4-5	NA	NA	NA	NA	NA	NA	NA	NA
	OCH3	KU2-2	NA	NA	NA	NA	NA	NA	127.2 ± 15.6	20.3 ± 7.6
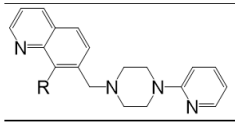	OH	NCGC2-5	97.1 ± 0.9	0.3 ± 0.09	NA	NA	58 ± 8.4	0.9 ± 0.3	NA	NA
	Cl	KU2-4	56.8 ± 8.3	6.6 ± 5.5	108.6 ± 89	34.6 ± 21.6	30.1 ± 1.1	7.3 ± 1.8	79.9 ± 12.1	17.9 ± 9.4
	CH3	KU2-7	48.9 ± 5.4	1.4 ± 0.7	45.8 ± 12.6	11.5 ± 4	22 ± 1.6	9.3 ± 2.9	69.3 ± 9.8	4.6 ± 1.7

Yellow compounds are previously reported in Chapter 3. Red compounds appear in multiple tables.

SAR: a carbonyl group on the linker region causes complete loss in D2R activation

We next investigated the importance of the linker between rings B and C of the scaffold (Figure 29B, area 3) by converting the methylene group to a carbonyl group (Table 8). While each of the parent scaffolds (KU7-6, KU8-1, KU7-1 and KU8-2) were relatively unbiased agonists, the creation of a carbonyl linker resulted in a complete loss of agonist activity for the resulting compounds (KU7-14, KU7-15, KU7-7 and KU7-8). There are two likely explanations for these results. First, the creation of an amide bond will lower the pKa of the proximal nitrogen group such that is not protonated at physiological pH. This will result in the loss of the positively charged feature in the MLS1547 pharmacophore model (Figure 29A). Secondly, the introduction of a carbonyl group removes flexibility between the A/B and C/D ring groupings, which likely has adverse effects on the ability of the compound to dock to the receptor.

Table 8: Adding a carbonyl group to linker causes loss in G protein and arrestin activity.

Scaffold	R	Sibley ID	D2 cAMP HitHunter Assay				D2 Arrestin PathHunter Assay			
			E_{max} (% Control ± SEM)	EC_{50} (μM ± SEM)	I_{max} (% Control ± SEM)	IC_{50} (μM ± SEM)	E_{max} (% Control ± SEM)	EC_{50} (μM ± SEM)	I_{max} (% Control ± SEM)	IC_{50} (μM ± SEM)
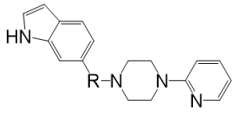	CH2	KU7-6	51.9 ± 13.8	1.6 ± 1.3	43.2 ± 11.6	11.3 ± 1.8	60.8 ± 6.0	9.3 ± 6.1	38.8 ± 4.1	1.6 ± 1.0
	CO	KU7-14	NA	NA	NA	NA	NA	NA	NA	NA
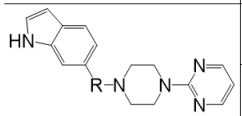	CH2	KU8-1	58.2 ± 1.4	0.04 ± 0.01	50 ± 6.8	1.3 ± 0.7	75.1 ± 7.1	0.1 ± 0.01	41.9 ± 9	5.9 ± 2.5
	CO	KU7-15	NA	NA	NA	NA	NA	NA	NA	NA
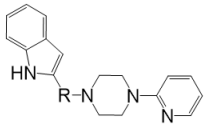	CH2	KU7-1	75.4 ± 7.6	0.2 ± 0.1	45.6 ± 12	11.8 ± 6	60.9 ± 6.4	0.7 ± 0.1	30 ± 1.0	3.3 ± 0.9
	CO	KU7-7	NA	NA	NA	NA	NA	NA	NA	NA
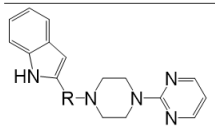	CH2	KU8-2	44.4 ± 1.7	0.6 ± 0.5	56 ± 1.3	6 ± 3.1	61.4 ± 11.7	1 ± 0.2	46 ± 5.7	4.1 ± 1.1
	CO	KU7-8	NA	NA	NA	NA	NA	NA	NA	NA

Yellow compounds are previously reported in Chapter 3. Red compounds appear in multiple tables.

SAR: aromaticity of ring D and nitrogen placement around ring D are integral to G protein and arrestin agonist activity

Based on previously published SAR and the pharmacophore model, the pyridine moiety of MLS1547 (Figure 29B, area 4) is believed to confer increased agonist potency, likely through formation of a hydrogen bond to T412 of the D2R. To further dissect the influence of the pyridine ring, we initially replaced it with a non-aromatic cyclohexane group within the context of both G protein biased and non-biased scaffolds (Table 9). Notably, each of these analogs lost all agonist activity at both G protein- and arrestin-mediated signaling. These data indicate that the aromaticity of ring D is essential for agonist activity. All of the compounds with the cyclohexane substituents did retain affinity for the D2R as evidenced by their ability to antagonize both G protein and arrestin recruitment activities. Further, as illustrated in Table 10, the addition of a bulky functional group to ring D in the para position relative to the piperazine ring resulted in a complete loss of all activity (see MLS1547 vs. KU4-2, and KU1-6 vs. KU4-1 or KU3-12). This highlights the importance of ring D for compound activity and suggests that substitutions at the para position are detrimental for receptor interactions.

Table 9: Changing ring D from an aromatic group to non-aromatic cyclohexane causes loss in G protein and arrestin agonist activity.

Scaffold	R	Sibley ID	D2 cAMP HitHunter Assay				D2 Arrestin PathHunter Assay			
			E_{max} (% Control ± SEM)	EC_{50} (μM ± SEM)	I_{max} (% Control ± SEM)	IC_{50} (μM ± SEM)	E_{max} (% Control ± SEM)	EC_{50} (μM ± SEM)	I_{max} (% Control ± SEM)	IC_{50} (μM ± SEM)
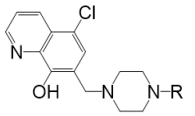		MLS1547	95.4 ± 8.9	2.2 ± 0.6	NA	NA	NA	NA	100 ± 0	20.4 ± 5.3
		KU5-4	NA	NA	58.3 ± 9.1	4.79 ± 0.57	NA	NA	114.9 ± 2.2	2.77 ± 0.11
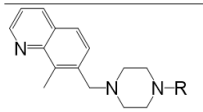		KU2-7	48.9 ± 5.4	1.4 ± 0.7	45.8 ± 12.6	11.5 ± 4	22 ± 1.6	9.3 ± 2.9	69.3 ± 9.8	4.6 ± 1.7
		KU5-5	NA	NA	109.6 ± 4	7.51 ± 3.14	NA	NA	109 ± 4.3	3.4 ± 0.21
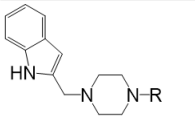		KU7-1	75.4 ± 7.6	0.2 ± 0.1	45.6 ± 12	11.8 ± 6	60.9 ± 6.4	0.7 ± 0.1	30 ± 1.0	3.3 ± 0.9
		KU7-3	NA	NA	84.3 ± 10.7	36.5 ± 10.9	NA	NA	109.8 ± 3.3	6.7 ± 0.9
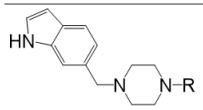		KU7-6	51.9 ± 13.8	1.6 ± 1.3	43.2 ± 11.6	11.3 ± 1.8	60.8 ± 6.0	9.3 ± 6.1	38.8 ± 4.1	1.6 ± 1.0
		KU8-5	NA	NA	90 ± 4.1	12.4 ± 8.7	NA	NA	97.4 ± 5.2	2.8 ± 1.0

Yellow compounds are previously reported in Chapter 3. Red compounds appear in multiple tables.

Table 10: Adding a bulky functional group para to the linker on ring D causes loss in G protein and arrestin agonist activity.

Scaffold	R	Sibley ID	D2 cAMP HitHunter Assay				D2 Arrestin PathHunter Assay			
			E_{max} (% Control ± SEM)	EC_{50} (μM ± SEM)	I_{max} (% Control ± SEM)	IC_{50} (μM ± SEM)	E_{max} (% Control ± SEM)	EC_{50} (μM ± SEM)	I_{max} (% Control ± SEM)	IC_{50} (μM ± SEM)
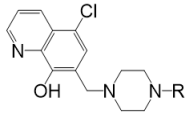		MLS1547	95.4 ± 8.9	2.2 ± 0.6	NA	NA	NA	NA	100 ± 0	20.4 ± 5.3
	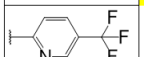	KU4-2	NA	NA	NA	NA	NA	NA	NA	NA
		KU1-6	83.8 ± 8.5	3.5 ± 3.4	15 ± 10.4	9.9 ± 5.4	NA	NA	127.2 ± 11.4	7.8 ± 1.6
	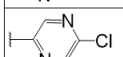	KU4-1	NA	NA	NA	NA	NA	NA	84.6 ± 12.5	36.4 ± 2.2
	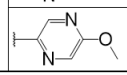	KU3-12	NA	NA	NA	NA	NA	NA	100 ± 0	12.29 ± 0.54

Yellow compounds are previously reported in Chapter 3. Red compounds appear in multiple tables.

To further investigate the role of the pyridine moiety in MLS1547 activity, we modified the location of the nitrogen atom within the ring. Firstly, Table 11 shows that removing the nitrogen altogether reduces agonist efficacy, as previously reported[212]. Further, moving the nitrogen to the meta position (Table 11) results in a complete loss of activity within the context of MLS1547 (see KU3-6 and KU3-5) as well as the active analogs KU7-1 and KU7-6 (see KU7-4 and KU8-3). Similarly, moving the nitrogen to the para position (Table 11) is not tolerated and results in a complete loss of activity within the context of several active scaffolds (see MLS1547, KU7-1, and KU2-7 vs. KU3-5, KU7-2 and KU3-11). These latter results correlate with those obtained with analogs containing substitutions at the para position on ring D (Table 5), which were likewise not tolerated. Overall, these data illustrate the importance of a nitrogen at the ortho position of ring D in order for the compound to exert agonist activity at the D2R.

We were next interested in examining the effects of adding a second nitrogen to ring D while maintaining the presence of a nitrogen at the ortho position (Table 12, Table 13, and Table 14). Initially, a second nitrogen was added at the second ortho (Table 12) position within the context of highly (MLS1547) or moderately (KU2-4 and KU2-7) G protein biased, or non-biased (KU7-1 and KU7-6) agonists. In general, this substitution was well tolerated with respect to G protein-mediated signaling. In fact, the potencies for agonist activity increased in all cases. Additionally, for compounds with a benzene for ring B (MLS1547, KU2-4, and KU2-7), no significant change in G protein agonist efficacy was seen when ring D was changed (KU 1-1, KU2-6, and KU2-8). However, in compounds with a pyrrole for ring B (KU7-1 and KU7-6), adding a second ortho nitrogen to ring D caused a decrease in G protein agonist efficacy (see KU7-1 vs. KU8-1).

Notably, in most cases there was also an increase in arrestin-mediated recruitment (see KU1-1, KU2-6, KU2-8), although this was not seen when the parent compound was unbiased (see KU8-1, KU8-2). Thus, addition of a second ortho nitrogen in ring D generally resulted in loss of G protein bias when compared to compounds with a single ortho nitrogen, although the dual ortho nitrogen containing compounds did retain agonist activity at the D2R.

The effects of adding a second nitrogen at the meta position of ring D in the presence of a nitrogen at the ortho position was next investigated (Table 13). Within the context of the parent MLS1547 scaffold, this substitution was well tolerated (KU1-6) and G protein bias was maintained, albeit with a slight decrease in G protein-mediated signaling efficacy. Interestingly, within the context of the partial, but G protein biased agonist KU2-3, the addition of a meta nitrogen resulted in an increase in G protein signaling efficacy (KU2-2). Markedly, in these cases, both of the parent scaffolds contain a chloro group in area 1 (Figure 29A). In contrast, within the context of the less biased KU2-7 scaffold lacking a chloro group in area 1, the addition of a meta nitrogen resulted in a complete loss of activity (KU3-9).

Finally, we investigated the addition of a second nitrogen at the para position of ring D in the presence of a nitrogen at the ortho position (Table 14). In all cases (KU3-13, KU7-5 and KU8-4), this resulted in a complete loss of activity for both G protein- and arrestin-mediated D2R signaling. This finding is consistent with the results observed when the single nitrogen on the pyridine is moved from the ortho to para position (Table 11) or the addition of a bulky functional group at the para position (Table 10). These data

support the need for a single nitrogen ortho to the linker without any substitution at the para position to maintain the activity and bias of the parent compound.

Generally it has been observed that although the addition of a second ortho nitrogen increases potency, it also results in a less biased compound. Overall adding a second nitrogen ortho or meta to the linker causes somewhat scaffold-dependent effects, whereas a second nitrogen para to the linker causes a loss of agonist activity. Consequently, it seems that overall nitrogen number and location is an essentially component to the bias agonist activity of the pharmacophore.

Table 11: Removing the nitrogen from ring D or moving the ortho nitrogen to the meta/para position relative to the linker causes loss in G protein and arrestin activity.

Scaffold	R	Sibley ID	D2 cAMP HitHunter Assay				D2 Arrestin PathHunter Assay			
			E_{max} (% Control ± SEM)	EC_{50} (μM ± SEM)	I_{max} (% Control ± SEM)	IC_{50} (μM ± SEM)	E_{max} (% Control ± SEM)	EC_{50} (μM ± SEM)	I_{max} (% Control ± SEM)	IC_{50} (μM ± SEM)
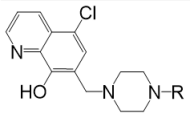		MLS1547	95.4 ± 8.9	2.2 ± 0.6	NA	NA	NA	NA	100 ± 0	20.4 ± 5.3
		NCGC1-D01	66.8 ± 3.9	2.8 ± 1.2			NA	NA		
		KU3-6	NA	NA	NA	NA	NA	NA	100 ± 0	3.06 ± 0.8
		KU3-5	NA	NA	NA	NA	NA	NA	100 ± 0	11.62 ± 6.33
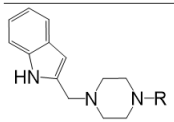		KU7-1	75.4 ± 7.6	0.2 ± 0.1	45.6 ± 12	11.8 ± 6	60.9 ± 6.4	0.7 ± 0.1	30 ± 1.0	3.3 ± 0.9
		KU7-4	NA	NA	80.4 ± 15.9	28.5 ± 9.9	NA	NA	88.9 ± 1.1	6.5 ± 1.2
		KU7-2	NA	NA	NA	NA	NA	NA	NA	NA
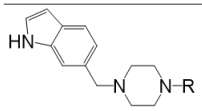		KU7-6	51.9 ± 13.8	1.6 ± 1.3	43.2 ± 11.6	11.3 ± 1.8	60.8 ± 6.0	9.3 ± 6.1	38.8 ± 4.1	1.6 ± 1.0
		KU8-3	NA	NA		>100		>39	NA	NA
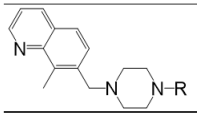		KU2-7	48.9 ± 5.4	1.4 ± 0.7	45.8 ± 12.6	11.5 ± 4	22 ± 1.6	9.3 ± 2.9	69.3 ± 9.8	4.6 ± 1.7
		KU3-11	NA	NA	NA	NA	NA	NA	NA	NA

Yellow compounds are previously reported in Chapter 3. Red compounds appear in multiple tables.

Table 12: Adding a second nitrogen ortho to the linker causes a gain in G protein agonist potency and arrestin agonist efficacy.

Scaffold	R	Sibley ID	D2 cAMP HitHunter Assay				D2 Arrestin PathHunter Assay			
			E_{max} (% Control ± SEM)	EC_{50} (μM ± SEM)	I_{max} (% Control ± SEM)	IC_{50} (μM ± SEM)	E_{max} (% Control ± SEM)	EC_{50} (μM ± SEM)	I_{max} (% Control ± SEM)	IC_{50} (μM ± SEM)
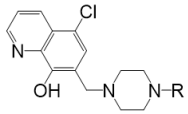		MLS1547	95.4 ± 8.9	2.2 ± 0.6	NA	NA	NA	NA	100 ± 0	20.4 ± 5.3
		KU1-1	92.8 ± 2.1	0.7 ± 0.2	NA	NA	21.6 ± 5.7	0.5 ± 0.3	92.8 ± 2.2	4.6 ± 2.4
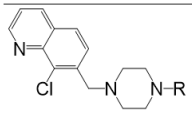		KU2-4	56.8 ± 8.3	6.6 ± 5.5	108.6 ± 89	34.6 ± 21.6	30.1 ± 1.1	7.3 ± 1.8	79.9 ± 12.1	17.9 ± 9.4
		KU2-6	59.3 ± 4.9	1.2 ± 0.4	NA	NA	53.4 ± 7.8	15.6 ± 8.8	NA	NA
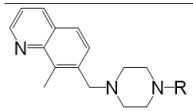		KU2-7	48.9 ± 5.4	1.4 ± 0.7	45.8 ± 12.6	11.5 ± 4	22 ± 1.6	9.3 ± 2.9	69.3 ± 9.8	4.6 ± 1.7
		KU2-8	58.7 ± 2.8	0.8 ± 0.4	NA	NA	46.5 ± 1.5	7.6 ± 1	73.2 ± 10.6	8.3 ± 2.9
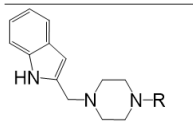		KU7-1	75.4 ± 7.6	0.2 ± 0.1	45.6 ± 12	11.8 ± 6	60.9 ± 6.4	0.7 ± 0.1	30 ± 1.0	3.3 ± 0.9
		KU8-1	58.2 ± 1.4	0.04 ± 0.01	50 ± 6.8	1.3 ± 0.7	75.1 ± 7.1	0.1 ± 0.01	41.9 ± 9	5.9 ± 2.5
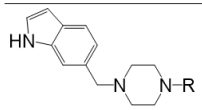		KU7-6	51.9 ± 13.8	1.6 ± 1.3	43.2 ± 11.6	11.3 ± 1.8	60.8 ± 6.0	9.3 ± 6.1	38.8 ± 4.1	1.6 ± 1.0
		KU8-2	44.4 ± 1.7	0.6 ± 0.5	56 ± 1.3	6 ± 3.1	61.4 ± 11.7	1 ± 0.2	46 ± 5.7	4.1 ± 1.1

Yellow compounds are previously reported in Chapter 3. Red compounds appear in multiple tables.

Table 13: Adding a second nitrogen meta to the linker causes decreased G protein activation potency, and scaffold dependent effects on G protein activation efficacy.

Scaffold	R	Sibley ID	D2 cAMP HitHunter Assay				D2 Arrestin PathHunter Assay			
			E_{max} (% Control ± SEM)	EC_{50} (μM ± SEM)	I_{max} (% Control ± SEM)	IC_{50} (μM ± SEM)	E_{max} (% Control ± SEM)	EC_{50} (μM ± SEM)	I_{max} (% Control ± SEM)	IC_{50} (μM ± SEM)
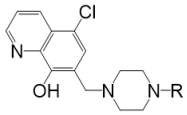		MLS1547	95.4 ± 8.9	2.2 ± 0.6	NA	NA	NA	NA	100 ± 0	20.4 ± 5.3
		KU1-6	83.8 ± 8.5	3.5 ± 3.4	15 ± 10.4	9.9 ± 5.4	NA	NA	127.2 ± 11.4	7.8 ± 1.6
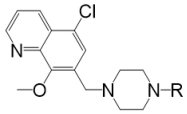		KU2-3	37.9 ± 8.1	13.4 ± 11.7	79.9 ± 0.8	2.5 ± 0.8	NA	NA	114.9 ± 0.7	4.5 ± 0.8
		KU2-2	57.2 ± 11.4	20.2 ± 12.1	NA	NA	NA	NA	127.2 ± 15.6	20.3 ± 7.6
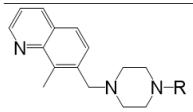		KU2-7	48.9 ± 5.4	1.4 ± 0.7	45.8 ± 12.6	11.5 ± 4	22 ± 1.6	9.3 ± 2.9	69.3 ± 9.8	4.6 ± 1.7
		KU3-9	NA	NA	NA	NA	NA	NA	NA	NA

Yellow compounds are previously reported in Chapter 3. Red compounds appear in multiple tables.

Table 14: Adding a second nitrogen para to the linker causes loss in G protein and arrestin agonist activity.

Scaffold	R	Sibley ID	D2 cAMP HitHunter Assay				D2 Arrestin PathHunter Assay			
			E_{max} (% Control ± SEM)	EC_{50} (μM ± SEM)	I_{max} (% Control ± SEM)	IC_{50} (μM ± SEM)	E_{max} (% Control ± SEM)	EC_{50} (μM ± SEM)	I_{max} (% Control ± SEM)	IC_{50} (μM ± SEM)
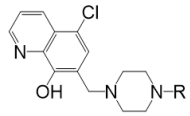		MLS1547	95.4 ± 8.9	2.2 ± 0.6	NA	NA	NA	NA	100 ± 0	20.4 ± 5.3
		KU3-13	NA	NA	NA	NA	NA	NA	100 ± 0	5.66 ± 2.24
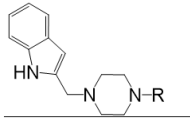		KU7-1	75.4 ± 7.6	0.2 ± 0.1	45.6 ± 12	11.8 ± 6	60.9 ± 6.4	0.7 ± 0.1	30 ± 1.0	3.3 ± 0.9
		KU7-5	NA	NA	NA	NA	NA	NA	NA	NA
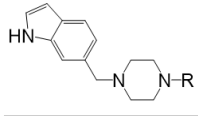		KU7-6	51.9 ± 13.8	1.6 ± 1.3	43.2 ± 11.6	11.3 ± 1.8	60.8 ± 6.0	9.3 ± 6.1	38.8 ± 4.1	1.6 ± 1.0
		KU8-4	NA	NA	NA	NA	NA	NA	NA	NA

Yellow compounds are previously reported in Chapter 3. Red compounds appear in multiple tables.

Discussion

In Chapter 3, the first identification of a G protein biased agonist, MLS1547, for the D2R was reported. Here, additional aspects were investigated with respect to MLS1547 SAR and G protein biased signaling. First, it was investigated whether or not MLS1547 would stimulate D2R internalization, which is believed to be dependent on β-arrestin-2 recruitment to the D2R[27,200]. The data generated from experiments performed in both non-native cells and MSNs indicated that MLS1547 is a strongly biased compound that stimulated only a very low degree of arrestin recruitment to the D2R (Figure 27 and Figure 28). It is possible that the discrepancy between the functional arrestin-recruitment assays, which report no arrestin recruitment to the D2R (Figure 23), and the internalization assays, which report D2R internalization (Figure 27 and Figure 28) is due to a combination of factors involving experimental design and/or cellular context.

The differences between β-arrestin-2 recruitment and internalization data may also be due to differences in assay sensitivity. This is supported by the different results seen in the ICC vs. TIRF data, which share the exact same batches of cells harvested and transfected on the same days, and differ only in the technique applied to detect receptor internalization. In the ICC data, MLS1547 stimulates a low, but statistically significant amount of D2R internalization when compared to the control (Figure 28A). However, while the TIRF microscopy method showed a trend towards an elevated level of MLS1547-stimulated D2R internalization, it was not statistically significant (Figure 28B). These results suggest that MLS1547 may stimulate a low degree of β-arrestin-2 recruitment that was not measurable in the direct assays utilized which results in a low

amount of receptor internalization with prolonged treatment. In this scenario, the conclusion would be that MLS1547 is highly, but incompletely biased for G protein signaling. Alternatively, the small amount of MLS1547-induced D2R internalization may be occurring through an arrestin-independent mechanism. There is precedent for this in other receptor systems where arrestin-independent internalization has been observed[215].

Although MLS1547 stimulates a low degree of D2R internalization, this does not mean that a D2R internalization deficient agonist cannot be found. It has been demonstrated that G protein activation can function independently from arrestin recruitment when the D2R is activated. One study found that mutating four D2R residues (I212A+Y213A+I214A+V215A) in the third ICL caused the receptor to activate G protein signaling without causing arrestin-mediated D2R internalization when treated with a non-biased agonist[204,216]. Another study showed that a different set of mutations within the 3rd TM domain caused either G protein biased (L125N+Y133L) or arrestin biased (A135R+M140D) signaling when the D2R was stimulated with a non-biased agonist[205]. Our molecular modeling (Figure 26) adds to this body of work, showing that when interacting with a ligand, three residues in the 2nd extracellular loop (I184) and the 5th TM domain (F189, V190) may confer bias for G protein signaling[212]. Interestingly, mutating the D2LR at F189Y conferred D4R-like affinities to the mutated D2R for D4R ligands, indicating that this might be an important residue for receptor function[217]. Coincidentally, MLS1547 has the highest affinity for D4R, followed by D2R, then D3R (Figure 24 and Figure 25).

Because MLS1547 stimulated a small degree of D2R internalization, we sought to optimize the compound by increasing G protein activation potency while maintaining a

lack of detectable arrestin recruitment, and hopefully create a D2R compound that is internalization deficient. Such a compound might represent a lead for a therapeutic drug (for instance, in treating Parkinson's disease) as it might elicit prolonged stimulation of the D2R due to a lack of receptor desensitization/internalization. In addition, we wanted to build upon and refine the pharmacophore model by generating additional SAR.

Previously, we obtained 22 MLS1547 analogs and tested them in D2R functional assays for cAMP accumulation and β-arrestin-2 recruitment (see Chapter 3)[212]. These original analogs were chosen based on commercial availability and none showed improved G protein activation potency while maintaining bias. These data did, however, help us to devise a molecular model for how G protein biased signaling of the D2R can occur (Figure 26). Using this model, 46 additional MLS1547 analogs were synthesized. While a compound with improved potency at G protein signaling was not found, these compounds enabled the development of additional SAR which both reinforced and refined the existing model for G protein biased D2R agonist binding.

Most of the SAR confirmed the importance of molecular signatures proposed to be essential for G protein bias, such as a hydrophobic binding moiety and the aromaticity at ring D as well as the placement of the nitrogens around that ring. Beyond that, two new chemical characteristics were proposed to be important for G protein bias D2R activation: the hydroxyl group on ring B (Table 7; Figure 29, area 2) and the linker region between rings B and C (Table 8; Figure 29, area 3). These areas open the door for a better understanding of ligand binding to the D2R, and will enable us to identify residues that may interact with biased ligands at the D2R.

Chapter 5: D2R β-arrestin-2 biased Ligands Screen

Background

As described in the introduction sections of Chapters 3 and 4, there may be utility for either G protein or arrestin biased ligands. Chapters 3 and 4 outlined the results of a G protein biased agonist screen, of which there were no preceding examples for the D2R. However, there was precedent for low efficacy arrestin biased D2R agonists[165,166], indicating that more potent and efficacious arrestin biased D2R ligands may exist.

In addition to functional selectivity, targeting allosteric receptor sites is a novel way to narrow the signaling capabilities of a ligand. Allosteric ligands can affect the receptor in one of three ways (Figure 30): altering the affinity of an orthosteric binding ligand, altering the efficacy of an orthosteric binding ligand, or independently stimulating or inhibiting receptor signaling. It is important to note that by definition, a functionally selective antagonist must be allosteric, as it would inhibit one pathway while allowing the activation of other parallel pathways. Because allosteric binding sites are separate from the orthosteric binding site, where residues are more highly conserved, an allosteric ligand is more likely to interact with residues that are divergent between receptors of the same class and/or family. As a result, an allosteric *and* functionally selective D2R ligand could potentially function as a highly subtype-selective, biased probe for D2R function.

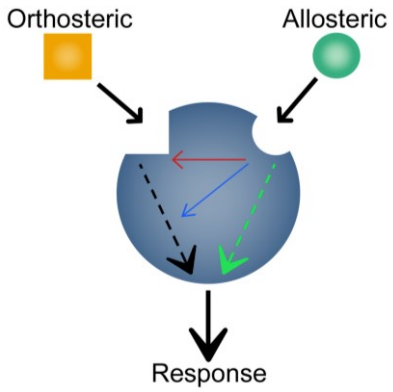

Figure 30: Allosteric modulation of GPCRs.
Allosteric compounds either directly alter downstream signaling (green line) or alter the affinity (red line) or efficacy (blue line) of the orthosteric compound).

Allosteric binding sites have already been identified for the D2R[218], and theoretically, there is almost unlimited potential for the identification of other allosteric sites[219–221]. With the therapeutic and investigative value of a functionally selective/allosteric D2R ligand in mind, a screen to detect arrestin biased D2R agonists, antagonists, and potentiators was performed by our lab.

Materials and Methods

See Chapters 3 and 4 Materials and Methods section for assays. See Results section for screening procedure.

Results

The arrestin biased D2R ligand screen was performed using the same compound library and functional assays used in the G protein biased D2R ligand screen (Chapter 3). The key difference was in the way the screen was performed (cf. Figure 20 and Figure 31). This assay was performed twice, once using an EC_{20} concentration of DA to detect potentiators, and once using an EC_{80} concentration of DA to detect potential antagonists. Each screen employed a two-add, two-read protocol (Figure 32) applied to the DiscoveRx D2R-β-arrestin-2 assay. First the library compound was added, followed by a detector read, then an $EC_{20/80}$ concentration of DA was added, followed by a second detector read. Consequently, three assay scenarios resulted in a three pools of "hits":

1. Agonists (either allosteric or orthosteric): the library compound exhibited agonist activity in the first read, producing a signal.
2. Potentiators (allosteric): the compound potentiated the signal stimulated by an EC_{20} concentration of DA.
3. Antagonists (allosteric): the compound inhibited the signal stimulated by an EC_{80} concentration of DA.

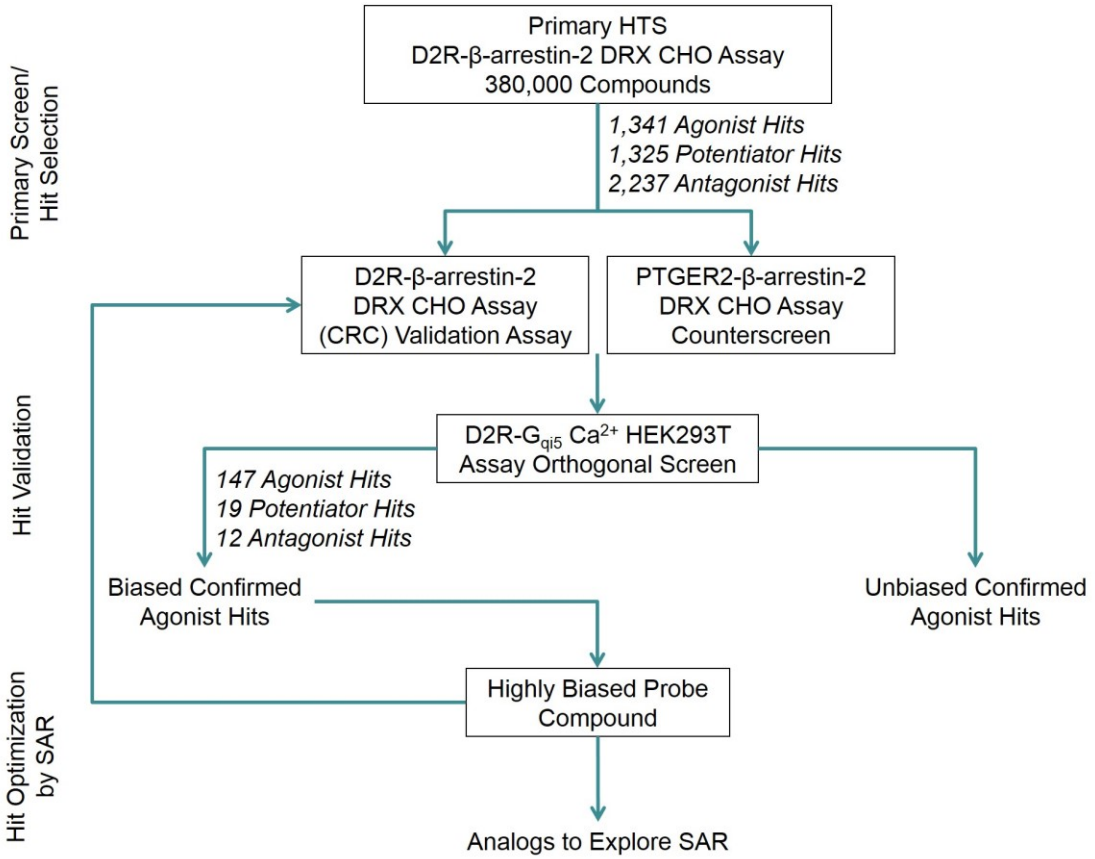

Figure 31: Flowchart of the D2R arrestin biased screen protocol.
Abbreviations: CRC (concentration response curve), HTS (high-throughput screen), PTGER2 (prostaglandin receptor 2), SAR (structure-activity relationships).

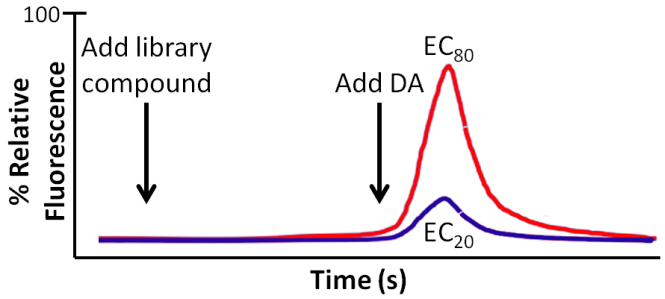

Figure 32: Compound add steps for arrestin biased D2R screens.
This schematic depicts the screening paradigm for detecting agonists (first compound add, both red and purple lines), antagonists (red line, second add), and potentiators (purple line, second add).

Compounds were selected from each pool of hits, based on their potency, efficacy, and chemical diversity, and were subjected to various secondary counterscreens (Figure 31), similar to the G protein biased agonist screen. 1,341 agonists, 1,325

potentiators, and 2,237 antagonist hits were detected in the primary screen. For the antagonists, an additional prostaglandin counter screen was performed to weed out compounds that inhibited the β-galactosidase enzyme integral to the arrestin assay instead of the receptor itself. Twelve antagonists passed the prostaglandin counter screen, and 6 were sent to us by our collaborators at NCATS. The other 6 antagonists were unavailable commercially, and were dropped from the validation step. None of the potentiators or antagonists were validated in our lab as biased compounds. However, one agonist, dihydroergocornine showed arrestin biased signaling (Figure 33). Unfortunately, a pure formulation of this compound was not available commercially and it was not cost effective to synthesize this compound, so we were not able to do further testing on this compound.

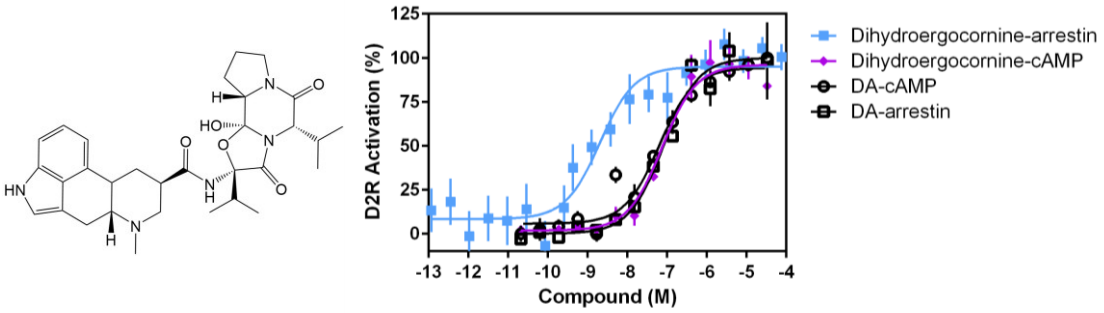

Figure 33: Comparison of cAMP and arrestin assay data for β-arrestin-2 biased D2R agonist. Compounds were tested as agonists in the arrestin recruitment and cAMP accumulation DiscoveRx assays. Dihydroergocornine showed a 100-fold bias towards arrestin recruitment by potency which was not seen with the dopamine (DA) control. Data are representative of 3-4 independent experiments and plotted as a percentage of the maximum response observed with dopamine (arrestin assay), or as a percentage of the maximum inhibition of forskolin response (cAMP assay). Dihydroergocornine cAMP E_{max} = 81.9% ± 12.1, EC_{50} = 74.1 nM ± 38.7; dihydroergocornine arrestin E_{max} = 86.3% ± 8.1, EC_{50} = 0.8 nM ± 0.7; DA cAMP E_{max} = 94.8% ± 2.3, EC_{50} = 24.4 nM ± 12.5; DA arrestin E_{max} = 100% ± 0, EC_{50} = 102.5 nM ± 17.4.

Discussion

The goal of this screen was to identify allosteric or orthosteric arrestin biased ligands targeting the D2R. These compounds could then be used as scaffold for SAR interrogation and pharmacological optimization to increase selectivity, potency, and stability. However, we were unable to identify any compounds that could move out of the screening stage into the optimization/development stage.

The preliminary identification of dihydroergocornine as an arrestin biased agonist seemed promising (Figure 33). Dihydroergocornine is a member of the ergopeptine (a.k.a. ergopeptide) family of compounds. Ergopeptines and ergolines are validated agonists of several neurotransmitter receptors including the DARs. In fact, another ergopeptine, bromocriptine, is used to treat Parkinson's disease[222,223]. Dihydroergocornine is often found in a tripartite mix of ergopeptines (dihydroergocristine, dihydroergocryptine, and dihydroergocornine) called dihydroergotoxine or ergoloid mesylate, which is used to treat age-related cognitive impairment and also stroke victims. Unfortunately, no sources for pure dihydroergocornine could be found for further testing. A dihydroergocornine analog, ergocornine, which differs only by the saturation of a double bond was also of interest (Figure 34, red bonds). However, like dihydroergocornine, a source for ergocornine could not be found.

In the hopes that other ergopeptines might exhibit arrestin biased agonism, several compounds belonging to the ergopeptine class were tested using the DiscoveRx cAMP accumulation and arrestin recruitment assays. They were found to be unbiased D2R agonists (see Figure 34 for structures, data not shown). However, a more systematic testing of other ergolines and ergopeptines for biased signaling may be warranted in future studies.

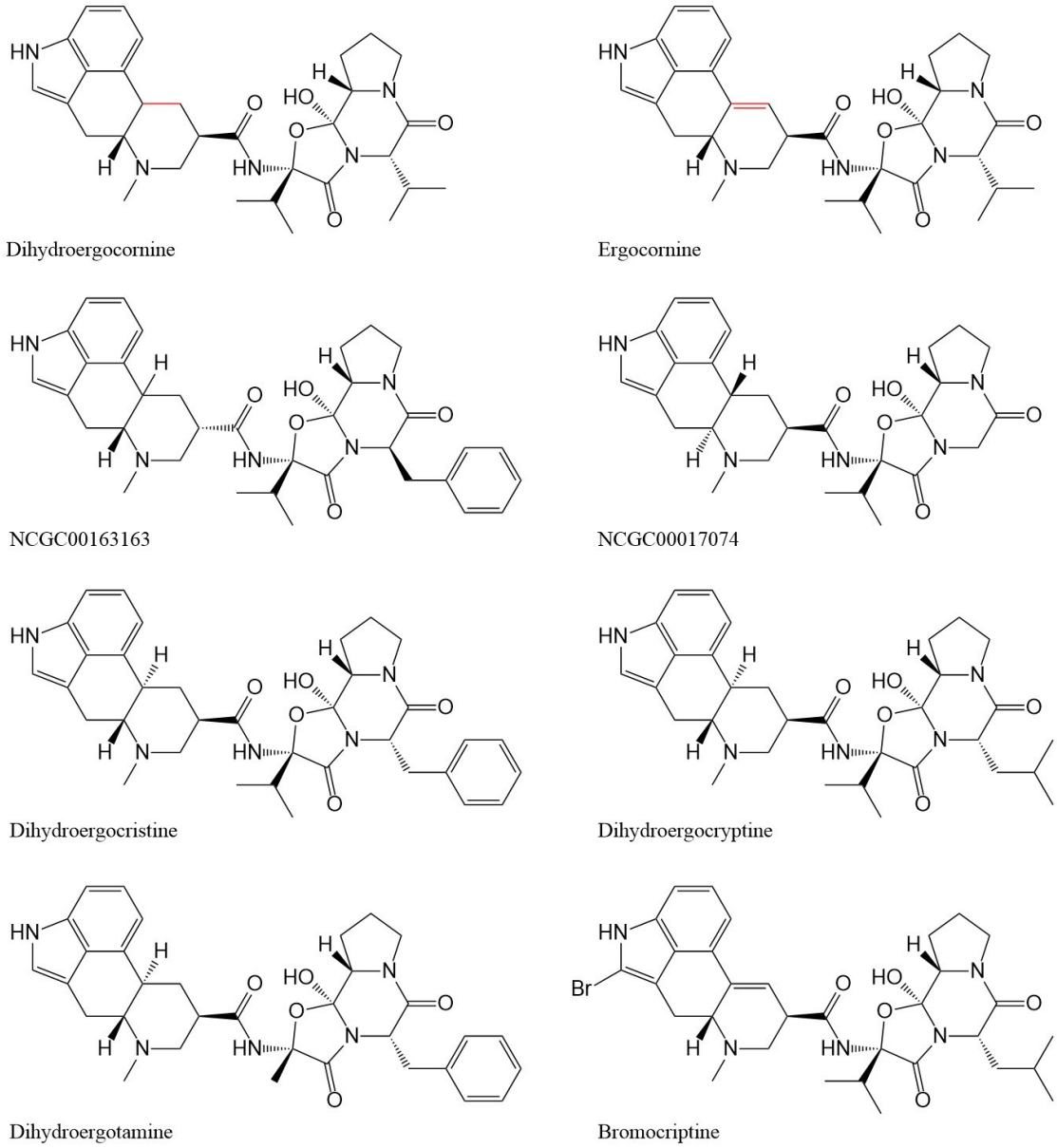

Figure 34: Non-biased ergopeptines tested in cAMP accumulation and arrestin recruitment assays.

Dihydroergocornine was found to show some D2R arrestin biased agonist activity (Figure 33). Ergocornine was a close analogue of dihydroergocornine that differed only in that a single bond became a double bond (red bonds), but could not be obtained for testing. Six other ergopeptines were tested in D2R cAMP and D2R arrestin DiscoveRx assays and were found to be unbiased D2R agonists (data not shown).

Chapter 6: Conclusions and Future Directions

The aim of this dissertation was to develop a better understanding of DAR function by investigating two aspects of D1R and D2R signaling: synergistic D1R-D2R activation of Ca^{2+} mobilization, and functionally selective signaling of the D2R. Both signaling mechanisms take advantage of the conformational fluidity inherent in the DARs and other GPCRs to cause selective activation of specific signaling cascades. This idea is supported by a body of work that indicates there are many different ways to manipulate GPCR protein conformation to modulate signaling[224]. The B2 bradykinin receptor has been shown to respond directly to cell membrane fluidity, changing its conformation and consequent signaling capabilities depending on the state of the membrane, independently of ligand-mediated modulation[225]. Using the β2 adrenergic receptor, it was shown that different ligands could stimulate slow or fast activation of signaling. The speed of receptor activation was thought to be due to the number of intermediate protein conformations (a.k.a. sequential binding states) between the inactive and active state, and the amount of time spent in each intermediate conformation[226]. Modeling has supported the idea of GPCR conformation plasticity[172,227,228], and the change in protein conformations has been more directly observed through crystallization of inactive- and active-state receptors[196,197,229].

In Chapter 2, the proposed D1R-D2R heteromer was investigated. There is evidence for the existence of heteromers involving other GPCRs[110], and our studies show that it is likely that the D1R and D2R work cooperatively to stimulate the observed Ca^{2+} response, but this cooperativity may not be due to direct interactions between the D1R and D2R in a heteromeric complex (Figure 18)[42]. In fact, one study found that the D1R-D2R could not cooperatively activate the G_q protein at all[78]. Furthermore, a presumed

D1R-D2R heteromer selective agonist, SKF83959, actually acted as a D1R-D2R antagonist (Figure 12) in our assays and has subsequently been shown to act as a homomeric D1R agonist[131,208]. SKF83959 was also found to bind to a wide variety of GPCRs and non-GPCRs such as the σ1 receptor (Table 1)[133], calling into question any *in vivo* studies where SKF83959 was used as a selective agonist of the D1R-D2R heteromer. It is entirely possible that atypical behavioral effects caused by SKF83959 that were previously attributed to activation of D1R-D2R heteromers or D1-like DARs are instead due to the activation of non-DAR targets[133].

In Chapters 3 and 5, a library of small molecules was screened against the D2R to detect G protein biased agonists and β-arrestin-2 biased agonists, antagonists, and potentiators. The arrestin screen was not successful in generating a biased antagonist or potentiator, but it did result in the detection of an arrestin biased agonist, dihydroergocornine (Figure 33), a member of the ergot alkaloid family. However, while further studies with dihydroergocornine, and its close analog ergocornine, were not possible due to cost and availability constraints, other ergopeptines were tested using β-arrestin-2 recruitment and cAMP accumulation assays (Figure 34). These ergopeptines were not found to be biased. However, many other ergot alkaloids (ergolines and ergopeptines) exist that might be of interest to test to see if one would serve as an arrestin biased agonist scaffold.

The G protein biased D2R screen was more fruitful and led to the identification and further characterization of the G protein biased agonist, MLS1547. A pharmacophore model based on preliminary SAR of twenty-two MLS1547 analogs was developed (Figure 26) and further refined by the SAR of an additional forty-six analogs in Chapter

4. It was confirmed that a hydrophobic binding moiety (Figure 29, Table 5, and Table 6) is important for G protein bias. Two additional regions of interest were identified on the MLS1547 chemical scaffold that contributed to D2R G protein signaling bias: a hydroxyl group (designated area 2 in Figure 29B; Table 7) and the linker between two aromatic rings (designated area 3 in Figure 29B; Table 8). Further, it was determined that the location of a single nitrogen or the placement of additional of nitrogens to ring D (Figure 29B) can affect G protein signaling bias and activity (Table 9 - Table 14). This SAR can be used to generate a more refined pharmacophore model. In addition, it may be used to rationally design an MLS1547 analog that has improved G protein activation potency while maintaining signaling bias.

Thus far, studying the chemical scaffold of MLS1547 and the resulting pharmacophore model has been helpful in understanding G protein biased signaling of the D2R. It will also be important to test the receptor side of the pharmacophore model; in particular, interrogation of the residues hypothesized to be important for MLS1547 binding and G protein bias. The hydrophobic moiety on MLS1547 is thought to interact with a binding pocket made up of the residues I184, F189, and V190. Likewise, the single nitrogen on ring D is thought to interact with T412. In future work, the D2R can be mutated at these residues and tested for G protein activation and β-arrestin-2 recruitment to see if this affects the signaling bias of the MLS1547 scaffold.

Notably, we found that in some cellular systems and assays, MLS1547 stimulated a low degree of D2R internalization (Figure 27 and Figure 28), but it is unclear whether this is due to arrestin-dependent or arrestin-independent mechanisms. Further studies are needed to determine the answer to this question.

Overall, this dissertation attempts to increase the understanding of DAR signaling through studying events that arise from changes in GPCR conformation. While many advances have been made, there are many remaining avenues of study to better understand D1R-D2R cooperativity and D2R biased signaling. It is my hope that this dissertation provides a meaningful body of work that will lead to improved targeting of the D1R and D2R for the purposes of probing *in vivo* signaling as well as the treatment of DAR-associated diseases.

References

1. Sunahara, R. K. *et al.* Human dopamine D1 receptor encoded by an intronless gene on chromosome 5. *Nature* **347,** 80–83 (1990).
2. Zhou, Q.-Y. *et al.* Cloning and expression of human and rat D1 dopamine receptors. *Nature* **347,** 76–80 (1990).
3. Dearry, A. *et al.* Molecular cloning and expression of the gene for a human D1 dopamine receptor. *Nature* **347,** 72–76 (1990).
4. Tiberi, M. *et al.* Cloning, molecular characterization, and chromosomal assignment of a gene encoding a second D1 dopamine receptor subtype: differential expression pattern in rat brain compared with the D1A receptor. *Proc. Natl. Acad. Sci.* **88,** 7491–7495 (1991).
5. Sunahara, R. K. *et al.* Cloning of the gene for a human dopamine D5 receptor with higher affinity for dopamine than D1. *Nature* **350,** 614–619 (1991).
6. Bunzow, J. R. *et al.* Cloning and expression of a rat D2 dopamine receptor cDNA. *Nature* **336,** 783–787 (1988).
7. Giros, B. *et al.* Alternative splicing directs the expression of two D2 dopamine receptor isoforms. *Nature* **342,** 923–926 (1989).
8. Monsma, F. J., McVittie, L. D., Gerfen, C. R., Mahan, L. C. & Sibley, D. R. Multiple D2 dopamine receptors produced by alternative RNA splicing. *Nature* **342,** 926–929 (1989).
9. Sokoloff, P., Giros, B., Martres, M.-P., Bouthenet, M.-L. & Schwartz, J.-C. Molecular cloning and characterization of a novel dopamine receptor (D3) as a target for neuroleptics. *Nature* **347,** 146–151 (1990).
10. Van Tol, H. H. M. *et al.* Cloning of the gene for a human dopamine D4 receptor with high affinity for the antipsychotic clozapine. *Nature* **350,** 610–614 (1991).
11. Tol, H. H. M. V. *et al.* Multiple dopamine D4 receptor variants in the human population. *Nature* **358,** 149–152 (1992).
12. Missale, C., Nash, S. R., Robinson, S. W., Jaber, M. & Caron, M. G. Dopamine receptors: from structure to function. *Physiol. Rev.* **78,** 189 –225 (1998).
13. Chien, E. Y. T. *et al.* Structure of the human dopamine D3 receptor in complex with a D2/D3 selective antagonist. *Science* **330,** 1091–1095 (2010).
14. Meador-Woodruff, J. H. *et al.* Comparison of the distributions of D1 and D2 dopamine receptor mRNAs in rat brain. *Neuropsychopharmacology* **5,** 231–242 (1991).
15. Yung, K. K. L. *et al.* Immunocytochemical localization of D1 and D2 dopamine receptors in the basal ganglia of the rat: Light and electron microscopy. *Neuroscience* **65,** 709–730 (1995).
16. Meador-Woodruff, J. H. *et al.* Distribution of D2 dopamine receptor mRNA in rat brain. *Proc. Natl. Acad. Sci. U. S. A.* **86,** 7625–7628 (1989).

17. Bouthenet, M. L. *et al.* Localization of dopamine D3 receptor mRNA in the rat brain using in situ hybridization histochemistry: comparison with dopamine D2 receptor mRNA. *Brain Res.* **564,** 203–219 (1991).

18. Picetti, R. *et al.* Dopamine D2 receptors in signal transduction and behavior. *Crit. Rev. Neurobiol.* **11,** 121–142 (1997).

19. Prou, D. *et al.* Intracellular retention of the two isoforms of the D(2) dopamine receptor promotes endoplasmic reticulum disruption. *J. Cell Sci.* **114,** 3517–3527 (2001).

20. Khan, Z. U., Mrzljak, L., Gutierrez, A., de la Calle, A. & Goldman-Rakic, P. S. Prominence of the dopamine D2 short isoform in dopaminergic pathways. *Proc. Natl. Acad. Sci.* **95,** 7731 –7736 (1998).

21. Meador-Woodruff, J. H. *et al.* Distribution of D5 dopamine receptor mRNA in rat brain. *Neurosci. Lett.* **145,** 209–212 (1992).

22. Khan, Z. U. *et al.* Dopamine D5 receptors of rat and human brain. *Neuroscience* **100,** 689–699 (2000).

23. Muly, E. C., Maddox, M. & Khan, Z. U. Distribution of D1 and D5 dopamine receptors in the primate nucleus accumbens. *Neuroscience* **169,** 1557–1566 (2010).

24. Stark, A. K. & Pakkenberg, B. Histological changes of the dopaminergic nigrostriatal system in aging. *Cell Tissue Res.* **318,** 81–92 (2004).

25. Little, K. Y. *et al.* Decreased brain dopamine cell numbers in human cocaine users. *Psychiatry Res.* **168,** 173–180 (2009).

26. Iversen, S. D. & Iversen, L. L. Dopamine: 50 years in perspective. *Trends Neurosci.* **30,** 188–193 (2007).

27. Beaulieu, J.-M. & Gainetdinov, R. R. The physiology, signaling, and pharmacology of dopamine receptors. *Pharmacol. Rev.* **63,** 182–217 (2011).

28. Holmes, A., Lachowicz, J. E. & Sibley, D. R. Phenotypic analysis of dopamine receptor knockout mice; recent insights into the functional specificity of dopamine receptor subtypes. *Neuropharmacology* **47,** 1117–1134 (2004).

29. Perreault, M. L. *et al.* The dopamine D1-D2 receptor heteromer localizes in dynorphin/enkephalin neurons. *J. Biol. Chem.* **285,** 36625 –36634 (2010).

30. Cools, A. R., Lubbers, L., van Oosten, R. V. & Andringa, G. SKF 83959 is an antagonist of dopamine D1-like receptors in the prefrontal cortex and nucleus accumbens: a key to its antiparkinsonian effect in animals? *Neuropharmacology* **42,** 237–245 (2002).

31. Pei, L. *et al.* Uncoupling the dopamine D1-D2 receptor complex exerts antidepressant-like effects. *Nat. Med.* **16,** 1393–1395 (2010).

32. Neves, S. R., Ram, P. T. & Iyengar, R. G Protein Pathways. *Science* **296,** 1636–1639 (2002).

33. Preininger, A. M. & Hamm, H. E. G Protein Signaling: Insights from New Structures. *Sci. Signal.* **2004,** re3–re3 (2004).

34. Hewavitharana, T. & Wedegaertner, P. B. Non-canonical signaling and localizations of heterotrimeric G proteins. *Cell. Signal.* **24,** 25–34 (2012).

35. Sibley, D. R. & Monsma Jr, F. J. Molecular biology of dopamine receptors. *Trends Pharmacol. Sci.* **13,** 61–69 (1992).

36. Gould, T. D. & Manji, H. K. DARPP-32: A molecular switch at the nexus of reward pathway plasticity. *Proc. Natl. Acad. Sci. U. S. A.* **102,** 253–254 (2005).

37. Valjent, E. *et al.* Regulation of a protein phosphatase cascade allows convergent dopamine and glutamate signals to activate ERK in the striatum. *Proc. Natl. Acad. Sci. U. S. A.* **102,** 491–496 (2005).

38. Flores-Hernández, J. *et al.* Dopamine Enhancement of NMDA Currents in Dissociated Medium-Sized Striatal Neurons: Role of D1 Receptors and DARPP-32. *J. Neurophysiol.* **88,** 3010–3020 (2002).

39. Friedman, E. *et al.* D1-like dopaminergic activation of phosphoinositide hydrolysis is independent of D(1A) dopamine receptors: Evidence from D(1A) knockout mice. *Mol. Pharmacol.* **51,** 6–11 (1997).

40. Sahu, A., Tyeryar, K. R., Vongtau, H. O., Sibley, D. R. & Undieh, A. S. D5 Dopamine Receptors are Required for Dopaminergic Activation of Phospholipase C. *Mol. Pharmacol.* **75,** 447 –453 (2009).

41. So, C. H. *et al.* Calcium signaling by dopamine D5 receptor and D5-D2 receptor hetero-oligomers occurs by a mechanism distinct from that for dopamine D1-D2 receptor hetero-oligomers. *Mol. Pharmacol.* **75,** 843 –854 (2009).

42. Chun, L. S. *et al.* D1-D2 dopamine receptor synergy promotes calcium signaling via multiple mechanisms. *Mol. Pharmacol.* **84,** 190–200 (2013).

43. Missale, C., Nash, S. R., Robinson, S. W., Jaber, M. & Caron, M. G. Dopamine Receptors: From Structure to Function. *Physiol. Rev.* **78,** 189–225 (1998).

44. Hernandez-Lopez, S. *et al.* D2 dopamine receptors in striatal medium spiny neurons reduce L-type Ca2+ currents and excitability via a novel PLC[beta]1-IP3-calcineurin-signaling cascade. *J. Neurosci. Off. J. Soc. Neurosci.* **20,** 8987–8995 (2000).

45. Kuzhikandathil, E. V., Yu, W. & Oxford, G. S. Human Dopamine D3 and D2L Receptors Couple to Inward Rectifier Potassium Channels in Mammalian Cell Lines. *Mol. Cell. Neurosci.* **12,** 390–402 (1998).

46. Lavine, N. *et al.* G Protein-coupled Receptors Form Stable Complexes with Inwardly Rectifying Potassium Channels and Adenylyl Cyclase. *J. Biol. Chem.* **277,** 46010–46019 (2002).

47. Yan, Z., Song, W.-J. & Surmeier, D. J. D2 Dopamine Receptors Reduce N-Type Ca2+ Currents in Rat Neostriatal Cholinergic Interneurons Through a Membrane-Delimited, Protein-Kinase-C-Insensitive Pathway. *J. Neurophysiol.* **77,** 1003–1015 (1997).

48. Lee, S. P. *et al.* Dopamine D1 and D2 receptor co-activation generates a novel phospholipase C-mediated calcium signal. *J. Biol. Chem.* **279,** 35671 –35678 (2004).

49. Evron, T., Daigle, T. L. & Caron, M. G. GRK2: multiple roles beyond G protein-coupled receptor desensitization. *Trends Pharmacol. Sci.* **33,** 154–164 (2012).

50. Ribas, C. *et al.* The G protein-coupled receptor kinase (GRK) interactome: Role of GRKs in GPCR regulation and signaling. *Biochim. Biophys. Acta BBA - Biomembr.* **1768,** 913–922 (2007).

51. Gainetdinov, R. R., Premont, R. T., Bohn, L. M., Lefkowitz, R. J. & Caron, M. G. Desensitization of G Protein–Coupled Receptors and Neuronal Functions. *Annu. Rev. Neurosci.* **27,** 107–144 (2004).

52. Felder, R. A. *et al.* G protein-coupled receptor kinase 4 gene variants in human essential hypertension. *Proc. Natl. Acad. Sci. U. S. A.* **99,** 3872–3877 (2002).

53. Ferguson, S. S. *et al.* Role of beta-arrestin in mediating agonist-promoted G protein-coupled receptor internalization. *Science* **271,** 363–366 (1996).

54. Namkung, Y., Dipace, C., Urizar, E., Javitch, J. A. & Sibley, D. R. G Protein-coupled Receptor Kinase-2 Constitutively Regulates D2 Dopamine Receptor Expression and Signaling Independently of Receptor Phosphorylation. *J. Biol. Chem.* **284,** 34103–34115 (2009).

55. Kang, D. S. *et al.* Structure of an arrestin2-clathrin complex reveals a novel clathrin binding domain that modulates receptor trafficking. *J. Biol. Chem.* **284,** 29860–29872 (2009).

56. Kim, Y.-M. & Benovic, J. L. Differential roles of arrestin-2 interaction with clathrin and adaptor protein 2 in G protein-coupled receptor trafficking. *J. Biol. Chem.* **277,** 30760–30768 (2002).

57. Laporte, S. A., Oakley, R. H., Holt, J. A., Barak, L. S. & Caron, M. G. The interaction of beta-arrestin with the AP-2 adaptor is required for the clustering of beta 2-adrenergic receptor into clathrin-coated pits. *J. Biol. Chem.* **275,** 23120–23126 (2000).

58. Goodman, O. B. *et al.* Beta-arrestin acts as a clathrin adaptor in endocytosis of the beta2-adrenergic receptor. *Nature* **383,** 447–450 (1996).

59. Kang, D. S., Tian, X. & Benovic, J. L. Role of β-arrestins and arrestin domain-containing proteins in G protein-coupled receptor trafficking. *Curr. Opin. Cell Biol.* **0,** 63–71 (2014).

60. Arriza, J. L. *et al.* The G-protein-coupled receptor kinases beta ARK1 and beta ARK2 are widely distributed at synapses in rat brain. *J. Neurosci. Off. J. Soc. Neurosci.* **12,** 4045–4055 (1992).

61. Gurevich, E. V., Benovic, J. L. & Gurevich, V. V. Arrestin2 and arrestin3 are differentially expressed in the rat brain during postnatal development. *Neuroscience* **109,** 421–436 (2002).

62. Kim, K. M. *et al.* Differential regulation of the dopamine D2 and D3 receptors by G protein-coupled receptor kinases and beta-arrestins. *J. Biol. Chem.* **276,** 37409–37414 (2001).

63. Oakley, R. H., Laporte, S. A., Holt, J. A., Barak, L. S. & Caron, M. G. Molecular determinants underlying the formation of stable intracellular G protein-coupled receptor-beta-arrestin complexes after receptor endocytosis*. *J. Biol. Chem.* **276,** 19452–19460 (2001).

64. Conner, D. A. *et al.* beta-Arrestin1 knockout mice appear normal but demonstrate altered cardiac responses to beta-adrenergic stimulation. *Circ. Res.* **81,** 1021–1026 (1997).

65. Butcher, A. J. *et al.* Differential G-protein-coupled receptor phosphorylation provides evidence for a signaling bar code. *J. Biol. Chem.* **286,** 11506–11518 (2011).

66. Nobles, K. N. *et al.* Distinct phosphorylation sites on the β(2)-adrenergic receptor establish a barcode that encodes differential functions of β-arrestin. *Sci. Signal.* **4,** ra51 (2011).

67. Namkung, Y., Dipace, C., Javitch, J. A. & Sibley, D. R. G Protein-Coupled Receptor Kinase-Mediated Phosphorylation Regulates Post-Endocytic Trafficking of the D2 Dopamine Receptor. *J. Biol. Chem.* **284,** 15038–15051 (2009).

68. Naga Prasad, S. V. *et al.* Phosphoinositide 3-kinase regulates beta2-adrenergic receptor endocytosis by AP-2 recruitment to the receptor/beta-arrestin complex. *J. Cell Biol.* **158,** 563–575 (2002).

69. Naga Prasad, S. V., Barak, L. S., Rapacciuolo, A., Caron, M. G. & Rockman, H. A. Agonist-dependent recruitment of phosphoinositide 3-kinase to the membrane by beta-adrenergic receptor kinase 1. A role in receptor sequestration. *J. Biol. Chem.* **276,** 18953–18959 (2001).

70. Ruiz-Gómez, A. & Mayor, F. Beta-adrenergic receptor kinase (GRK2) colocalizes with beta-adrenergic receptors during agonist-induced receptor internalization. *J. Biol. Chem.* **272,** 9601–9604 (1997).

71. Shiina, T. *et al.* Clathrin box in G protein-coupled receptor kinase 2. *J. Biol. Chem.* **276,** 33019–33026 (2001).

72. Ren, X.-R. *et al.* Different G protein-coupled receptor kinases govern G protein and beta-arrestin-mediated signaling of V2 vasopressin receptor. *Proc. Natl. Acad. Sci. U. S. A.* **102,** 1448–1453 (2005).

73. Kim, J. *et al.* Functional antagonism of different G protein-coupled receptor kinases for beta-arrestin-mediated angiotensin II receptor signaling. *Proc. Natl. Acad. Sci. U. S. A.* **102,** 1442–1447 (2005).

74. Guo, Q., Subramanian, H., Gupta, K. & Ali, H. Regulation of C3a Receptor Signaling in Human Mast Cells by G Protein Coupled Receptor Kinases. *PLoS ONE* **6,** (2011).

75. Perrino, C. *et al.* Restoration of beta-adrenergic receptor signaling and contractile function in heart failure by disruption of the betaARK1/phosphoinositide 3-kinase complex. *Circulation* **111,** 2579–2587 (2005).

76. Gerfen, C. *et al.* D1 and D2 dopamine receptor-regulated gene expression of striatonigral and striatopallidal neurons. *Science* **250,** 1429 –1432 (1990).

77. Hersch, S. *et al.* Electron microscopic analysis of D1 and D2 dopamine receptor proteins in the dorsal striatum and their synaptic relationships with motor corticostriatal afferents. *J. Neurosci.* **15,** 5222 –5237 (1995).

78. Frederick, A. L. *et al.* Evidence against dopamine D1/D2 receptor heteromers. *Mol. Psychiatry* (2015). doi:10.1038/mp.2014.166

79. Aizman, O. *et al.* Anatomical and physiological evidence for D1 and D2 dopamine receptor colocalization in neostriatal neurons. *Nat. Neurosci.* **3,** 226–230 (2000).

80. Bertran-Gonzalez, J. *et al.* Opposing patterns of signaling activation in dopamine D1 and D2 receptor-expressing striatal neurons in response to cocaine and haloperidol. *J. Neurosci.* **28,** 5671 –5685 (2008).

81. Lester, J., Fink, S., Aronin, N. & DiFiglia, M. Colocalization of D1 and D2 dopamine receptor mRNAs in striatal neurons. *Brain Res.* **621,** 106–110 (1993).

82. Le Moine, C., Normand, E. & Bloch, B. Phenotypical characterization of the rat striatal neurons expressing the D1 dopamine receptor gene. *Proc. Natl. Acad. Sci.* **88,** 4205 –4209 (1991).

83. Le Moine, C. & Bloch, B. D1 and D2 dopamine receptor gene expression in the rat striatum: Sensitive cRNA probes demonstrate prominent segregation of D1 and D2 mRNAS in distinct neuronal populations of the dorsal and ventral striatum. *J. Comp. Neurol.* **355,** 418–426 (1995).

84. Surmeier, D. J. *et al.* Dopamine receptor subtypes colocalize in rat striatonigral neurons. *Proc. Natl. Acad. Sci.* **89,** 10178 –10182 (1992).

85. Surmeier, D. J., Song, W.-J. & Yan, Z. Coordinated expression of dopamine receptors in neostriatal medium spiny neurons. *J. Neurosci.* **16,** 6579 –6591 (1996).

86. Kebabian, J. W. & Calne, D. B. Multiple receptors for dopamine. *Nature* **277,** 93–96 (1979).

87. Calne, D. B., Kebabian, J., Silbergeld, E. & Evarts, E. Advances in the neuropharmacology of parkinsonism. *Ann. Intern. Med.* **90,** 219 –229 (1979).

88. Clark, D. & White, F. J. Review: D1 dopamine receptor-the search for a function: a critical evaluation of the DUD2 dopamine receptor classification and its functional implications. *Synapse* **1,** 347–388 (1987).

89. Calabresi, P., Maj, R., Mercuri, N. B. & Bernardi, G. Coactivation of D1 and D2 dopamine receptors is required for long-term synaptic depression in the striatum. *Neurosci. Lett.* **142,** 95–99 (1992).

90. Gerfen, C., Keefe, K. & Gauda, E. D1 and D2 dopamine receptor function in the striatum: coactivation of D1- and D2-dopamine receptors on separate populations of

neurons results in potentiated immediate early gene response in D1-containing neurons. *J. Neurosci.* **15,** 8167 –8176 (1995).

91. Kita, K., Shiratani, T., Takenouchi, K., Fukuzako, H. & Takigawa, M. Effects of D1 and D2 dopamine receptor antagonists on cocaine-induced self-stimulation and locomotor activity in rats. *Eur. Neuropsychopharmacol.* **9,** 1–7 (1999).

92. Svenningsson, P., Fredholm, B. B., Bloch, B. & Le Moine, C. Co-stimulation of D1/D5 and D2 dopamine receptors leads to an increase in c-fos messenger RNA in cholinergic interneurons and a redistribution of c-fos messenger RNA in striatal projection neurons. *Neuroscience* **98,** 749–757 (2000).

93. Mahan, L. C., Burch, R. M., Monsma, F. J. & Sibley, D. R. Expression of striatal D1 dopamine receptors coupled to inositol phosphate production and Ca2+ mobilization in Xenopus oocytes. *Proc. Natl. Acad. Sci.* **87,** 2196 –2200 (1990).

94. Pacheco, M. A. & Jope, R. S. Comparison of [3H]phosphatidylinositol and [3H]phosphatidylinositol 4,5-bisphosphate hydrolysis in postmortem human brain membranes and characterization of stimulation by dopamine D1 receptors. *J. Neurochem.* **69,** 639–644 (1997).

95. Undie, A. S. & Friedman, E. Stimulation of a dopamine D1 receptor enhances inositol phosphates formation in rat brain. *J. Pharmacol. Exp. Ther.* **253,** 987–992 (1990).

96. Wang, H. Y., Undie, A. S. & Friedman, E. Evidence for the coupling of Gq protein to D1-like dopamine sites in rat striatum: possible role in dopamine-mediated inositol phosphate formation. *Mol. Pharmacol.* **48,** 988–994 (1995).

97. Hasbi, A. *et al.* Calcium signaling cascade links dopamine D1–D2 receptor heteromer to striatal BDNF production and neuronal growth. *Proc. Natl. Acad. Sci.* **106,** 21377 –21382 (2009).

98. Perreault, M. L., Hasbi, A., O'Dowd, B. F. & George, S. R. The Dopamine D1–D2 Receptor Heteromer in Striatal Medium Spiny Neurons: Evidence for a Third Distinct Neuronal Pathway in Basal Ganglia. *Front. Neuroanat.* **5,** (2011).

99. Perreault, M. L., Hasbi, A., Alijaniaram, M., O'Dowd, B. F. & George, S. R. Reduced striatal dopamine D1–D2 receptor heteromer expression and behavioural subsensitivity in juvenile rats. *Neuroscience* **225,** 130–139 (2012).

100. So, C. H. *et al.* D1 and D2 dopamine receptors form heterooligomers and cointernalize after selective activation of either receptor. *Mol. Pharmacol.* **68,** 568 – 578 (2005).

101. O'Dowd, B. F. *et al.* Dopamine receptor oligomerization visualized in living cells. *J. Biol. Chem.* **280,** 37225 –37235 (2005).

102. Rashid, A. J. *et al.* D1–D2 dopamine receptor heterooligomers with unique pharmacology are coupled to rapid activation of Gq/11 in the striatum. *Proc. Natl. Acad. Sci.* **104,** 654 –659 (2007).

103. Rashid, A. J., O'Dowd, B. F., Verma, V. & George, S. R. Neuronal Gq/11-coupled dopamine receptors: an uncharted role for dopamine. *Trends Pharmacol. Sci.* **28,** 551–555 (2007).

104. Panchalingam, S. & Undie, A. S. SKF83959 exhibits biochemical agonism by stimulating [35S]GTP[gamma]S binding and phosphoinositide hydrolysis in rat and monkey brain. *Neuropharmacology* **40,** 826–837 (2001).

105. O'Sullivan, G. J. *et al.* Ethological resolution of behavioural topography and D1-like versus D2-like agonist responses in congenic D5 dopamine receptor mutants: Identification of D5:D2-like interactions. *Synapse* **55,** 201–211 (2005).

106. Andringa, G., Stoof, J. C. & Cools, A. R. Sub-chronic administration of the dopamine D1 antagonist SKF 83959 in bilaterally MPTP-treated rhesus monkeys: stable therapeutic effects and wearing-off dyskinesia. *Psychopharmacology (Berl.)* **146,** 328–334 (1999).

107. Kendall, R. T. & Senogles, S. E. Isoform-specific uncoupling of the D2 dopamine receptors subtypes. *Neuropharmacology* **60,** 336–342 (2011).

108. Ferre, S. *et al.* Building a new conceptual framework for receptor heteromers. *Nat. Chem. Biol.* **5,** 131–134 (2009).

109. Ferré, S. *et al.* G Protein–Coupled Receptor Oligomerization Revisited: Functional and Pharmacological Perspectives. *Pharmacol. Rev.* **66,** 413–434 (2014).

110. Ferré, S. The GPCR heterotetramer: challenging classical pharmacology. *Trends Pharmacol. Sci.* **36,** 145–152 (2015).

111. Prinster, S. C., Hague, C. & Hall, R. A. Heterodimerization of G protein-coupled receptors: specificity and functional significance. *Pharmacol. Rev.* **57,** 289 –298 (2005).

112. George, S. R., O'Dowd, B. F. & Lee, S. P. G protein-coupled receptor oligomerization and its potential for drug discovery. *Nat. Rev. Drug Discov.* **1,** 808–820 (2002).

113. Milligan, G. G protein-coupled receptor dimerization: function and ligand pharmacology. *Mol. Pharmacol.* **66,** 1 –7 (2004).

114. Missale, C., Fiorentini, C., Collo, G. & Spano, P. The neurobiology of dopamine receptors: evolution from the dual concept to heterodimer complexes. *J. Recept. Signal Transduct. Res.* **30,** 347–354 (2010).

115. Terrillon, S. & Bouvier, M. Roles of G-protein-coupled receptor dimerization. *Eur. Mol. Biol. Organ. Rep.* **5,** 30–34 (2004).

116. Hubbell, W. L., Altenbach, C., Hubbell, C. M. & Khorana, H. G. in *Membrane Proteins* **Volume 63,** 243–290 (Academic Press, 2003).

117. Milan-Lobo, L. & Whistler, J. L. Heteromerization of the μ- and δ-Opioid Receptors Produces Ligand-Biased Antagonism and Alters μ-Receptor Trafficking. *J. Pharmacol. Exp. Ther.* **337,** 868 –875 (2011).

118. Waldhoer, M. *et al.* A heterodimer-selective agonist shows in vivo relevance of G protein-coupled receptor dimers. *Proc. Natl. Acad. Sci. U. S. A.* **102,** 9050 –9055 (2005).

119. Ng, J., Rashid, A. J., So, C. H., O'Dowd, B. F. & George, S. R. Activation of calcium/calmodulin-dependent protein kinase II[alpha] in the striatum by the heteromeric D1-D2 dopamine receptor complex. *Neuroscience* **165,** 535–541 (2010).

120. Perreault, M. L., Fan, T., Alijaniaram, M., O'Dowd, B. F. & George, S. R. Dopamine D1–D2 Receptor Heteromer in Dual Phenotype GABA/Glutamate-Coexpressing Striatal Medium Spiny Neurons: Regulation of BDNF, GAD67 and VGLUT1/2. *PLoS ONE* **7,** e33348 (2012).

121. Takebe, Y. *et al.* SR alpha promoter: an efficient and versatile mammalian cDNA expression system composed of the simian virus 40 early promoter and the R-U5 segment of human T-cell leukemia virus type 1 long terminal repeat. *Mol. Cell. Biol.* **8,** 466–472 (1988).

122. Monsma, F. J., Mahan, L. C., McVittie, L. D., Gerfen, C. R. & Sibley, D. R. Molecular cloning and expression of a D1 dopamine receptor linked to adenylyl cyclase activation. *Proc. Natl. Acad. Sci.* **87,** 6723–6727 (1990).

123. Zhang, L. J., Lachowicz, J. E. & Sibley, D. R. The D2S and D2L dopamine receptor isoforms are differentially regulated in Chinese hamster ovary cells. *Mol. Pharmacol.* **45,** 878–889 (1994).

124. Schetz, J. A. & Sibley, D. R. The binding-site crevice of the D4 dopamine receptor is coupled to three distinct sites of allosteric modulation. *J. Pharmacol. Exp. Ther.* **296,** 359–363 (2001).

125. Koch, W. J., Hawes, B. E., Inglese, J., Luttrell, L. M. & Lefkowitz, R. J. Cellular expression of the carboxyl terminus of a G protein-coupled receptor kinase attenuates G beta gamma-mediated signaling. *J. Biol. Chem.* **269,** 6193–6197 (1994).

126. Freedman, N. J. *et al.* Phosphorylation and desensitization of the human beta-adrenergic receptor: involvemenf of G protein-coupled receptor kinases and cAMP-dependent protein kinase. *J. Biol. Chem.* **270,** 17953–17961 (1995).

127. Namkung, Y. & Sibley, D. R. Protein kinase C mediates phosphorylation, desensitization, and trafficking of the D2 dopamine receptor. *J. Biol. Chem.* **279,** 49533–49541 (2004).

128. Seeman, P. & Van Tol, H. H. M. Dopamine D4 receptors bind inactive (+)-aporphines, suggesting neuroleptic role. Sulpiride not stereoselective. *Eur. J. Pharmacol.* **233,** 173–174 (1993).

129. Millan, M., Newman-Tancredi, A., Quentric, Y. & Cussac, D. The 'selective' dopamine D1 receptor antagonist, SCH23390, is a potent and high efficacy agonist at cloned human serotonin2C receptors. *Psychopharmacology (Berl.)* **156,** 58–62 (2001).

130. O'Sullivan, G. J., Roth, B. L., Kinsella, A. & Waddington, J. L. SKF 83822 distinguishes adenylyl cyclase from phospholipase C-coupled dopamine D1-like receptors: behavioural topography. *Eur. J. Pharmacol.* **486,** 273–280 (2004).

131. Zhang, Z.-J. *et al.* The paradoxical effects of SKF83959, a novel dopamine D1-like receptor agonist, in the rat acoustic startle reflex paradigm. *Neurosci. Lett.* **382,** 134–138 (2005).

132. Hasbi, A., O'Dowd, B. F. & George, S. R. Dopamine D1-D2 receptor heteromer signaling pathway in the brain: emerging physiological relevance. *Mol. Brain* **4,** 26 (2011).

133. Guo, L. *et al.* SKF83959 is a Potent Allosteric Modulator of Sigma-1 Receptor. *Mol. Pharmacol.* (2013). doi:10.1124/mol.112.083840

134. la Cour, C. M., Salles, M.-J., Pasteau, V. & Millan, M. J. Signaling Pathways Leading to Phosphorylation of Akt and GSK-3β by Activation of Cloned Human and Rat Cerebral D2 and D3 Receptors. *Mol. Pharmacol.* **79,** 91–105 (2011).

135. Okajima, F., Sato, K., Sho, K. & Kondo, Y. Stimulation of adenosine receptor enhances α1 -adrenergic receptor-mediated activation of phospholipase C and Ca2+ mobilization in a pertussis toxin-sensitive manner in FRTL-5 thyroid cells. *FEBS Lett.* **248,** 145–149 (1989).

136. Carroll, R. C., Morielli, A. D. & Peralta, E. G. Coincidence detection at the level of phospholipase C activation mediated by the m4 muscarinic acetylcholine receptor. *Curr. Biol.* **5,** 536–544 (1995).

137. Toms, N. J. & Roberts, P. J. Group 1 mGlu receptors elevate [Ca2+]i in rat cultured cortical type 2 astrocytes: [Ca2+]i synergy with adenosine A1 receptors. *Neuropharmacology* **38,** 1511–1517 (1999).

138. Rebres, R. A. *et al.* Synergistic Ca2+ Responses by Gαi- and Gαq-coupled G-protein-coupled Receptors Require a Single PLCβ Isoform That Is Sensitive to Both Gβγ and Gαq. *J. Biol. Chem.* **286,** 942–951 (2011).

139. González, S. *et al.* Circadian-Related Heteromerization of Adrenergic and Dopamine D4 Receptors Modulates Melatonin Synthesis and Release in the Pineal Gland. *PLoS Biol* **10,** e1001347 (2012).

140. Kern, A., Albarran-Zeckler, R., Walsh, H. E. & Smith, R. G. Apo-Ghrelin Receptor Forms Heteromers with DRD2 in Hypothalamic Neurons and Is Essential for Anorexigenic Effects of DRD2 Agonism. *Neuron* **73,** 317–332 (2012).

141. O'Dowd, B. F., Ji, X., Nguyen, T. & George, S. R. Two amino acids in each of D1 and D2 dopamine receptor cytoplasmic regions are involved in D1–D2 heteromer formation. *Biochem. Biophys. Res. Commun.* **417,** 23–28 (2012).

142. Dziedzicka-Wasylewska, M. *et al.* Fluorescence Studies Reveal Heterodimerization of Dopamine D1 and D2 Receptors in the Plasma Membrane. *Biochemistry (Mosc.)* **45,** 8751–8759 (2006).

143. Łukasiewicz, S., Faron-Górecka, A., Dobrucki, J., Polit, A. & Dziedzicka-Wasylewska, M. Studies on the role of the receptor protein motifs possibly involved

in electrostatic interactions on the dopamine D1 and D2 receptor oligomerization. *FEBS J.* **276,** 760–775 (2009).

144. Liu, Y. F., Civelli, O., Zhou, Q. Y. & Albert, P. R. Cholera toxin-sensitive 3',5'-cyclic adenosine monophosphate and calcium signals of the human dopamine-D1 receptor: selective potentiation by protein kinase A. *Mol. Endocrinol.* **6,** 1815–1824 (1992).

145. Camps, M. *et al.* Stimulation of phospholipase C by guanine-nucleotide-binding protein βγ subunits. *Eur. J. Biochem.* **206,** 821–831 (1992).

146. Sallese, M., Mariggiò, S., D'Urbano, E., Iacovelli, L. & Blasi, A. D. Selective Regulation of Gq Signaling by G Protein-Coupled Receptor Kinase 2: Direct Interaction of Kinase N Terminus with Activated Gαq. *Mol. Pharmacol.* **57,** 826–831 (2000).

147. Carman, C. V. *et al.* Selective Regulation of Gαq/11 by an RGS Domain in the G Protein-coupled Receptor Kinase, GRK2. *J. Biol. Chem.* **274,** 34483–34492 (1999).

148. Allen, J. A., Halverson-Tamboli, R. A. & Rasenick, M. M. Lipid raft microdomains and neurotransmitter signalling. *Nat. Rev. Neurosci.* **8,** 128–140 (2006).

149. Korade, Z. & Kenworthy, A. K. Lipid rafts, cholesterol, and the brain. *Neuropharmacology* **55,** 1265–1273 (2008).

150. Björk, K. & Svenningsson, P. Modulation of Monoamine Receptors by Adaptor Proteins and Lipid Rafts: Role in Some Effects of Centrally Acting Drugs and Therapeutic Agents. *Annu. Rev. Pharmacol. Toxicol.* **51,** 211–242 (2011).

151. Kong, M. M. C., Verma, V., O'Dowd, B. F. & George, S. R. The role of palmitoylation in directing dopamine D1 receptor internalization through selective endocytic routes. *Biochem. Biophys. Res. Commun.* **405,** 445–449 (2011).

152. Sebastião, A. M., Assaife-Lopes, N., Diógenes, M. J., Vaz, S. H. & Ribeiro, J. A. Modulation of brain-derived neurotrophic factor (BDNF) actions in the nervous system by adenosine A2A receptors and the role of lipid rafts. *Biochim. Biophys. Acta BBA - Biomembr.* **1808,** 1340–1349 (2011).

153. Celver, J., Sharma, M. & Kovoor, A. D2-Dopamine receptors target regulator of G protein signaling 9-2 to detergent-resistant membrane fractions. *J. Neurochem.* **120,** 56–69 (2012).

154. Bateup, H. S. *et al.* Cell-type specific regulation of DARPP-32 phosphorylation by psychostimulant and antipsychotic drugs. *Nat. Neurosci.* **11,** 932–939 (2008).

155. Svenningsson, P. *et al.* DARPP-32: an integrator of neurotransmission. *Annu. Rev. Pharmacol. Toxicol.* **44,** 269–296 (2004).

156. Pozzi, L. *et al.* Opposite regulation by typical and atypical anti-psychotics of ERK1/2, CREB and Elk-1 phosphorylation in mouse dorsal striatum. *J. Neurochem.* **86,** 451–459 (2003).

157. Beaulieu, J.-M. *et al.* Lithium antagonizes dopamine-dependent behaviors mediated by an AKT/glycogen synthase kinase 3 signaling cascade. *Proc. Natl. Acad. Sci. U. S. A.* **101,** 5099–5104 (2004).

158. Emamian, E. S., Hall, D., Birnbaum, M. J., Karayiorgou, M. & Gogos, J. A. Convergent evidence for impaired AKT1-GSK3beta signaling in schizophrenia. *Nat. Genet.* **36,** 131–137 (2004).

159. Beaulieu, J.-M. *et al.* An Akt/beta-arrestin 2/PP2A signaling complex mediates dopaminergic neurotransmission and behavior. *Cell* **122,** 261–273 (2005).

160. Beaulieu, J.-M. *et al.* Regulation of Akt Signaling by D2 and D3 Dopamine Receptors In Vivo. *J. Neurosci.* **27,** 881–885 (2007).

161. Beaulieu, J.-M. *et al.* A beta-arrestin 2 signaling complex mediates lithium action on behavior. *Cell* **132,** 125–136 (2008).

162. Beaulieu, J.-M., Gainetdinov, R. R. & Caron, M. G. The Akt-GSK-3 signaling cascade in the actions of dopamine. *Trends Pharmacol. Sci.* **28,** 166–172 (2007).

163. Masri, B. *et al.* Antagonism of dopamine D2 receptor/β-arrestin 2 interaction is a common property of clinically effective antipsychotics. *Proc. Natl. Acad. Sci.* **105,** 13656–13661 (2008).

164. Urs, N. M., Snyder, J. C., Jacobsen, J. P. R., Peterson, S. M. & Caron, M. G. Deletion of GSK3β in D2R-expressing neurons reveals distinct roles for β-arrestin signaling in antipsychotic and lithium action. *Proc. Natl. Acad. Sci. U. S. A.* **109,** 20732–20737 (2012).

165. Allen, J. A. *et al.* Discovery of β-Arrestin–Biased Dopamine D2 Ligands for Probing Signal Transduction Pathways Essential for Antipsychotic Efficacy. *Proc. Natl. Acad. Sci.* **108,** 18488–18493 (2011).

166. Chen, X. *et al.* Structure-Functional Selectivity Relationship Studies of β-arrestin-biased Dopamine D2 Receptor Agonists. *J. Med. Chem.* (2012). doi:10.1021/jm300603y

167. Urban, J. D. *et al.* Functional Selectivity and Classical Concepts of Quantitative Pharmacology. *J. Pharmacol. Exp. Ther.* **320,** 1–13 (2007).

168. Whalen, E. J., Rajagopal, S. & Lefkowitz, R. J. Therapeutic potential of β-arrestin- and G protein-biased agonists. *Trends Mol. Med.* **17,** 126–139 (2011).

169. Kenakin, T. Collateral efficacy in drug discovery: taking advantage of the good (allosteric) nature of 7TM receptors. *Trends Pharmacol. Sci.* **28,** 407–415 (2007).

170. Kenakin, T. Functional selectivity through protean and biased agonism: who steers the ship? *Mol. Pharmacol.* **72,** 1393–1401 (2007).

171. Kenakin, T. P. Pharmacological onomastics: what's in a name? *Br. J. Pharmacol.* **153,** 432–438 (2008).

172. Kobilka, B. K. & Deupi, X. Conformational complexity of G-protein-coupled receptors. *Trends Pharmacol. Sci.* **28,** 397–406 (2007).

173. Wess, J., Han, S.-J., Kim, S.-K., Jacobson, K. A. & Li, J. H. Conformational changes involved in G-protein-coupled-receptor activation. *Trends Pharmacol. Sci.* **29,** 616–625 (2008).

174. Rajagopal, S., Rajagopal, K. & Lefkowitz, R. J. Teaching old receptors new tricks: biasing seven-transmembrane receptors. *Nat. Rev. Drug Discov.* **9,** 373–386 (2010).

175. Hudson, B. D., Hébert, T. E. & M. Kelly, M. E. Ligand- and Heterodimer-Directed Signaling of the CB1 Cannabinoid Receptor. *Mol. Pharmacol.* **77,** 1 –9 (2010).

176. Carr, R. *et al.* Development and Characterization of Pepducins as Gs-biased Allosteric Agonists. *J. Biol. Chem.* **289,** 35668–35684 (2014).

177. White, K. L. *et al.* Identification of Novel Functionally Selective κ-Opioid Receptor Scaffolds. *Mol. Pharmacol.* **85,** 83–90 (2014).

178. Valant, C. *et al.* A novel mechanism of G protein-coupled receptor functional selectivity. Muscarinic partial agonist McN-A-343 as a bitopic orthosteric/allosteric ligand. *J. Biol. Chem.* **283,** 29312–29321 (2008).

179. Lane, J. R., Sexton, P. M. & Christopoulos, A. Bridging the gap: bitopic ligands of G-protein-coupled receptors. *Trends Pharmacol. Sci.* **34,** 59–66 (2013).

180. Wacker, D. *et al.* Structural Features for Functional Selectivity at Serotonin Receptors. *Science* **340,** 615–619 (2013).

181. Quoyer, J. *et al.* Pepducin targeting the C-X-C chemokine receptor type 4 acts as a biased agonist favoring activation of the inhibitory G protein. *Proc. Natl. Acad. Sci.* 201312515 (2013). doi:10.1073/pnas.1312515110

182. Gay, E. A., Urban, J. D., Nichols, D. E., Oxford, G. S. & Mailman, R. B. Functional selectivity of D2 receptor ligands in a Chinese hamster ovary hD2L cell line: evidence for induction of ligand-specific receptor states. *Mol. Pharmacol.* **66,** 97–105 (2004).

183. Kilts, J. D. *et al.* Functional selectivity of dopamine receptor agonists. II. Actions of dihydrexidine in D2L receptor-transfected MN9D cells and pituitary lactotrophs. *J. Pharmacol. Exp. Ther.* **301,** 1179–1189 (2002).

184. Lane, J. R., Powney, B., Wise, A., Rees, S. & Milligan, G. Protean Agonism at the Dopamine D2 Receptor: (S)-3-(3-Hydroxyphenyl)-N-propylpiperidine Is an Agonist for Activation of Go1 but an Antagonist/Inverse Agonist for Gi1,Gi2, and Gi3. *Mol. Pharmacol.* **71,** 1349–1359 (2007).

185. Lane, J. R., Powney, B., Wise, A., Rees, S. & Milligan, G. G Protein Coupling and Ligand Selectivity of the D2L and D3 Dopamine Receptors. *J. Pharmacol. Exp. Ther.* **325,** 319–330 (2008).

186. Mottola, D. M. *et al.* Functional selectivity of dopamine receptor agonists. I. Selective activation of postsynaptic dopamine D2 receptors linked to adenylate cyclase. *J. Pharmacol. Exp. Ther.* **301,** 1166–1178 (2002).

187. Liu, J. J., Horst, R., Katritch, V., Stevens, R. C. & Wüthrich, K. Biased signaling pathways in β2-adrenergic receptor characterized by 19F-NMR. *Science* **335,** 1106–1110 (2012).

188. Kruse, A. C. *et al.* Muscarinic receptors as model targets and antitargets for structure-based ligand discovery. *Mol. Pharmacol.* **84,** 528–540 (2013).

189. Dror, R. O. *et al.* Structural basis for modulation of a G-protein-coupled receptor by allosteric drugs. *Nature* **503,** 295–299 (2013).

190. Banala, A. K. *et al.* N-(3-fluoro-4-(4-(2-methoxy or 2,3-dichlorophenyl)piperazine-1-yl)butyl)arylcarboxamides as selective dopamine D3 receptor ligands: critical role of the carboxamide linker for D3 receptor selectivity. *J. Med. Chem.* **54,** 3581–3594 (2011).

191. Bergman, J. *et al.* Modification of cocaine self-administration by buspirone (buspar®): potential involvement of D3 and D4 dopamine receptors. *Int. J. Neuropsychopharmacol. Off. Sci. J. Coll. Int. Neuropsychopharmacol. CINP* **16,** 445–458 (2013).

192. Hamdan, F. F., Audet, M., Garneau, P., Pelletier, J. & Bouvier, M. High-throughput screening of G protein-coupled receptor antagonists using a bioluminescence resonance energy transfer 1-based beta-arrestin2 recruitment assay. *J. Biomol. Screen.* **10,** 463–475 (2005).

193. Klewe, I. V. *et al.* Recruitment of beta-arrestin2 to the dopamine D2 receptor: insights into anti-psychotic and anti-parkinsonian drug receptor signaling. *Neuropharmacology* **54,** 1215–1222 (2008).

194. Kenakin, T., Watson, C., Muniz-Medina, V., Christopoulos, A. & Novick, S. A Simple Method for Quantifying Functional Selectivity and Agonist Bias. *ACS Chem. Neurosci.* **3,** 193–203 (2012).

195. Greene, J., Kahn, S., Savoj, H., Sprague, P. & Teig, S. Chemical Function Queries for 3D Database Search. *J. Chem. Inf. Comput. Sci.* **34,** 1297–1308 (1994).

196. Cherezov, V. *et al.* High-resolution crystal structure of an engineered human beta2-adrenergic G protein-coupled receptor. *Science* **318,** 1258–1265 (2007).

197. Rasmussen, S. G. F. *et al.* Crystal structure of the β2 adrenergic receptor-Gs protein complex. *Nature* **477,** 549–555 (2011).

198. Boeckler, F., Lanig, H. & Gmeiner, P. Modeling the similarity and divergence of dopamine D2-like receptors and identification of validated ligand-receptor complexes. *J. Med. Chem.* **48,** 694–709 (2005).

199. Newman, A. H. *et al.* Molecular determinants of selectivity and efficacy at the dopamine D3 receptor. *J. Med. Chem.* **55,** 6689–6699 (2012).

200. Skinbjerg, M. *et al.* Arrestin3 Mediates D2 Dopamine Receptor Internalization. *Synap. N. Y. N* **63,** 621–624 (2009).

201. Baum, B. *et al.* More than a simple lipophilic contact: a detailed thermodynamic analysis of nonbasic residues in the s1 pocket of thrombin. *J. Mol. Biol.* **390,** 56–69 (2009).

202. Kenakin, T. & Christopoulos, A. Signalling bias in new drug discovery: detection, quantification and therapeutic impact. *Nat. Rev. Drug Discov.* **12,** 205–216 (2013).

203. Stahl, E. L., Zhou, L., Ehlert, F. J. & Bohn, L. M. A Novel Method for Analyzing Extremely Biased Agonism at G Protein–Coupled Receptors. *Mol. Pharmacol.* **87,** 866–877 (2015).

204. Lan, H., Liu, Y., Bell, M. I., Gurevich, V. V. & Neve, K. A. A Dopamine D2 Receptor Mutant Capable of G Protein-Mediated Signaling but Deficient in Arrestin Binding. *Mol. Pharmacol.* **75,** 113–123 (2009).

205. Peterson, S. M. *et al.* Elucidation of G-protein and β-arrestin functional selectivity at the dopamine D2 receptor. *Proc. Natl. Acad. Sci.* **112,** 7097–7102 (2015).

206. Kenakin, T. & Christopoulos, A. Signalling bias in new drug discovery: detection, quantification and therapeutic impact. *Nat. Rev. Drug Discov.* **12,** 205–216 (2013).

207. Whistler, J. L., Chuang, H., Chu, P., Jan, L. Y. & von Zastrow, M. Functional Dissociation of μ Opioid Receptor Signaling and Endocytosis: Implications for the Biology of Opiate Tolerance and Addiction. *Neuron* **23,** 737–746 (1999).

208. Conroy, J. L., Free, R. B. & Sibley, D. R. Identification of G Protein-Biased Agonists That Fail To Recruit β-Arrestin or Promote Internalization of the D1 Dopamine Receptor. *ACS Chem. Neurosci.* **6,** 681–692 (2015).

209. Daly, K. M., Li, Y. & Lin, D.-T. Imaging the Insertion of Superecliptic pHluorin-Labeled Dopamine D2 Receptor Using Total Internal Reflection Fluorescence Microscopy. *Curr. Protoc. Neurosci. Editor. Board Jacqueline N Crawley Al* **70,** 5.31.1–5.31.20 (2015).

210. Li, Y. *et al.* Imaging pHluorin-tagged receptor insertion to the plasma membrane in primary cultured mouse neurons. *J. Vis. Exp. JoVE* (2012). doi:10.3791/4450

211. Li, Y. *et al.* Identification of Two Functionally Distinct Endosomal Recycling Pathways for Dopamine D2 Receptor. *J. Neurosci.* **32,** 7178–7190 (2012).

212. Free, R. B. *et al.* Discovery and Characterization of a G Protein-biased Agonist that Inhibits β-arrestin Recruitment to the D2 Dopamine Receptor. *Mol. Pharmacol.* mol.113.090563 (2014). doi:10.1124/mol.113.090563

213. Mancini, A. *et al.* β-arrestin recruitment and biased agonism at free fatty acid receptor 1. *J. Biol. Chem.* (2015). doi:10.1074/jbc.M115.644450

214. Lee, F. J. S. *et al.* Dopamine transporter cell surface localization facilitated by a direct interaction with the dopamine D2 receptor. *EMBO J.* **26,** 2127–2136 (2007).

215. Bailey, C. & Kelly, E. in *Methods for the Discovery and Characterization of G Protein-Coupled Receptors* (ed. Stevens, C. W.) **60,** 323–346 (Humana Press, 2011).

216. Clayton, C. C., Donthamsetti, P., Lambert, N. A., Javitch, J. A. & Neve, K. A. Mutation of Three Residues in the Third Intracellular Loop of the Dopamine D2 Receptor Creates an Internalization-defective Receptor. *J. Biol. Chem.* **289,** 33663–33675 (2014).

217. Simpson, M. M. *et al.* Dopamine D4/D2 Receptor Selectivity Is Determined by A Divergent Aromatic Microdomain Contained within the Second, Third, and Seventh Membrane-Spanning Segments. *Mol. Pharmacol.* **56,** 1116–1126 (1999).

218. Schetz, J. Allosteric Modulation of Dopamine Receptors. *Mini-Rev. Med. Chem.* **5,** 555–561 (2005).

219. Conn, P. J., Christopoulos, A. & Lindsley, C. W. Allosteric modulators of GPCRs: a novel approach for the treatment of CNS disorders. *Nat. Rev. Drug Discov.* **8,** 41–54 (2009).

220. Burford, N. T., Watson, J., Bertekap, R. & Alt, A. Strategies for the identification of allosteric modulators of G-protein-coupled receptors. *Biochem. Pharmacol.* **81,** 691–702 (2011).

221. Keov, P., Sexton, P. M. & Christopoulos, A. Allosteric modulation of G protein-coupled receptors: A pharmacological perspective. *Neuropharmacology* **60,** 24–35 (2011).

222. Christopher L Schardl, D. G. P. Chapter 2 Ergot Alkaloids - Biology and Molecular Biology. *Alkaloids Chem. Biol.* **63,** 45–86 (2006).

223. Mukherjee, J. & Menge, M. Progress and prospects of ergot alkaloid research. *Adv. Biochem. Eng. Biotechnol.* **68,** 1–20 (2000).

224. Kenakin, T. Ligand-selective receptor conformations revisited: the promise and the problem. *Trends Pharmacol. Sci.* **24,** 346–354 (2003).

225. Chachisvilis, M., Zhang, Y.-L. & Frangos, J. A. G protein-coupled receptors sense fluid shear stress in endothelial cells. *Proc. Natl. Acad. Sci. U. S. A.* **103,** 15463–15468 (2006).

226. Swaminath, G. *et al.* Sequential Binding of Agonists to the β2 Adrenoceptor KINETIC EVIDENCE FOR INTERMEDIATE CONFORMATIONAL STATES. *J. Biol. Chem.* **279,** 686–691 (2004).

227. Deupi, X. & Kobilka, B. K. Energy landscapes as a tool to integrate GPCR structure, dynamics and function. *Physiol. Bethesda Md* **25,** 293–303 (2010).

228. Deupi, X. *et al.* Structural models of class a G protein-coupled receptors as a tool for drug design: insights on transmembrane bundle plasticity. *Curr. Top. Med. Chem.* **7,** 991–998 (2007).

229. Hofmann, K. P. *et al.* A G protein-coupled receptor at work: the rhodopsin model. *Trends Biochem. Sci.* **34,** 540–552 (2009).

Curriculum Vitae

Lani S. Chun

9978 Guilford Road, Apt. 202 ▪ Jessup, MD 20794 ▪ (253) 737-7426 ▪ lchun3@jhu.edu

EDUCATION

Johns Hopkins University (Sept. 2009 - Aug. 2015): CMD Biology & Biophysics Program
- Doctor of Philosophy in Biology
- NIH IRTA fellow

University of Washington (Sept. 2003 - Jun. 2007): Dual BS/BS completed
- Bachelor of Science in Cellular, Molecular, and Developmental Biology
- Bachelor of Science in Biochemistry

RELEVANT POSITIONS HELD

David Sibley Lab, NINDS, NIH, Rockville, MD
2010 - Present, Ph.D. Candidate
- First-authored a *Molecular Pharmacology* and *Neuromethods* paper.
- Second-authored a *Molecular Pharmacology* paper.
- Lead efforts to test hits from a high-throughput screen for functionally biased D_2 dopamine receptor ligands and make SAR determinations based on data from hit analogues.
- Work with collaborators to do additional testing on our main compound of interest.
- Presented data at several large conferences, including at the Society for Neuroscience 2011, Catecholamine Symposium 2012, Experimental Biology 2013, and Experimental Biology 2014.

Undergraduate Biochemistry/Biology Lab Class, JHU, Baltimore, MD
2009 - 2010, Spring and Fall Semester, Teacher's Assistant
- Explained and demonstrated experiments to students.
- Instructed students on basic concepts and solved any issues that might occur.
- Worked with the professor and other TAs to grade lab reports, grade exams, and proctor exams.

Puget Sound VA Medical Center, Seattle, WA
2007 - 2009, Research Assistant
- Worked with nurses and other lab techs to draw and process blood samples from patients.
- Tested blood samples and analyzed data in a case/control study of genomic variants in the human Nurr1 gene using TaqMan genotyping and BigDye sequencing assays.
- Selectively lesioned intracranial noradrenergic neurons and tested effect on addiction formation and extinction in the mouse model using behavioral tests such as CPP, water maze, and T-maze tests.

Wendy Raskind Lab, University of Washington, Seattle, WA
2004 - 2007, Undergraduate Research Assistant
- Performed independent research involving a linkage disequilibrium study on a family with congenital heart abnormalities using PCR, microsatellite probes, and BigDye sequencing.
- Co-authored a paper published in the *American Journal of Cardiology*.
- Co-authored a paper published in the *American Journal of Medical Genetics*.
- Presented data at the Undergraduate Research Symposium 2006

Cyrus Zabetian Lab, Puget Sound VA Medical Center, Seattle, WA
2004 - 2007, Undergraduate Research Assistant
- Performed independent research project involved a case-control study of how variants within the DBH gene might affect plasma dopamine-hydroxylase levels and its consequent effect on risk for onset of Parkinson's disease.
- Presented data at the Undergraduate Research Symposium 2005.
- First-authored an *Annals of Neurology* paper.

PUBLICATIONS AND MANUSCRIPTS

- Chun LS, Free RB, Sibley DR. **Calcium and PLC signaling through dopamine receptors**. In M. Tiberi, ed. *Dopamine Receptor Technologies, Neuromethods*. Springer Science and Business Media (in press).
- Meade JA, Free RB, Miller NR, Doyle TB, Moritz AE, Conroy JL, Chun LS, Watts VJ, Sibley DR. **(-)-Stepholidine is a potent pan-dopamine receptor antagonist of both G protein- and β-arrestin-mediated signaling**. *Psychopharm*, 2015 Mar; 232(5):917-30.
- Free RB, Chun LS, Moritz AE, Miller B, Doyle TB, Conroy JL, Padron A, Meade JA, Xiao J, Hu X, Dulcey AE, Han Y, Duan L, Titus S, Bryant-Genevier M, Barnaeva E, Ferrer M, Javitch JA, Beuming T, Shi L, Southall N, Marugan JJ, Sibley DR. **Discovery and characterization of a G protein-biased agonist that inhibits β-arrestin recruitment to the D_2 dopamine receptor**. *Mol Pharmacol*, 2014 Jul; 86(1):96-105.
- Chun LS, Free RB, Doyle TB, Huang X-P, Sibley DR. **Investigation of the D_1-D_2 heteromer: pharmacology, subunit composition, and mechanisms of signaling.** In: Eiden LE, ed. *Catecholamine Research in the 21st Century*. Boston: Academic Press; 2014:106.
- Chun LS, Free RB, Doyle TB, Huang XP, Rankin ML, Sibley DR. **D_1-D_2 dopamine receptor synergy promotes calcium signaling via multiple mechanisms.** *Mol Pharmacol*, 2013 Aug;84(2):190-200.
- Guntheroth W, Lani LS, Patton KK, Matsushita MM, Page RL, Raskind WH. **Wenckebach periodicity at rest that normalizes with tachycardia in a family with NKX2.5 mutation.** *Am J Cardiol*, 2012 Dec; 110(11):1646-1650.
- Chun LS, Samii A, Hutter CM, Griffith A, Roberts JW, Leis BC, Mosley AD, Wander PL, Edwards KL, Payami H, Zabetian CP. **DBH -1021C→T does not modify risk or age at onset in Parkinson's disease.** *Annals of Neurl*, 2007 Jul; 62(1):99-101.
- Brkanac Z, Chapman NH, Matsushita MM, Chun L, Nielsen K, Cochrane E, Berninger VW, Wijsman EM, Raskind WH. **Evaluation of candidate genes for DYX1 and DYX2 in families with dyslexia.** *Am J Med Genet*, 2007 Jun 5; 144(4):556-60.

ABSTRACTS

Development of structure-activity relationships for a G protein-biased agonist of the D_2 dopamine receptor
Experimental Biology 2015, Boston, MA
Chun LS, Free RB, Vekariya RH, Beuming T, Shi L, Aubé J, Frankowski K, Sibley DR
124 analogs of a D_2R G protein-biased agonist (1547) were tested to develop structure-activity relationships (SAR). This SAR supported and refined a previously published molecular model for 1547 binding to the D_2R.

Discovery and characterization of a G protein-biased agonist of the D_2 dopamine receptor
Experimental Biology 2014, San Diego, CA
Chun LS, Free RB, Moritz AE, Conroy JL, Meade JA, Xiao J, Dulcey AE, Vekariya RH, Ferrer M, Javitch JA, Beuming T, Shi L, Southall N, Marugan JJ, Aubé J, Frankowski KJ, Sibley DR
A high-throughput screen was conducted on a library of small molecule compounds for G protein-biased D_2 dopamine receptor signaling. A biased ligand was found, and signaling activity as well as molecular modeling were used to determine preliminary structure-activity relationships.

Discovery and characterization of a G protein-biased agonist of the D_2 dopamine receptor
Graduate Research Symposium 2014, NIH, Bethesda, MD
Chun LS, Free RB, Moritz AE, Conroy JL, Meade JA, Xiao J, Dulcey AE, Ferrer M, Javitch JA, Beuming T, Shi L, Southall N, Marugan JJ, Aubé J, Frankowski KJ, Sibley DR
See above for description. Findings submitted to *Molecular Pharmacology*, and this poster was selected as one of eleven winners of the Graduate Student Research Awards.

Discovery and characterization of a G protein-biased agonist that inhibits β-arrestin recruitment to the D_2 dopamine receptor
2013 GPCR Workshop, Maui, HI
Free RB, Chun LS, Moritz AE, Miller B, Doyle TB, Conroy JL, Padron A, Meade JA, Xiao J, Hu X, Dulcey AE, Han Y, Duan L, Titus S, Bryant-Genevier M, Barnaeva E, Ferrer M, Javitch JA, Beuming T, Shi L, Southall N, Marugan JJ, Sibley DR
See above for description.

Discovery and characterization of a completely G-protein biased D_2 dopamine receptor agonist
Society for Neuroscience 2013, San Diego, CA
Free RB, Chun LS, Conroy JL, Moritz AE, Miller B, Doyle TB, Padron A, Han Y, Southall N, Xiao J, Marugan JJ, Ferrer M, Javitch JA, Sibley DR
See above for description.

Discovery and characterization of a G protein-biased agonist that inhibits β-arrestin recruitment to the D_2 dopamine receptor
American College of Neuropsychopharmacology 2013, Hollywood, FL
Sibley DR, Free RB, Chun LS, Moritz AE, Miller B, Doyle TB, Conroy JL, Padron A, Meade JA, Xiao J, Han Y, Duan L, Ferrer M, Javitch JA, Southall N, Marugan JJ.
See above for description.

Investigation of the D_1-D_2 dopamine receptor heteromer reveals a complex signaling mechanism not limited to G_q protein activation
Experimental Biology 2013, Boston, MA
Chun LS, Free RB, Doyle TB, Huang XP, Sibley DR
This poster presents data which implicates multiple contributing pathways affecting D_1-D_2 dopamine receptor heteromer signaling. Data also clarifies other mechanistic and pharmacological aspects of the heteromer.

Investigation of the D_1-D_2 heteromer: pharmacology, subunit composition, and mechanisms of signaling
10th Annual Catecholamine Symposium 2012, Pacific Grove, CA
Chun LS, Free RB, Doyle TB, Huang XP, Sibley DR
Invited to give an oral presentation. Data was shown which implicated multiple pathways involved in D_1-D_2 dopamine receptor heteromer signaling. The subunit composition as well as the pharmacology of the heteromer were also further elucidated.

Both D_{2L} and D_{2S} dopamine receptor isoforms are able to form functional heteromeric complexes with the D_1 dopamine receptor
Society for Neuroscience 2011, Washington, DC
Chun LS, Free RB, Doyle TB, Sibley DR
This poster presents data on the pharmacology of the D_1-D_2 dopamine receptor heteromer, and the effects of various antagonists and agonists on the D_1-D_{2S} and D_1-D_{2L} dopamine receptor heteromer.

Possible differences in signal transduction for the D_1-D_{2L} and D_1-D_{2S} dopamine receptor heteromers
Graduate Research Symposium 2011, NIH, Bethesda, MD
Chun LS, Free RB, Sibley DR
This poster presents data on the pharmacology of the D_1-D_2 dopamine receptor heteromer, and the effects of various antagonists and agonists on the D_1-D_{2S} and D_1-D_{2L} dopamine receptor heteromer.

Divergent neuroadaptations in noradrenergic signaling underlie resilience and vulnerability in an animal model of PTSD
Society for Neuroscience 2008, Washington, DC
Olson VG, Rockett H, Reh R, Redila V, Chun LS, Raskind M, McMillan PJ, Szot P
The poster was on the new post traumatic stress disorder mouse model that has been developed by this lab.

Finding a gene for a new distal myopathy
Summer Undergraduate Research Symposium 2006, University of Washington, Seattle, WA
Chun LS, Raskind WH
This presentation was on an independent research project, funded by the NASA Space Grant Consortium. It
involved a genomic, linkage disequilibrium study of a family with a history co-inheritance of pancytopenia with distal myopathy via microsatellite haplotype analysis and BigDye sequencing.

A transmission disequilibrium test of DCDC2 markers in dyslexia
Undergraduate Research Symposium 2006, University of Washington, Seattle, WA
Chun LS, Raskind WH
Presented data on an investigation of several candidate genes that were believed to cause dyslexia. Responsibilities included sequencing and genotyping probands.

Lack of association between DBH -1021C→T and susceptibility to Parkinson's disease
Undergraduate Research Symposium 2005, University of Washington, Seattle, WA
Chun LS, Zabetian CP
Participated by presenting a poster on the preliminary results regarding linkage between the DBH -1021 gene and Parkinson's disease.

SKILLS

Techniques: Mammalian cell transfection, cell culture, compound screening, live cell-based BRET/FRET assays, PCR, Taqman genotyping, competition and saturation radioligand binding, molecular cloning, mouse behavioral tests, mouse dissection, confocal.

Software: Microsoft Word, PowerPoint, and Excel; GraphPad PRISM; ImageJ.

AWARDS AND HONORS

- **JHU-NIH Graduate Partnership Program IRTA fellow** (2009 - Present)
- **ASPET Robert F. Furchgott Travel Award**, $1000 for travel to EB 2015
- **ASPET Graduate Student Travel Award,** $1000 for travel to EB 2014
- **NIH Graduate Student Research Symposium Competition Award,** $1000 travel award (2014)
- **ASPET Steven E. Mayer Travel Award,** $1000 for travel to EB 2013
- **International Society for Neurochemistry Catecholamine Research Travel Fellowship**, $1000 for travel to 10th Annual Catecholamine Symposium (2012)
- **Mary Gates Scholar**
- **NASA Space Grant Consortium/Bill and Melinda Gates Research Endowment**, $1800 (2006)
- **Robert C. Byrd Scholarship**, $1500 per academic year (2003 - 2007)

PROFESSIONAL SOCIETY MEMBERSHIPS

- **American Society for Pharmacology and Experimental Therapeutics**, Graduate student member (2010 - 2015)
- **NIH Science Policy Discussion Group**, Graduate student member and blog contributor (2014 - 2015)